MASTERARBEIT | MASTER'S THESIS

Titel | Title

Zooarchaeology by Mass Spectrometry Analyses of Denisova Cave Layers

verfasst von | submitted by

Lidia Martin

angestrebter akademischer Grad | in partial fulfilment of the requirements for the degree of

Master of Science (MSc)

Wien | Vienna, 2025

1.   Abstracts

Abstract in English

The genus *Homo* has spread from its origins in Africa several times. The latest such expansion is linked to the dispersal of modern humans (*Homo sapiens*) into Eurasia where several other, so-called archaic hominin species already lived. Such archaic hominins are the Neanderthals and Denisovans, the latter first attested at Denisova Cave in the Altai mountains of southern Siberia, Russia. Denisova Cave has yielded numerous hominin fossils and a rich stratigraphic sequence. However, the distribution of fossils and hominin DNA in the cave's sediments varies considerably between layers. This renders our understanding of hominin occupation, alternation of hominin species and possible overlap, difficult to establish with certainty.

In this thesis, I aim to close the gap created by the lack of hominin fossils from layers 13 and 14 of the East Chamber of Denisova Cave. These are some of the oldest cultural layers in the cave, dating to the late Middle Pleistocene between 190-150 ka (ka=thousand years ago), but lack hominin remains until now. The layers differ distinctively in the amount of archaeological remains, as well as the markers for climatic conditions prevailing at the time. In addition, layer 14 is the richest archaeological layer of the site, hence understanding who the maker of the lithic assemblages was, is crucial.

To discover new hominin remains from these layers, I use a palaeoproteomics method known as Zooarchaeology by Mass Spectrometry (or ZooMS) to taxonomically categorize bone fragments that cannot be identified through morphology and therefore could be potentially of human origin. The method is based on subtle differences in the collagen peptide sequences of different taxa.

Of the ~650 bone fragments I analysed from the East Chamber using ZooMS, two yielded results consistent with their origin as Hominidae. These were photographed and analysed isotopically before ancient DNA analyses. The non-hominin bones allowed me to explore differences in the faunal composition of these two climatic differing layers, and these observations are discussed in the thesis.

Deutschsprachige Kurzfassung (Abstract in German)

Diese Arbeit fokussiert sich auf die Analyse von Knochenfragmenten der Schichten 13 und 14 der östlichen Kammer der Denisova-Höhle. Die Denisova-Höhle im Altai-Gebirge Südsibiriens hat zahlreiche hominide Fossilien sowie eine komplexe Stratigraphie hervorgebracht. Allerdings variiert die Verteilung von Fossilien und hominider DNA erheblich zwischen den Schichten der Höhle. Dies erschwert die Erforschung der Besiedlungsmuster, des Wechsels von Hominidenarten und möglicher zeitlicher Überschneidungen ihrer Präsenz.

Die untersuchten Schichten 13 und 14 sind die ältesten Schichten der östlichen Kammer, in denen kulturelle Artefakte gefunden wurden. Sie datieren auf das späte mittlere Pleistozän (ca. 190–150 ka) und unterscheiden sich sowohl in der Menge archäologischer Überreste als auch in den klimatischen Bedingungen, die sie widerspiegeln. Schicht 14 ist die fundreichste archäologische Schicht in diesem Teil der Höhle. Daher ist es von zentraler Bedeutung zu bestimmen, welche Hominiden die in dieser Schicht gefundenen Artefakte geschaffen haben.

Zur Entdeckung neuer Hominiden-Überreste wurde eine Methode aus der Paläoproteomik angewandt: die Zooarchäologie durch Massenspektrometrie (ZooMS). Diese Technik ermöglicht die taxonomische Identifikation von Knochenfragmenten, die morphologisch nicht bestimmbar sind, basierend auf Unterschieden in den Kollagenpeptidsequenzen verschiedener Arten.

Von den rund 650 analysierten Knochenfragmenten konnten zwei als hominid identifiziert werden, da ihre Kollagenpeptidsequenzen mit bekannten Hominiden-Markern übereinstimmten. Diese wurden anschließend durch aDNA-Analysen bestätigt. Die nicht-hominiden Knochenfunde erlauben zudem Rückschlüsse auf Unterschiede in der Faunenzusammensetzung zwischen den beiden klimatisch unterschiedlichen Schichten. Diese Beobachtungen werden in der vorliegenden Arbeit diskutiert.

Acknowledgments

I would like to express my sincere gratitude to my supervisor, Dr. Katerina Douka, for her guidance, support, and encouragement throughout my research. Her expertise and insights have been invaluable in shaping my work. Without her help this master's thesis would not have been possible.

I would also like to thank the lab manager and lab technician Laura van der Sluis and Maddalena Giannì for their help and guidance in the lab, as well as the postdoctoral researchers Emese Vegh, Annette Oertle, and Naihui Wang for their assistance and support in conducting experiments and analysing data. Their technical expertise and dedication to their work have been instrumental in the success of this project.

I would also like to thank my family, friends and my partner for their unwavering support and encouragement throughout my academic journey. Their love and encouragement have been a constant source of motivation. I would like to especially thank my parents for giving me everything they could.

I would like to thank all the people and tools that helped me with the proofreading and paraphrasing.

Finally, I would like to acknowledge the University of Vienna for providing me with the opportunity to pursue my master's degree. The resources and facilities provided by the university have been instrumental in the completion of this thesis. Thank you all for your contributions to my academic and personal growth.

2. Table of Content

3. List of Illustrations

4. List of Tables

5. List of Abbreviations

MALDI-TOF MS	Matrix-assisted laser desorption/ionization time-of-flight mass spectrometry
NISP	Number of identified specimens
ZooMS	Zooarchaeology by Mass Spectrometry
AMH	Anatomically Modern Human
ka	Thousand years ago
MIS	Marine Isotope Stage
MNI	Minimum Number of Individuals
aDNA	Ancient DNA
mtDNA	Mitochondrial DNA
LC-MS/MS	Liquid chromatography and mass spectrometry
AA	Amino Assets

Introduction

Denisova Cave is an archaeologically significant site that was repeatedly occupied from around 300 ka (ka=thousand years ago) until 20 ka (Jacobs et al. 2019). During this time, the cave was inhabited by Neanderthals, Denisovans, and anatomically modern humans (AMH), both separately and with some overlap (Jacobs et al. 2019). Evidence of interaction and interbreeding between these three hominin types has been found during this intensively investigated period (Douka et al. 2019; Zavala et al. 2021; Slon et al. 2018). In addition, this is the site where the first Denisovan was ever discovered, identified through its genome (Reich et al. 2010).

Denisova Cave is currently the only site where the occupation of all three hominins has been confirmed. For a long time, Denisova Cave was the only place where Denisovan remains had been found, but recent evidence suggests that Denisovans spread further than this specific cave or even the Altai Mountains (Chen et al. 2019; Demeter et al. 2022; Xia et al. 2024). Genetic data shows that several East Asian populations share genes due to a Denisovan ancestor, implying one or more interbreeding events between Denisovans and AMH, likely occurring outside of Central Asia (Reich et al. 2011). This evidence also provides insights into the wide adaptive range of Denisovans, as they show genetic adaptations to high-altitude environments associated with the Altai Denisovans (Zhang et al. 2022).

Neanderthals were a sister group of the Denisovans, with overlapping occupations found in Denisova Cave. Neanderthals were long believed to be highly adapted to cold climates, but scientific beliefs have changed. Neanderthals likely had to deal with significant climatic changes over time and in the vast territory they occupied, which extended from southern Spain to the Altai Mountains, encompassing a wide variety of habitats and potential climatic conditions (Gavan 2018; Stewart et al. 2019; Yaworsky et al. 2024).

Despite the adaptive abilities of the Denisovans and the extensive occupation range of Neanderthals, both hominin groups went extinct. The reasons for their extinction are highly debated (Timmermann 2020; Chu 2023). Finding new hominin remains could help create a clearer picture of our genetic cousin groups, potentially leading to a broader understanding of the migration, extinction, and living conditions of Denisovans and Neanderthals.

The East Chamber of Denisova Cave has been extensively explored, with excavations conducted over a decade (2004-2017) yielding numerous artifacts and bone fragments from hominins and faunal remains (Shunkov et al. 2020; Vasiliev et al. 2017).

Layer 13 of the East Chamber is associated with significant hyena activity, resulting in highly fragmented and digested bone fragments that are challenging to identify morphologically (Morley et al. 2019; Jacobs et al. 2019). Numerous bone fragments (around 6,000) have been collected, however the vast majority of them are morphologically non-identifiable (Vasiliev et al. 2017), leading to a lack of information about taxonomic diversity in the layer (Brown et al. 2016; Brown et al. 2021; Vasiliev et al. 2017).

Below it, Layer 14 has been extensively studied, with over 1,000 bone fragments identified through previous ZooMS analysis and more than 1,000 bones identified morphologically (Brown et al. 2021; Vasiliev et al. 2017). This makes Layer 14 one of the most thoroughly researched layers in the East Chamber and an excellent reference point for comparison with Layer 13. Evidence of hominin occupation in Layer 14 has been diagnosed through the study of both archaeological assemblages and sediment DNA analysis (Jacobs et al. 2019; Zavala et al. 2021). However, previous ZooMS analyses have not yielded any hominin remains from this layer (Brown et al. 2016; Brown et al. 2021), underscoring the importance of further research on this stratum.

This thesis aims to provide significant new information about the fauna diversity and the human taxonomic consistency of these two layers (Layer 13 and Layer 14) of the East Chamber in Denisova Cave. The analysed material consists of bone fragments excavated in 2012 and 2013, and the data produced using ZooMS will be analysed and compared to shed light on the taxonomy of these two layers. This approach aims to create a clearer picture of the taxonomy during these periods and help assess climatic changes. Additionally, it is hoped that further hominin remains will be discovered, as approximately 1 in 1,000 ZooMS-analysed bones from Denisova Cave is found to be hominin (Brown et al. 2016).

The second part of this thesis intends to generate stable isotope values for Layers 13, 14, 15, and 17. This includes a time frame of around 150,000 to up to 500,000 years ago. Five species, including herbivores and carnivores, have been analysed for their carbon and nitrogen isotope ratios.

A previous analysis of stable isotopic data from sites also located in the Altai region shows nitrogen values that are higher than expected when Neanderthal bone fragments from European sites are compared (Dobrovolskaya et al. 2011). The ecology at a site

can influence the isotopic values, thereby disrupting the trophic model with which dietary assumptions of a taxonomic group are made (Ambrose 1991). For Denisova Cave, it is not clear whether the climatic conditions and ecology caused this or if the diet of the inhabitants was responsible for the unique stable isotope values in this region, as both arguments are highly debated. All of this leads to the needs for further research on stable isotope values to conclude information about the dietary situation and the climatic living conditions of the inhabitants in the Altai region.

The generated data is used for a better understanding of the habitat and the climatic changes during this time, as well as the dietary aspects of Neanderthals and Denisovans, the hominin groups expected to live in the timeframe these layers have built up.

The chapters below include an introduction to the current scientific state of the three hominin groups found in Denisova Cave (Background) and a summary of the hominin remains found in the cave. Further, they include a stratigraphic description of the cave and an introduction to the taxonomic and climatic variability of the different layers. The thesis continues with an explanation of the methods and material used (Methods and Materials), followed by Results and finally in the Discussion I summarise and discuss the new findings.

Background

From Africa to Siberia

Africa is considered the cradle of humankind. *Homo sapiens* evolved there; however, they are not the first hominin to cross the borders of this continent and enter Eurasia. *Homo erectus* appears to be the pioneer when it comes to exploring and establishing themselves in new locations. *Homo erectus* also evolved in Africa, but by 1.8 million years ago the earliest members of these species outside Africa are found in Dmanisi, in the Georgian Caucasus (Lordkipanidze et al. 2005; Ferring et al. 2011). This suggests that a migration out of Africa happened before that; however, the timing and route these archaic hominins selected is highly debated (Carotenuto et al. 2016).

Between 500,000–300,000 years ago, another migration wave out of Africa took place. These hominins are believed to be the ancestors of *Homo neanderthalensis* (Neanderthals) and are considered to share a last common ancestor with Denisovans and the anatomically modern human, scholars argue that this individual almost certainly belongs to *Homo heidelbergensis* (Di Vincenzo et al. 2023). Originating in Africa, the ancestors of the Neanderthals developed in Eurasia and occupied the European continent for more than 400,000 years (Stringer and Crété 2022), reaching as far east as southern Siberia (Skov et al. 2022). To the north, Neanderthals were limited by the cold arid conditions during the last Ice Ages.

Anatomically modern humans evolved in Africa and migrated several times to populate the rest of the world. Evidence for this is that the genetic diversity in the African population is the highest globally, disregarding the lack of admixture with Neanderthals and Denisovans (Bergström et al. 2020; Stringer & Andrews 1988).

The timing of modern human dispersals out of Africa is unknown, and at least two models have been proposed, with early dispersals as old as 200 ka based on the Apidima 1 cranium in Greece (Harvati et al. 2019) or as early as 170 ka based on a maxilla found at Misliya Cave in present-day Israel (Hershkovitz et al. 2018). The main dispersal event is thereby believed to be between 70-60 ka, whereby stable colonisation of the Eurasian continent can be seen only after ~ 45 ka based on direct dates as well as DNA age estimates from fossil remains found all around Eurasia (Vallini et al. 2024; Fu et al. 2015; Hublin et al. 2020; Hershkovitz et al. 2015; Slimak et al. 2022).

The expansion of modern humans out of Africa probably occurred multiple times, although several early modern human lineages did not contribute to the genetics of later

Eurasian populations (Fu et al. 2015). Two primary routes are hypothesised for anatomically modern humans (AMH) entering Eurasia: one through the Near East to southern Europe, the Mediterranean region, the Caucasus Mountains, and the Danube Corridor (Mellars et al. 2004); the other through West Asia towards the east (Mellars 2006; Derevianko & Shunkov 2009). The dispersal was not a direct, linear process, but rather a back-and-forth movement over centuries, heavily influenced by climatic conditions and environmental factors (Bae et al. 2017).

When the earliest *H. sapiens* arrived in Europe around 54,000 years ago (Hublin et al. 2020; Slimak et al. 2022) the continent was exclusively inhabited by Neanderthals. Within several millennia, *H. sapiens* had completely occupied the region. This period is archaeologically referred to as the Middle to Upper Palaeolithic transition. Chronological data indicates that Neanderthals and modern humans coexisted in Europe for at least 2,600-5,400 years (Higham et al. 2014). *H. sapiens* not only settled in Europe but expanded in the rest of Eurasia very quickly, reaching Sahul probably even earlier than 55 ka (Pedro 2020), and inhabiting also the Altai region, more specifically the Denisova Cave, where the focus of this research lies.

The advancement of biomolecular methods in archaeological science, particularly in the field of ancient DNA (aDNA), has significantly expanded research possibilities. While genetic evidence has provided insights into the relationships between Neanderthals and anatomically modern humans (Fu et al. 2015; Hajdinjak et al. 2021), it also laid the groundwork for the discovery of a new hominin species – the Denisovans and their connection to modern humans and Neanderthals.

Hominin groups found at Denisova Cave

The following chapter will summarise the information about the three hominin groups found in the Denisova Cave.

Denisovans

The first Denisovan human remains were discovered in 1984 in the Denisova Cave in the Siberian Altai. However, while they were identified as human their assignation to Denisovans took place much later. In 2010, an international team led by geneticist S. Pääbo and his group sequenced DNA from a human finger bone found at the site, revealing a genetic signature distinct from both *H. sapiens* and Neanderthals. This new

hominin group was subsequently named Denisovan after the cave where it was discovered (Krause et al. 2010).

Genetic analyses, based on nuclear genome sequences, indicate that Denisovans, Neanderthals, and modern humans share a common ancestral population that separated approximately 630,000 to 520,000 years ago. (Peyrégne et al. 2024; Prüfer et al. 2017). However, nuclear DNA studies suggest a more recent divergence between Denisovans and Neanderthals around 440,000 to 390,000 years ago (Peyrégne et al. 2024; Prüfer et al. 2017). This divergence is further supported by the morphology of Denisovan teeth, which exhibit primitive traits more commonly found in hominins outside the genus *Homo*, suggesting a separation predating the emergence of Neanderthal-specific dental features (Reich et al. 2010).

The separation of Neanderthals and Denisovans is thought to have resulted from a geographical separation of Neanderthals between the west and the east of Eurasia. There is evidence of Denisovans in Asia as early as 250–170 ka, based on sediment DNA from Denisova Cave. The oldest bone fragments (Denisova 19, 20, and 21) were found in the East Gallery, Layer 15, dated to 206-252 thousand years ago (Brown et al. 2022). These represent the oldest archaeological layer at the site, with sediments dated from 197 ± 12 to 238 ± 20 ka ago (Jacobs et al. 2019). The youngest Denisovan remains genetically date to 76–52 ka and were found in Layer 11.2 of the East Chamber.

In 2018, Slon et al. analysed a bone fragment from Denisova 11, revealed to be the offspring of a Neanderthal mother and a Denisovan father. This fragment, dated to approximately 79,300–118,100 years ago (Douka et al. 2019), provides compelling evidence of multiple instances of admixture between Neanderthals and Denisovans during overlapping geographical occupation between 200,000 and 60,000 years ago (Slon et al. 2018). All of these discoveries show evidence of Neanderthal ancestry, some less recent (Denisova 2 and 8) than others (Denisova 11). Nevertheless, sediment DNA analysis shows an inconsistency in the occupation of the cave, indicating a population exchange of Denisovans in the Denisova Cave, which is consistent with the comparison of genetic analyses of bone fragments of different layers at the site (Peyrégne et al. 2024). Further studies of Neanderthal remains in other caves in this region (Chagyrskaya Cave) could also show Denisova admixture, nevertheless admixture in further west living Neanderthals is not known (Peyrégne et al. 2024).

The analysis of the Denisovan DNA revealed an even more surprising fact, the gene flow from archaic hominins, that diverged from the modern human ancestor more than a million years ago, shows the Denisovans have admixed with the ancestors of the

present-day humans from Oceania (Prüfer et al. 2014). This gene flow from Denisovans to anatomically modern humans occurred after the separation of the Neanderthal and Denisovan lineages (Reich et al. 2010). Studies of contemporary Indigenous populations in Australia, Papua New Guinea, and parts of East and Southeast Asia, as well as Indigenous Philippine and American populations, indicate at least two distinct instances of interbreeding between Denisovan populations and anatomically modern humans (Massilani et al. 2020). One admixture event seems to be the introduction of the Denisovan Genome, closely related to Denisova 3 found at the Denisova Cave in Siberia, into the modern human genome. This variant of Denisovan ancestry is mainly found in Oceanians and Native Americans.

The Denisovan introgression was estimated to be between 54–44 ka for Indigenous Australians and Melanesians and 46 ka for the ancestors of Oceanians. This genetic exchange contributed approximately 4–6% of the genetic material found in recent Melanesian populations. (Browning et al. 2018; Reich et al. 2010; Sankararaman et al. 2016; Peyrégne et al. 2024), while it only contributes to 0.2% of Denisova ancestry in Asians and Native Americans. The Philippine Indigenous group of the Negritos shows the highest levels of Denisovan ancestry.

These findings collectively highlight the complexity of human evolution, demonstrating that our ancestral story is far from linear. Instead, it involves a network of interactions and genetic exchanges between various hominin groups, contributing to the diverse genetic landscape of modern human populations.

Visualizing the Altai region and the Denisova Cave as one remarkable site, the melting pot where archaic hominin living occurred.

Neanderthals

The Neanderthals (*Homo neanderthalensis*) and *H. sapiens* shared a common mitochondrial DNA ancestor approximately 520,000 to 630,000 years ago, following the divergence of the Denisovan and Neanderthal lineages (Prüfer et al. 2017). The oldest discovered Neanderthal remains, or fossils that potentially belonged to the lineage linked to Neanderthals, are estimated to be around 430,000 years old (Arnold et al. 2014; Hajdinijak et al. 2018). For many years, *Homo heidelbergensis* was believed to be the last common ancestor of Neanderthals and *H. sapiens* (Rightmire 1998; Stringer 1988, 2012) Some researchers even propose that *H. heidelbergensis'* transition to *H. neanderthalensis* can be displayed by fossil records (Di Vincento and Manzi 2023).

However, recent studies have challenged this view, suggesting that *H. heidelbergensis* might instead be a sister group of Neanderthals. (Gomez-Robles 2019). Given these conflicting perspectives, it remains uncertain whether the last common ancestor of Neanderthals and *H. sapiens* has been definitively identified in the fossil record.

Neanderthals evolved in Eurasia and thrived there for over 200,000 years, occupying vast territories before their extinction around 40,000 years ago (Higham et al. 2014). Throughout this extensive period, Neanderthals demonstrated remarkable adaptability to various environments and climatic conditions, which fluctuated dramatically between glacial and interglacial periods. Scientists previously believed Neanderthals to be primarily carnivorous, relying heavily on hunting large herbivorous prey due to their adaptations to cold climates supported by earlier studies on Neanderthal diet and physiology (Bocherens et al. 2005; Richards et al. 2000, Ocobock et al. 2021), newer research has challenged this notion, suggesting a more complex and diverse dietary pattern for Neanderthals. Dental plaque analysis, for instance, has provided evidence of a much more diverse range of food sources for Neanderthals (Henry et al. 2011; Hardy & Moncel 2011; Power et al. 2018). This suggests that Neanderthals' dietary choices were not rigid but rather influenced by local resources and habitat conditions.
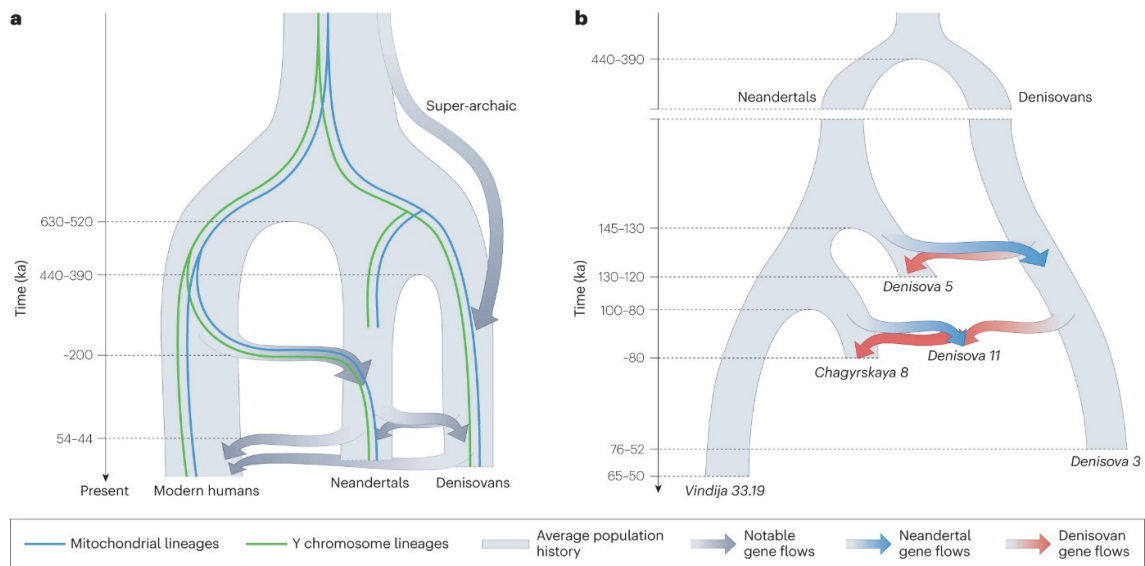
Figure 1: Relationships of Denisovans, Neanderthals and modern humans reconstructed from nuclear DNA, mtDNA, and the Y chromosome. a) Describes the Relationship between all human groups b) Describes the Relationship between Denisovans and Neanderthals (Peyrégne et al. 2024).

Evidence suggests that Neanderthals practiced self-medication using plants with antibiotic and antiseptic properties, demonstrating their knowledge and resourcefulness in addressing health concerns (Hardy et al. 2012). This sophisticated practice indicates a nuanced understanding of their environment and medicinal resources. The discovery

of symbolic items, burial rituals, and specialized bone tools among Neanderthals reveals their capacity for complex social structures, resembling those observed in modern humans (Radovčić et al. 2015; Zilhão et al. 2010). Notably, several artifacts suggest that Neanderthals may have been the first to engage in cave painting, challenging the long-held belief that this artistic expression was exclusive to *H. sapiens*.

These findings collectively refute the outdated portrayal of Neanderthals as primitive cave dwellers, instead revealing advanced behaviours and social dynamics remarkably similar to those of early anatomically modern humans. The concurrent existence of such sophisticated social behaviour among Neanderthals and the initial occupation of Europe by modern humans raises intriguing questions about potential cultural exchanges or influences between the two species. (Mellars 2005).

This question is further emphasised by the discovery of several transitional stone tool industries (Uluzzian, Chatelperronian, Szeletian, and Bohunician) across Eurasia (Hublin 2015) and the uncertainty to which specific homo species they belong to (Higham et al. 2014). Dating of the Mousterian stone tool industry, unequivocally associated with Neanderthals, reveals that these tools disappeared around the same time across regions spanning from the Black Sea and the Near East to the Atlantic coast. Interestingly, in areas where transitional stone tools have been found, the Mousterian industry, and consequently Neanderthals, persisted longer in Europe (Higham et al. 2014).

Exchanges between the two species are believed to have occurred not only on cultural and technological levels but also genetically. Evidence suggests that *H. sapiens* and Neanderthals interbred, likely on multiple occasions during their 2,600-5,400 years of coexistence (Higham et al. 2014). The discovery of Neanderthal genetic ancestry in the modern human genome (Green et al. 2010; Kuhlwilm et al. 2016; Reich et al. 2010) and fossil findings with recent Neanderthal admixture (Fu et al. 2014; Hajdinjak et al. 2021) provide evidence of interbreeding. We now know that gene exchange between Neanderthals and anatomically modern humans occurred multiple times and across different temporal scales (Kuhlwilm et al. 2016; Prüfer et al. 2014; Reich et al. 2010). These multiple interbreeding events support the concept that the evolution of the *H. sapiens* and our close archaic relatives resembles a network rather than a linear progression (Harvati et al. 2011) and is unsurprising given their shared abilities and overlapping territories (Kuhlwilm et al. 2016; Reich et al. 2010).

These findings reinforce the argument that Neanderthals, like modern humans, possessed the ability to adapt rapidly to new environments and conditions. Considering

their migration patterns and the diverse climates they inhabited, it is reasonable to infer their flexibility in response to varied habitats. Despite this adaptability, Neanderthals ultimately went extinct, leaving anatomically modern humans as the sole surviving *Homo* species. Yet, Neanderthals did not disappear without a trace, given that their genes live within our very own genome still today (Green et al. 2010; Hardy et al. 2020; Leder et al. 2021).

Modern humans

Homo sapiens is the only *Homo* genus that has persisted into modern times. The term anatomical modern human (AMH) is used to separate the *H. sapiens* (the only hominin species still existing) from the archaic human species, which have shown the same anatomical traits. Its origins trace back to the African continent. The global spread of modern humans outside Africa, where they evolved as early as 300 ka, occurred through two (or more) potential migration routes: the northern and the southern routes.

The southern route is characterised by a trajectory through Ethiopia, the Bab-el-Mandeb strait, and the Arabian Peninsula. The northern route is believed to traverse Egypt and Sinai. The latter seems more plausible, especially considering that the oldest anatomically modern human remains were discovered near this path, close to Israel (Hublin et al. 2017; Richter et al. 2017). These ancient AMH bones were unearthed in Jebel Irhoud, and their dating coincides with remains found at the Florisbad site (Grün et al. 1996; Richter et al. 2017).

Anatomically modern humans were thought to have emerged around 300,000 years ago, a conclusion initially drawn from human fossils, as well as mtDNA-based calculations estimating the most recent common ancestor (Behar et al. 2008). However, assemblages found in East and South Africa linked to AMH suggest a much earlier development. For instance, artifacts associated with the oldest *H. sapiens* remains in the Jebel Irhoud cave, including Levallois-based Middle Stone Age stone tools, have been dated to 315 ± 34 ka. This prompts a conjecture that the transition to anatomically modern humans might have taken place around that time (Richter et al. 2017). For example, a series of hypotheses are explored in a recently published review (Bergström et al. 2021).

The oldest modern human remains outside Africa were discovered in southern Greece, at the site of Apidima Cave (Harvati et al. 2019) and date to as early as 200 ka. After a long pause in early modern human remains, potentially because the earlier modern

human expansions were unsuccessful, early modern human presence is attested at the site of Mandrin in southern France, dated to around 54 ka (Slimak et al. 2022), and at Bacho Kiro in Bulgaria, dating to as early as 47-45 ka (Hublin et al. 2020), followed in northern Asia by the Ust'-Ishim human remains from Russia at 45 ka (Fu et al. 2014). Indirectly dated *H. sapiens* remains include the Cavallo Cave teeth from southern Italy dating to between 45-43 ka (Benazzi et al. 2011). It is now widely accepted that AMH established themselves in Eurasia at least 45,000 years ago and potentially earlier too. This time coincides with the ending of the Middle Palaeolithic and the beginning of the Upper Palaeolithic and the transitional technocomplexes at the time, some of which may belong to AMH or Neanderthals. To what extent this has influenced the demise of Neanderthals is still up for debate.

It is clear from the description that Eurasia in the past 200,000 years was a different place with several human groups, and species, co-existing, sometimes for several thousand years. The only site in the world where we can claim a potential coexistence of AMH, Neanderthals, and Denisovans is Denisova Cave in Russia (Siberian Altai), a reason this thesis centres on it and aims to generate new information about the site.

Denisova Cave

Stratigraphy and Geography

Denisova Cave is situated in northwestern Altai, southern Siberia, near the Anui River basin. The entrance has an elevation of 30 meters above sea level (Shunkov et al. 2018; Derevianko et al. 2008). The cave and surrounding mountains formed during the Pleistocene epoch, shaped by alternating glacial and interglacial periods that created the region's distinctive landscape of mountains, valleys, and rivers (Chlachula 2001).

The cave is formed within a massive block of coarse-grained limestone and features a southwest-facing entrance. It comprises three relatively small, mostly horizontal chambers: the Main, South, and East Chambers, all interconnected through the Main Chamber.

Figure 2:Entrance of Denisova Cave, (1. Juli 2014, Flickr).

Russian paleontologist Nikolai D. Ovodov discovered the site in 1977. Systematic excavations began in 1982, initially focusing on Holocene deposits in the Main Chamber and cave entrance. Subsequent excavations in the Main Chamber (1984, 1993-95, 1997, and 2016) and the entrance (1990, 1991, and 1996) shifted to Pleistocene layers. From 2004 to 2016, excavations concentrated on Pleistocene deposits in the East Chamber.

While the stratigraphy varies between chambers, all chambers' upper layers (1.5-2 m deep) date to the Holocene. Based on consistent optical dating chronology, the sediments show minimal signs of mixing. However, post-depositional mixing could have occurred due to animal or human activities, freeze-thaw processes, and erosional events. In the East Chamber, Layer 13 dates from 156 ± 15 to 146 ± 11 ka, Layer 14 from 193 ± 12 to 187 ± 14 ka, and Layer 15 dates from 203 ± 14 to 197 ± 12 ka. Layer 17.1, the oldest in the East Chamber, accumulated around 300 ka (Jacobs et al. 2019; Zavala et al. 2021).
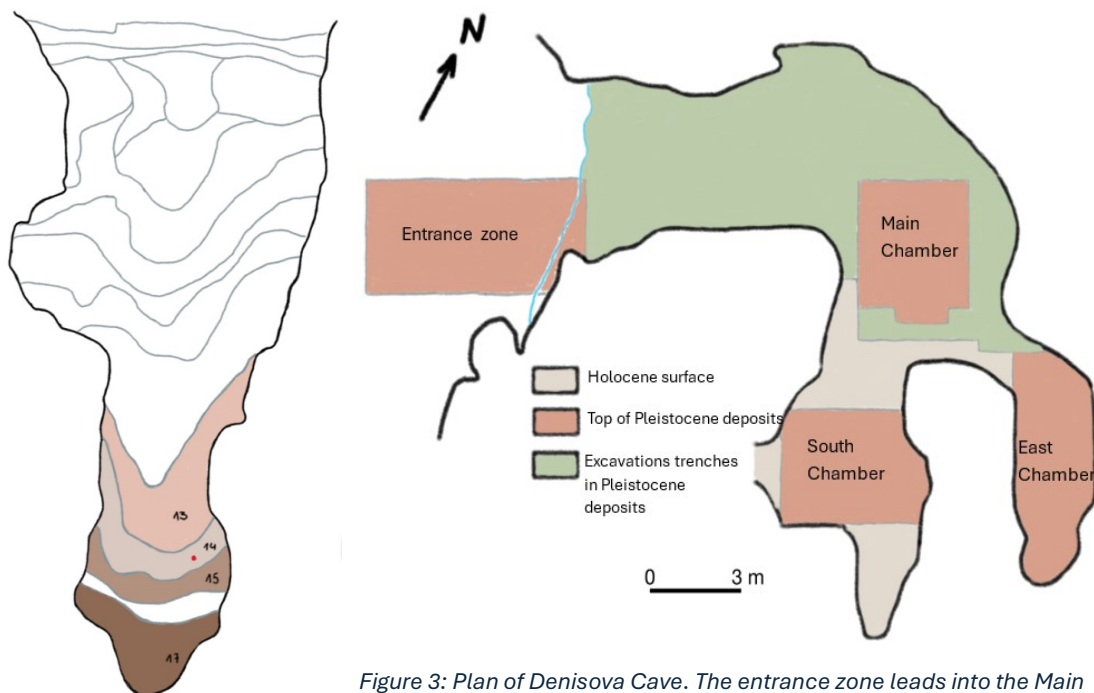
Figure 3: Plan of Denisova Cave. The entrance zone leads into the Main Chamber from where the South and East Chambers can be reached.

Figure 4: Stratigraphy of the East Chamber, Layers 13, 14, 15 and 17 are coloured. The red dot marks the locations of the newly found hominins in Layer 14.

Table 1: Bayesian model of optical ages for the deposits in the East Chamber. Ages (n = 28) have been modelled in OxCal version 4.2.4. Only random errors are included in the age model. Start and end ages have been modelled for each phase, age ranges shown ka.(after Jacobs et al. 2019; Zavala et al. 2021).

Archaeology	East Chamber Layer		Thousand years (ka)	
Upper Palaeolithic	9			
Initial Upper Palaeolithic	11.1	End	38 ± 9	Upper part: Arid climatic conditions
		Start	49 ± 6	Warm interstadial climatic conditions
		End	55 ± 6	
	11.2			- open periglacial mountain-steppe landscapes
		Start	63 ± 6	
Middle Palaeolithic	11.3	End	70 ± 8	- cooler and moister than before
		Start	80 ± 10	- dominated by Periglacial Fircedar-forest and mixed grass steppes
	Gap		25 ± 13	
	11.4	End	105 ± 11	- lower part: concluded during warm climatic conditions
				- period of cooling
	12.1	Start	120 ± 11	- dryer climate with steppe, meadow-steppe, dominant
	12.2	End	129 ± 11	- upper part: dryer climate with steppe, meadow-steppe, dominant
				- lower part: harsh cold glacial period
	12.3	Start	141 ± 10	- harsh, cold glacial period
		End	146 ± 11	
	13	Start	156 ± 15	- interglacial period, significantly warmer than present
				- lower part: decrease of warm and moisture
	Gap		32 ± 18	
Early Middle Palaeolithic				
	14	End	187 ± 14	- interglacial period, significantly warmer than present
		Start	193 ± 12	
	15	End	197 ± 12	
		Start	203 ± 14	
	Gap		36 ± 17	
Sterile	16	End	238 ± 20	
		Start	259 ± 28	
	17.1	End	284 ± 32	- Upper part: colder conditions
		Start	305 ± 37	- Lower part: milder climatic conditions, expansion of forested biotopes
	Gap		214 ± 74	
	17.2		508 ± 40	- Colder conditions Mountain-tundra of mountain-forest-tundra conditions

Paleoclimate changes are often categorized into Marine Isotope Stages (MIS), which represent cyclical climatic conditions alternating between warm and cold periods. These stages are determined by analysing oxygen isotope data from deep-sea core samples, where high Oxygen-18 levels indicate cold glacial periods and vice versa. This creates a timescale of climatic changes that is valuable for further research.

The pollen records of the different Layers from the East Chamber of Denisova Cave correlate with MIS and reveal a series of environmental changes. The section below is based on work by Jacobs et al. 2019; Brown et al. 2021; Bolikhovskaya et al. 2015; 2014; Zavala et al. 2021.

The explored layers of the East Chamber begin with Layer 17. The lower part of this layer was deposited during Marine Isotope Stage (MIS) 9, ranging from approximately 337,000 to 300,000 years ago. MIS 9 was an interglacial period with average temperatures above the modern climate. This is consistent with the sediment pollen found in this time period, which indicates a moderately warm and humid climate when the Altai was dominated by pine and birch forests and a mixture of broad-leaved species.

MIS 8 is associated with a generally cold climate, starting with a subsequent cooling phase 300,000 years ago. During MIS 8, the upper part of Layer 17 and the lower part of Layer 16 were deposited. In this time frame, pollen in the layers indicated a forest reduction at the beginning of MIS 8, followed by a phase of stable cold and humid climatic conditions, which led to the development of mountain and forest tundra, ending 243,000 years ago.

MIS 7 is considered an interglacial period with a complex structure, including three warm substages and two cooler intervals in between. These changes were highly influenced by variations in Earth's orbital parameters. In general, MIS 7 is considered a relatively cold interglacial compared to MIS 5 and 1 (Choudhury et al. 2020). Nevertheless, MIS 7 is associated with dry and warm climate conditions. MIS 7 occurred from 243,000 to 191,000 years ago. The climatic conditions of MIS 7 correspond with the climate markers found in Layers 14 and 15 deposited during this time.

Archaeology	East Chamber Layer			MIS
Upper Palaeolithic	9			
Initial Upper Palaeolithic	11.1	End	38 ± 9	3
		Start	49 ± 6	3
		End	55 ± 6	
	11.2	Start	63 ± 6	4
Middle Middle Palaeolithic	11.3	End	70 ± 8	4
		Start	80 ± 10	5
	Gap		25 ± 13	
	11.4	End	105 ± 11	5
	12.1	Start	120 ± 11	5
	12.2	End	129 ± 11	5 - 6
	12.3	Start	141 ± 10	6
		End	146 ± 11	6
	13	Start	156 ± 15	6
	Gap 32 ± 18			
Early Middle Palaeolithic	14 *	End	187 ± 14	6
		Start	193 ± 12	7
	15	End	197 ± 12	7
		Start	203 ± 14	7
	Gap 36 ± 17			
Sterile	16	End	238 ± 20	7
		Start	259 ± 28	8
	17.1	End	284 ± 32	8
		Start	305 ± 37	9
	Gap 214 ± 74			
	17.2		508 ± 40	

Figure 5: Timeline of layer formation combined with the Marine-Isotope Stages (Jacobs et al. 2019).

24

The pollen information in these layers is linked to pine-birch forests and broad-leaved species. The upper part of Layer 14 was also deposited in the early stages of MIS 6, suggesting that this early stage was associated with a rather warm climate. Later in MIS 6, the climatic conditions changed to cold and dry periglacial conditions, corresponding to the time frame of the lower part of Layer 12.2, Layer 12.3, and Layer 13.

During the Last Interglacial, MIS 5 (130,000 to 80,000 years ago), unstable fluctuating climatic conditions were observed, responsible for strong variations in temperature and humidity. At that time, pollen from Layer 12.1 shows signs of drier climatic conditions with a tendency towards steppes or meadow-steppes. The layer above, Layer 11.4, shows a change in climatic conditions. In the lower part, there are signs of warmer climatic conditions, considered to be warmer than those of the present. The upper part of this layer shows a change to a cooling period, associated with the disappearance of broad-leaved trees and an increase in Siberian pine species. Layer 11.3 began to form during a period of warmer temperatures, leading to the development of interstadial steppes and probably forest steppes. In the middle of this layer, a change in humidity leading to a drier climate can be observed, causing a dominance of periglacial dry steppe landscapes. The upper part of Layer 11.3 was formed in a cooler and more humid climate.

MIS 4, considered to be ranging from 71,000 – 57,000 years ago, had highly fluctuating dry and wet but consistently cold conditions. Steppe and meadow-steppe plants expanded, thereby replacing broad-leaved species. This corresponds to Layer 11.2, which developed in an open periglacial mountain-steppe landscape.

Marine Isotope Stage 3 shows different climatic periods: a cold and humid condition, leading to a dominance of dark coniferous forests, and a warmer one, with a dominance of mixed-grass communities and deciduous tree forests. This stage begins 57,000 and ends 29,000 years ago, this correlates with Layers 11.1 and 11.2, as well as the lower part of Layer 9.

As seen above, the Marine Isotope Stages can be verified by the spore-pollen analyses of Bolikhovskaya et al. (2015) found in the East Chamber of the Denisova Cave. Not only can spore-pollen be a good indication of climatic conditions and is often used (Bolikhovskaya et al. 2015; 2014; Jacobs et al. 2019), but faunal remains are also an excellent proxy for reconstructing the climatic conditions in a specific time frame. The optimal habitation conditions of animal species vary significantly according to their

tolerance and needs, making changes in faunal remains a good indication of changes in climatic conditions.

This was already used in previous studies (Jacobs et al. 2019; Brown et al. 2021), which include information about faunal remains alongside pollen analysis. This shows consistency in the climatic changes across all three studies, indicating that the faunal composition of a cave is an important indicator of the environmental conditions surrounding the cave.

Faunal composition of Denisova Cave

Denisova Cave is a crucial site for understanding the taxonomic diversity of the Pleistocene in the Altai region. More than 12 years of excavation at the East Chamber and analysis have yielded more than 177,000 identifiable bone fragments, and several million unidentified ones, belonging to over 80 species of large and small mammals, as well as several species of birds, amphibians, and fish. Small animal species, including rodents, insectivores, birds, bats, amphibians, and fish, comprise 39.3% of all morphologically identifiable remains (Vasiliev 2017). More than a decade of analyses expanded our knowledge, identifying 100 different species of small mammals and 66 bird taxa (Jacobs et al. 2019). The most common zooarchaeologically analysed species from the East Chamber of Denisova Cave are listed in the table below. These identifications are based on morphological analysis of bones from excavations conducted between 2005 and 2016 (Agadjanian et. al. 2019; Vasiliev et al. 2013; 2017).

Table 2: Possible mammalian species that have been found in the East Chamber of Denisova Cave. The column with the grouping gives further information about the animal species. Bats and Rodents species are not named specifically (Agadjanian et. al. 2019; Vasiliev et al. 2013; 2017).

Species	General name	Family	Genus	Group
Lepus tanaiticus	Don hare	Leporidae	*Lepus*	Small mammal
Lepus tolai	Tolai hare	Leporidae	*Lepus*	Small mammal
Erinaceus auratus	Hedgehog	Erinaceidae	*Erinaceus*	Small mammal
Asioscalops altaica	Siberian mole Talpa	Talpidae	*Eulipotyphla*	Small mammal
Chiropthera gen. indet.	Bats	n.k.	*Chiropthera*	Small mammal
Ochotona sp.	Pika	Ochotonidae	*Ochotona*	Small mammal
Pteromys volans	Siberian flying squirrel	Sciuridae	*Pteromys*	Small mammal

Tamias sibiricus	Siberian chipmunk	Sciuridae	*Tamias*	Small mammal
Citellus sp./ Spermophilus sp.	Ground squirrel	Sciuridae	*Spermophilus*	Small mammal
Allactaga sp.	Allactaga	Dipodidae	*Allactaga*	Small mammal
Cricetus sp.	Hamsters	Cricetidae	*Cricetus*	Small mammal
Rodentia gen. indet.	Rodent	Rodentia		Small mammal
Myospalax myospalax	Zokor	Spalacidae	*Myospalax*	Small mammal
Marmota baibacina	Gray marmot	Sciuridae	*Marmota*	Small mammal
Castor fiber	Eurasian beaver	Castoridae	*Castor*	Small mammal
Canis lupus	Wolf	Canidae	*Canis*	Carnivore
Vulpes vulpes	Red fox	Canidae	*Vulpes*	Carnivore
Vulpes corsak	Corsac fox	Canidae	*Vulpes*	Carnivore
Alopex lagopus	Arctic fox	Canidae	*Vulpes*	Carnivore
Cuon alpinus	Dhole	Canidae	*Cuon*	Carnivore
Ursus arctos	Brown bear	Ursidae	*Ursus*	Omnivore
U. (Spelaearctos) savini	Cave Bear	Ursidae	*Ursus*	Omnivore
Martes zibellina	Sable	Mustelidae	*Martes*	Small predators
Gulo gulo	Wolverine	Mustelidae	*Gulo*	Small predators
Mustela erminea	Stoat	Mustelidae	*Mustela*	Small predators
Mustela nivalis	Least weasel	Mustelidae	*Mustela*	Small predators
Mustela altaica	Mountain weasel	Mustelidae	*Mustela*	Small predators
Mustela eversmanni	Steppe polecat	Mustelidae	*Mustela*	Small predators
Mustela sibirica	Siberian weasel	Mustelidae	*Mustela*	Small predators
C. crocuta spelaea	Cave hyena	Hyaenidae	*Crocuta*	Carnivore
Panthera spelaea	Cave lion	Felidae	*Panthera*	Carnivore
Uncia uncia	Snow leopard	Felidae	*Panthera*	Carnivore
Lynx lynx	Eurasian lynx	Felidae	*Lynx*	Carnivore
Felis manul	Pallas's cat	Felidae	*Otocolobus*	Carnivore
Mammuthus primigenius	Woolly mammoth (extinct)	Elephantidae	*Mammuthus*	Megafauna
Equus (E.) ferus	*Tarpan*	Equidae	*Equus*	Stepp-related
E. (Sussemionus) ovodovi	Equus species (extinct)	Equidae	*Equus*	Stepp-related
E. ovodovi / ferus	Equus species (extinct)	Equidae	*Equus*	Stepp-related
Coelodonta antiquitatis	Woolly Rhino	Rhinocerotidae	*Coelodonta*	Megafauna
Cervus elaphus	Red deer	Cervidae	*Cervus*	Forest-related
Megaloceros giganteus	Megaloceros	Cervidae	*Megaloceros*	Forest-related
Alces cf. alces	Moose	Cervidae	*Alces*	Forest-related

Capreolus pygargus	Siberian roe deer	Cervidae	*Capreolus*	Forest-related
Rangifer tarandus	Reindeer	Cervidae	*Rangifer*	Forest-related
Bison priscus	Steppe bison	Bovidae	*Bison*	Step-related
Poëphagus mutus baicalensis	Wild yak	Bovidae	*Bos*	Step-related
Saiga tatarica borealis	Saiga antelope	Bovidae	*Saiga*	Step-related
Gazella guttursza/ Procapra Gutturosa	Mongolian gazelle	Bovidae	*Gazella*	Step-related
Capra sibirica	Siberian ibex	Bovidae	*Capra*	Rocky-related
Ovis ammon	Argali	Bovidae	*Ovis*	Rocky-related
Capra / Ovis	Goat / sheep species	Bovidae	*Capra*	Rocky-related
Spirocerus kiakhtensis	Screw-horned antelope	Bovidae	*Spirocerus*	Rocky-related
Pisces	Fish species			
Amphibia	Amphibian species			
Aves	Bird species			

In the East Chamber of Denisova Cave, steppe species dominated during the formation of Layers 9 to 13, accounting for 62.8% to 68.2% of the faunal remains, while forest species made up a minimal share of 5.2% to 7.5%. The percentages of forest-steppe and rocky biotope species varied slightly, ranging from 9.6% to 16.3% and 14.0% to 18.8%, respectively. In Layers 14 and 15, there was an increased presence of forest and forest-steppe species, primarily due to a notable rise in the remains of roe deer, red deer, and, to a lesser extent, brown bears. Conversely, the number of steppe species, including two horse species, bison, woolly rhinoceros, dzeren, Mongolian gazelle, and saiga antelope, declined significantly (Vasiliev et al. 2013; 2017).

Brown et al. (2021) highlight that 20% of the morphologically analysed bone fragments are identified as predator species. The variation in predator species across different layers remains consistent in Layers 9 to 13, with cave hyena (*Crocuta crocuta spelaea*) being the dominant predator. In Layers 13 to 17, Canidae emerged as the primary predator (Jacobs et al. 2019).

The examination of megafaunal remains allows researchers to trace changes in the natural environment during the sedimentation of cave deposits. The proportions of species associated with different biotope groups—steppe, forest-steppe, forest, and rocky—shift due to climatic variations. Each faunal species has a specific environmental range determined by factors such as temperature, water availability, and food resources.

These changes in the proportions of animal species serve as indicators for reconstructing climatic conditions during the Pleistocene.

Understanding which animals inhabited the surrounding area and when they were present is particularly important. Since caves are not easily accessible or preferred by most animals, the presence of specific animal taxa in archaeological deposits suggests either their occasion due to predators or human hunting activities. This information provides insights into hominin occupation patterns and living conditions.

Faunal remains also serve as indicators of hominin occupation. For example, the decline in bat remains during periods of human habitation is attributed to the use of fire by hominins (Agadjanian et al. 2019).

In the Altai region, animal migration patterns have significantly influenced human settlement and occupation. Seasonal migrations of large herbivores, such as reindeer and other ungulates, directly impacted resource availability for ancient human populations. Archaeological evidence from various sites in the region, including Gorno-Altai and surrounding areas, demonstrates that human activities were closely linked to these animal movements, influencing both hunting strategies and settlement locations (Agatova et al. 2016; Kuzmin et al. 2021).

The archaeological record in this mountainous region indicates that prehistoric and early historical human groups adapted their settlement patterns to align with the seasonal availability of migratory animals. For instance, sites featuring remains of hunting tools and animal bones suggest that people followed these herds to exploit seasonal hunting opportunities, as observed in studies conducted in the Southern Altai (Agatova et al. 2016; Kuzmin et al. 2021).

Moreover, evidence from burial constructions and petroglyphs indicates that human occupation in the area is often concentrated around key migratory routes (Chlachula 2019).
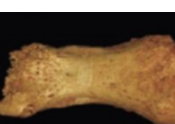
This dynamic interaction between environmental changes, animal behaviour, and human adaptation provides valuable insights into the broader ecological and cultural context of the region. It illustrates the complex relationships between early human populations and their environment, highlighting the importance of animal occupation in shaping human settlement patterns and subsistence strategies in the Altai region during prehistoric times. Leading to a closer look into the living conditions of the previous *H. sapiens* and their next relatives.
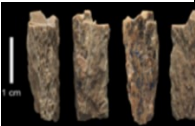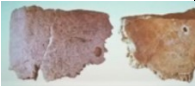
Homini fossils

The fossil record of Denisova is unique on a global scale and the site remains the only locus occupied by at least three distinct human groups. Neanderthals, Denisovans, and modern humans had all at one point taken residence in Denisova Cave. On several occasions, these groups interacted with each other and exchanged genetic material, as clearly evidenced by Denisova 11 (Slon et al. 2018), a female individual with a Neanderthal father and a Denisovan mother.

Seventeen hominin remains have been found and published from the site, discovered through morphological and biomolecular methods.

Table 3: Bone remains identified as hominin from Denisova Cave (data from Brown et al. 2021; Douka et al. 2019; Peyrégne et al. 2024)

Fossil ID	Excavation Date	Chamber & Layer	Age (ka)	Description / Identification
Denisova 2	1984	Main Chamber Layer 22.1	122.7 – 194.4	Second molar, deciduous of a female Denisovan
Denisova 3	2008	East Chamber Layer 11.2	51.6 – 76.2	Female proximal epiphysis of a distal manual phalanx, of a female Denisovan juvenile
Denisova 4	2000	South Chamber Layer 11.1	84,1 – 55,2	Maxilla molar of a male Denisovan individual
Denisova 5	2010	East Chamber Layer 11.4	90,9 – 130	Proximal pedal phalanx, known as "The Altai" Neanderthal
Denisova 6	2010	East Chamber Layer 11.4	91,2 – 130,3	Deciduous tooth, second left mandibular of a *Homo sapiens*

Denisova 8	2010	East Chamber

Interface between Layer 11.4 and 12 | 136,4 – 105,6 | Left maxillary molar, most likely the third one, of a male Denisovan individual |
| Denisova 9 | 2011 | East Chamber

Layer 12.3 | 119,1 – 147,3 | Distal manual phalanx of a male Neanderthal |
| Denisova 11 | 2012 | East Chamber

Layer 12.3 | 79,3 – 118,1 | Denisova-Neanderthal hybrid, also referred to as "Denny" |
| Denisova 13 | 2016 | South Chamber

Layer 22 | *Not dated* | Hominin.
Pair of conjoining posterior parietal fragments |
| Denisova 14 | 2012 | East Chamber

Layer 9.3 | 45,9 – 50 | Bone fragment from a *Homo* sp. |
| Denisova 15 | 2012 | East Chamber

Layer 11.4 | 91,4 – 130,3 | Neanderthal, bone fragment |
| Denisova 16 | 2016 | Main Chamber

Layer 9.1 | *Not dated* | *Homo* sp. bone fragment |
| Denisova 17 | 2021 | East Chamber

Layer 12 | *Not dated* | Neanderthal bone fragment |
| Denisova 18 | 2021 | East Chamber

Layer 15 | | *Homo* sp. bone fragment. aDNA analyses were insufficient for further specialisation |

Denisova 19	2021	East Chamber Layer 15	217 – 187	Denisovan bone fragment
Denisova 20	2021	East Chamber Layer 15	217 – 187	Denisovan bone fragment
Denisova 21	2021	East Chamber Layer 15	217 – 187	Denisovan bone fragment

The hominin remains, like most of the bones found at Denisova Cave, are highly fragmented and therefore hard to find and identify.

Several methods can be employed to formalize the identification of bones (whether of human or animal origin).

Methods of Zooarchaeology

As previously discussed, the taxonomic distribution of archaeofauna provides valuable information about the local environment and human hunting preferences, making it highly relevant to this research. Zooarchaeology, a field developed over several decades, has given rise to numerous methodologies. In this section, I will elaborate on some of these methods.

I.   Traditional Zooarchaeology

Traditional zooarchaeological methods rely on the morphological identification of bones, and often proceed in two steps: a categorisation into elements, and then, if possible, into body size classes or even better into taxa (Lyman 2002; Morin et al. 2017). This approach involves identifying species based on unique diagnostic characteristics. For several years, this has been the dominant method for identifying bone fragments at Denisova Cave (Vasiliev et al. 2017; 2013).

Species identification is frequently employed to gather information about the presence and prevalence of specific species at a given site, quantified through the NISP (Number

of Identified Specimens). However, as bones are often fragmented, each piece does not necessarily represent a distinct individual; multiple fragments may belong to the same animal (Morin et al. 2017). This limitation led to the development of a more precise quantification method: the MNI (Minimum Number of Individuals). MNI represents the lowest possible number of individual animals that could account for all identified bones in an assemblage (Lambacher et al. 2016; White 1953). To calculate MNI, bone fragments are first identified by species and then separated into left and right elements. The most abundant bone elements are then counted, with the highest number determining the MNI. Beyond species identification, morphological analysis of bones also provides valuable insights into hunting methods, butchery practices, mastication patterns, and evidence of craftsmanship (Agam & Barkai 2018; Shipman & Rose 1983).

Unfortunately, degradation and fragmentation caused by human or animal manipulation, compression, and weathering make it difficult to distinguish between different species (Morin et al. 2017; Brown et al. 2021). Most of the fragmentation is attributed to predatory actions, considering that the hominin and herbivore remains found are comparable in size.

II.   Biomolecular methods

One of the most well-known biomolecular methods for analysing bone fragments is ancient DNA (aDNA) analysis. aDNA is extracted from bone fragments, teeth or other organic tissues found at excavations. The aDNA is purified, amplified, sequenced, and compared with reference DNA from known species (Orlando et al. 2021). Genetic studies can be used to explore relationships between populations and their migration and colonisation tracks. When variation in one species is studied, mostly mitochondrial DNA (mtDNA) is used because it is extensively present in multiple copies within each cell, making it more likely to persist than nuclear DNA. Furthermore, mtDNA is much smaller than the nuclear genome and lacks a repair mechanism, leading to a higher mutation rate. This results in species-specific coded genes that are useful for species identification (Kowalczyk 2021). aDNA analyses can be used not only to identify species but also to determine relationships between two species or even within a single species (Kowalczyk 2021). Unfortunately, this method is often not feasible due to poor bone preservation and the high costs associated with sequencing. In such cases, protein sequencing is frequently employed as an alternative.

Proteins found in a bone can also be used as an identification method (Warinner et al. 2021; Hendy et al. 2018). Proteins are composed of peptides, themselves a composition of amino acids (AA) , with 20 different AA forming chains. The combination of different peptides creates different proteins. These peptides are identified often using liquid chromatography and mass spectrometry (LC-MS/MS). The outcome of this method is the exact amino acid sequence of the analysed peptide. This method enables the determination of novel protein sequences from extinct organisms, thereby allowing comparisons of evolutionary relationships between organisms. Unfortunately, this method is quite expensive and is therefore mainly used when the amino acid sequences or the information gained are crucial for the research question (Welker 2018; Hendy 2021).

Zooarchaeology by Mass Spectrometry

Zooarchaeology by Mass Spectrometry (or ZooMS) is a palaeoproteomics method developed about 15 years ago (Buckley et al. 2009; Buckley et al. 2014). The method has seen a large uptake in the past few years and a considerable number of publications produced (for a review see Richter et al. 2022).

ZooMS utilises type I collagen, which is the most abundant collagen type in bone, comprising 80% of the bone's proteome. Collagen itself is one of the most common and persistent proteins found in bones. In vertebrates, type I collagen (COL1) consists of three chains: two identical alpha 1 (α1) chains and one more variable alpha 2 (α2) chain. The α2 chain is less constrained by the amount of proline in the chain, creating the possibility for species differentiation (Buckley 2017; Buckley et al. 2009).

These differences in the peptides lead to variations in the mass of the collagen protein. Through purification and digestion of the collagen into its peptide components, individual peptides can be analysed by a mass spectrometer. This process creates a species- or family-specific distribution of masses, visualised as peaks.

ZooMS is a cost-efficient method that allows for the generation of numerous results in a short amount of time, with a high success rate. It is the method best suited for addressing the research question of this thesis and was therefore chosen for this study. For this thesis, a specific MALDI-ToF (Matrix-Assisted Laser Desorption/Ionization Time-of-Flight) analysis was employed.

Matrix-assisted laser desorption/ionization time-of-flight mass spectrometry (MALDI-ToF-MS) is an established method for analysing collagen peptide mass spectra. In this process, samples are spotted onto a ground steel target plate, which is then inserted into a Bruker Autoflex maX LRF MALDI MS instrument. A smartbeam-II solid-state laser ionises the matrix on the plate, charging it to +1 and causing it to evaporate along with the peptides.

The time of flight (ToF) for each peptide varies based on its mass. An electromagnet in the ToF tube detects these peptides as they travel a consistent distance from the plate to the detector. Smaller peptides arrive at the detector earlier than larger ones, creating a unique mass spectrum for each sample spot. The results are then converted into mass-to-charge ratios (m/z) (Richter et al. 2022).

ZooMS analyses peptides with masses between 800-3500 Da, corresponding to peptide lengths of 8-30 amino acids. This range includes all peptides present in COL1. The MALDI-ToF generates a mass spectrum where specific mass-to-charge ratio (m/z) peaks correspond to a particular peptide fragment. A unique sequence of peaks characterises a specific taxonomic group, sometimes at the family, genus, or species level, thereby creating a distinct collagen peptide mass fingerprint for that taxon. While not all peaks are useful for taxonomic identification, those that are are termed marker peptides (Brown et al. 2021; Richter et al. 2022).

There are 12 marker peptides that can be used to identify the taxonomy of bone fragments (**P1**: COL1α1 508 – 519; **A**: COL1α2 978 – 990; **A´**: COL1α2 978 – 990; **B**: COL1α2 484 – 498; **C**: COL1α2 502 – 519; **P2**: COL1α2 292 – 309; **D**: COL1α2 793 – 816; **E**: COL1α2 454 – 483; **F**: COL1α1 586 – 618; **F´**: COL1α1 586 – 618; **G**: COL1α2 757 – 789; **G´**: COL1α2 757 – 789). Each peptide is associated with a specific range of possible masses. For the identification process, 9 of these 12 peptides are searched for in a specific order, as outlined in Brown (2021).

This order is based on the potential intensity of the peaks. Therefore, the first peptide is B: COL1α2 484 – 498, which has a mass ranging around 1400 m/z. The most common peaks for mammalian collagen are 1427.7 and 1453.7.
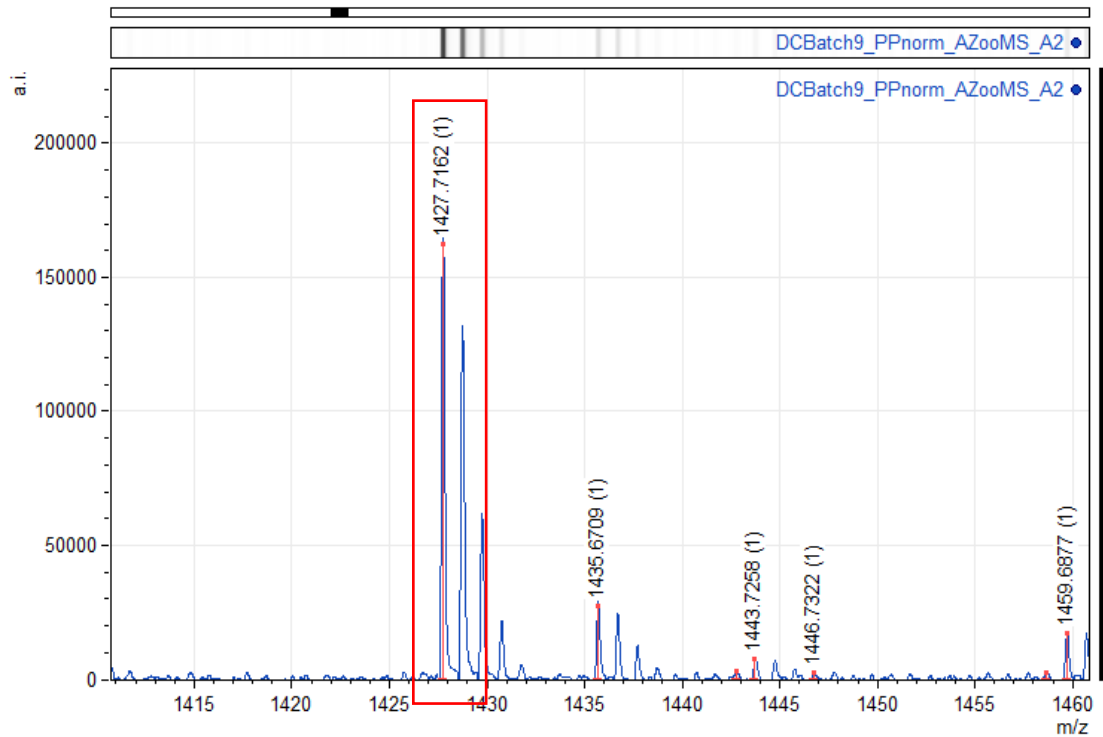
Figure 6: Peak for B: COL1α2 484 – 498 at m/z 1427.7, marked in red.

The identification continues with the D marker, COL1α2 793 – 816, which ranges around m/z 2100, with the most common peaks being 2115.1, 2131.1, and 2145.1 m/z. Marker C (COL1α2 502 – 519) is highly important for the differentiation between closely related species, but the preservation of this peptide is often poor. It ranges around 1500 m/z.
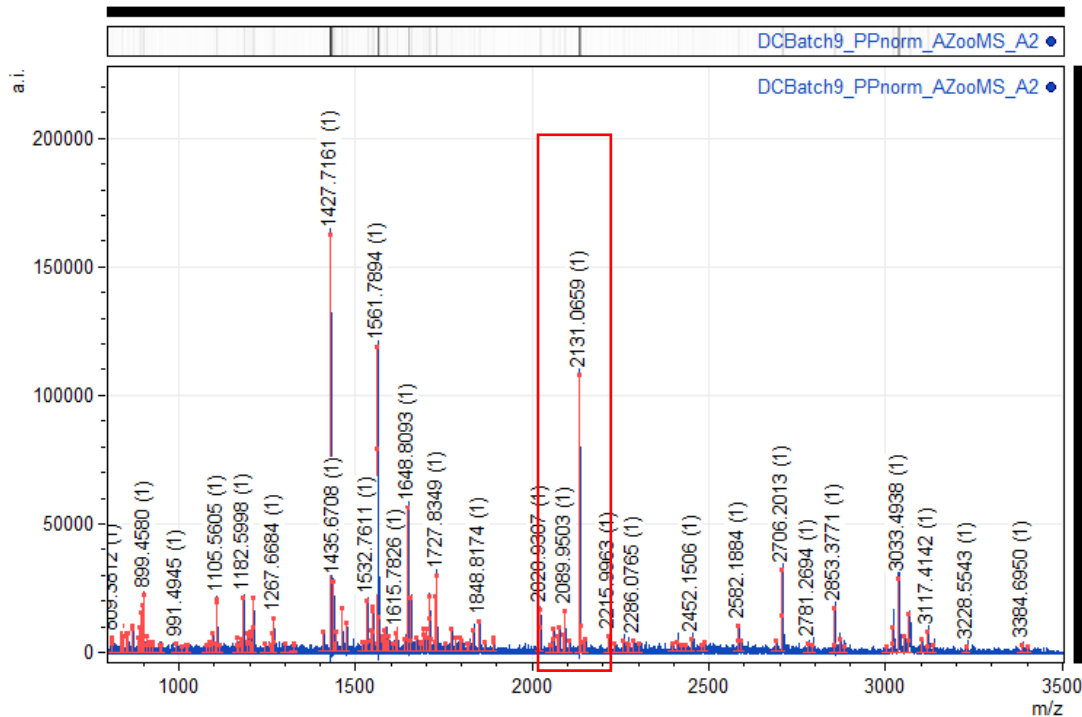
Figure 7: : Complete spectra of a Bos/Bison; Marker D is highlighted in red.

The peaks for further specification are oxidative pairs, meaning that the two markers COL1α2 978 – 990 (A) and COL1α2 978 – 990´ (A´) are 16 parts apart from each other. Both markers represent the same peptide; COL1α2 978 – 990 is the original peptide, while COL1α2 978 – 990´ represents the oxidated state. Both markers have a m/z ranging around 1100 – 1200, making distinguishing difficult. Therefore, these markers should always come in pairs; if the markers do not match, this could indicate high sample degradation or contamination. Considering this, the markers A and A' should be identified last.

COL1α2 757 – 789 (G) and COL1α2 757 – 789´ (G´) is another oxidative marker pair. This marker shows an m/z value that is not only specific for collagen but also for keratin (m/z=3017.1). Keratin is one of the most abundant structural proteins, mainly found in hair, fur, and skin, and is the most common lab contaminant. Therefore, contamination with keratin is highly possible, and for identifications, the marker at 3017.1 should not be used on its own without the matching G´ at m/z 3033.1.

Marker E (COL1α2 454 – 483) is the most vulnerable to collagen degradation, often leading to a complete loss of this marker. The low reliability of this marker makes it the last to assess.

Unfortunately, due to crosslinking, glycosylation, glycation, incomplete digestion, and poor ionisation, some of these peptide markers may not be visible or may give an unclear signal. Furthermore, sample contamination can create unexpected spectra. Matrix peaks and auto-digested trypsin peaks can also lead to misinterpretation of spectra. Matrix peaks are often found in a small m/z range; therefore, they overlap with small collagen peptides (smaller than 1000 Da). Based on this, the most reliable marker peptides are those found between 1000 and 3100 Da.

The most common change in peptide markers is deamidation, occurring through side chain hydrolysis or a condensation reaction, often seen in glutamine changing to glutamic acid and asparagine changing to aspartic acid. In any case, the m/z value increases by 1 Da based on the exchange of the amide with a carboxyl functional group.

The identification through peptide markers is often not decisive, as different animal species can share some markers. Therefore, a grouping of possible animal species is necessary. This means several species must be clustered into one group, known as "ZooMS taxon". These do not always correspond to Linnean taxonomic ranks, and several genera or families can be included under the same "ZooMS taxon".

Data analysis

The mass spectra were identified using QuickID, an in-house automated code developed by the Douka Lab. QuickID compares the markers present in a MALDI spectrum with a reference database of peptide markers and selects the most fitting taxon. The dataset contains several species, mostly mammals, which have been identified morphologically or genetically, and subsequently analysed with ZooMS to identify species-specific peaks. In recent years, the number of animals that can be characterised through this method has steadily increased, continually expanding the reference database for ZooMS analysis. The results were then manually verified using the open-source program mMass version 6.0.2 (created by Martin Strohalm 2005-13).

Stable Isotope Analysis

From Bones to Isotopes

Collagen is considered one of the most valuable proteins for archaeological science due to its remarkable stability, attributed to its tightly packed structure and the fact that it is the most common protein found in bones. This unique characteristic ensures excellent preservation, making collagen a valuable resource even in bones dating back over 1 million years. Collagen is not only used for ZooMS analyses but plays a significant role in other archaeological analyses, such as radiocarbon dating and stable isotopes. In 1990, the first stable isotope analyses on bone collagen from hominin remains were applied opening a scientific field that provides valuable insights into an individual's dietary preferences (Bocherens et al. 1991).

Isotopes are different forms of the same element, distinguished by the number of neutrons in the nuclei while maintaining a consistent number of protons. This variance in atomic mass dictates their position on the periodic table, with no impact on their chemical properties but a significant influence on their physical properties, like weight. An individual possesses a specific isotope signature, accrued through the utilisation and physiological processes. This creates a unique ratio of heavy and light isotopes, giving insights about the environment and trophy level of a species (Ben-David & Flaherty 2012).

Stable isotope analyses

Stable isotopes are broadly used in archaeology. The main stable isotopes analyses are on oxygen, strontium, carbon and nitrogen. The ratio of light and heavy stable isotopes contains information about the diet, the environment and the lifestyle of an individual as well as the age of a bone fragment. Information about migration patterns, the environmental conditions, ancient diets, social hierarchies and cultural rituals of ancient individuals can be generated by analysing organic materials like bones, hair and teeth. Heavy and light stable isotopes are ingested into the body of an individual through their diet, creating a specific stable isotope profile unique for every individual. This profile mirrors the stable isotope profile of the diet, allowing to recreate an ancient diet profile and the environmental conditions. For example, if the individual was mainly nourishing on terrestrial, fresh water or marine prey (Bocherens et al. 1991; Dawson et al. 2002).

Moreover, carbon isotope rations can reveal information about the types of plants the individuals where consuming due to different photosynthetic pathways of the plants. Two categories have been grouped, namely, C3 and C4 plants, that exhibit distinctive ^{13}C values (Smith & Epstein 1971). C4 plants, often adapted to hot and arid climates (Ben-David & Flaherty 2012) show higher C values and range between δ^{13}C: -15‰ to -11‰, whereas C3 plants range between δ^{13}C: -35‰ to -25‰ (Dawson et al. 2002; Marshall et al. 2007). Animals that consume these plants can be differentiated on the basis of their isotopic signal, providing invaluable insights into the environmental conditions of their respective habitats.

The ratio between N[15]/N[13]+N[14] has been used to estimate the trophic position of an organism for decades. The steps of the different isotopic positions were marked by a 3 ‰ border, creating a terrace-like pattern starting with the primary production (plants) and increasing through herbivore and omnivore species to the carnivores, expected to be the highest in the highest trophy-levels. Based on this, the trophic position can be calculated using the equation shown below. A species should cluster around a specific value depending on their dietary preferences, which refers to the trophic level of this species.

$$\text{trophic position} = \lambda + \frac{\delta^{15}N_{\text{secondary consumer}} - \delta^{15}N_{\text{base}}}{\Delta_n}$$

where, λ is the trophic level δ^{15}N Base is referring to (usually λ = 1, for the primary producer (plants)); Δn is the trophic discrimination (usually 3.4 ‰)

Due to the turnover of bones, the stable isotope values of the collagen only reflect the last 5 to 10 years of an individual's life, and its composition is directly determined by the diet of the individual (Hedges et al. 2004).

Materials and Methods

Zooarchaeology by Mass Spectrometry

In this thesis, I analysed 647 bone fragments excavated from the East Chamber of Denisova Cave in 2012 and 2013. These morphologically nonidentifiable bones were collected from Layers 13 and 14 and were brought to the University of Vienna for palaeoproteomic analyses.

Wet lab preparation

1. Weighing samples

All 647 samples were cleaned with compressed air and aluminium oxide powder. Between 20 – 40 mg of bone was sampled by drilling or clipping. The sampled bone chip was transferred into 1,5 ml tubes, and the leftover bone to a plastic bag, and both were labelled with a unique identification number (DC 15294 – DC 15941), see in the appendix.

2. Acid demineralisation

Each bone chip was demineralised in 500 µL of 0.6M hydrochloric acid (HCl) for 1 – 2 days at room temperature. The duration of the demineralisation depended on the bone's density, texture, preservation, and size. As the bones demineralise, textural changes become visible. For the bones that demineralised faster, the process was stopped, and samples were washed and stored in the refrigerator.

3. Washing

Following demineralisation, the bone chips were washed with 200 µL of ammonium bicarbonate buffer (AmBic) with a concentration of 50 mM, to neutral pH. The solution was vortexed and centrifuged, the supernatant was discarded, and the process was repeated a second time.

4. Gelatinisation

The collagen was then gelatinised in 100 µL of AmBic 50 mM and incubated for 1 hour at 65°C. This process dissolves the collagen in AmBic and unravels the collagen alpha chains, while retaining their long-form structure, through the swelling and dissolution of intermolecular collagen bonds. After gelatinisation, 50 µL of the supernatant was transferred from the tube in two micro-well plates, labelled "Extract" and "Second Extract". The second extract was stored in the freezer for further analyses.

5. Trypsin digestion

50µL of the gelatine ("Extract") underwent enzymatic digestion with 5 µL of trypsin for 18 hours at 37°C. Trypsin cleaves the C-terminal peptide bonds of lysine and arginine, leading to different peptide lengths and weights specific to the taxon. The digestion was stopped with trifluoroacetic acid (TFA).

6. Peptide extraction

To clean, desalt and concentrate the peptides, C18 filter pipette tips called ZipTips (ThermoFisher Scientific) were used, to which the purified peptides bind. After the activation of the ZipTips, by rinsing them twice with conditioning solution, consisting of

50% MilliQ water, 50% acetonitrile and 0.1% TFA and afterwards twice with washing solution, consisting of 100% MilliQ water and 0.1% TFA, the sample is loaded into the ZipTip. The sample was resuspended back and forth over the tips five to ten times. This step fills the C18 filter in the tips with the peptides while removing other contaminants. To remove non-necessary organic material, the tips were rinsed two times with 100 µL of washing solution. Finally, the sample was eluted using conditioning solution.

7. *Spotting on MALDI plate*

The purified and digested peptides were spotted on a MALDI ground steel plate alongside a matrix of α-cyano-4-hydroxycinamic acid (CHCA), and were left to crystalise. Peptide calibrant spots were also spotted on the plate. The spotted plates were left to dry prior to mass spectrometric analyses.

8. *Mass spectrometric analyses*

Once dried, the spotted plates are inserted in an in-house (Bruker Autoflex maX LRF) MALDI-ToF mass spectrometer, at the Department of Evolutionary Anthropology (Douka Lab) for measurement. Each sample is measured in triplicate.

Stable Isotopes

Bone samples from Layers 13, 14, 15, and 17 of the East Chamber were selected for stable isotope analyses (C and N). The selected bones represent various groups, including *Bos/Bison, Elephantidae, Canidae, Equidae*, and *Felidae*.

Layer 17 posed a unique challenge, as it is archaeologically sterile with limited collagen preservation. Consequently, finding enough bones within the appropriate species group proved challenging.

The selected bones were clipped into small bone chips, ranging from 150 to 200 mg, depending on their initial size.

Collagen extraction for stable isotopes

The stable isotope analysis is based on the "acid-base-acid" method developed by Longin in 1971 formally for radiocarbon dating. The bones underwent demineralisation in 0.6 M HCl until the bone mineral was completely dissolved. The demineralisation process itself could lead to damage or loss of collagen, creating the necessity for a less destructive procedure. For very old bone fragments, such as those found in Layer 17, a

more diluted HCl solution was used (0.3 M HCl) which slowed down the demineralisation process. Additionally, the samples and reagents were stored in the fridge during the demineralisation process, which further slows down the process.

The reaction was considered completed when no CO_2 evaporated out of the bone anymore. Demineralised bones tend to be transparent, with a spongy texture. The acid was removed, and the bone was washed with MilliQ water three times. Subsequently, the samples underwent base treatment, in which a weak NaOH solution was used to remove humic acid contamination from the collagen. However, basic solutions can also be harmful to the collagen structure, leading to decreased collagen yield (Chisholm et al. 1983; Liden et al. 1995; Szpak et al. 2017). Therefore, this step was excluded for samples expected to have poor collagen preservation. Samples excluded from the base treatment will be marked with an asterisk in the supplementary. Samples washed with NaOH solution were washed with MilliQ water afterwards three times.

The washed collagen was then gelatinised through incubation in pH3 MilliQ H_2O at 65°C for 16 hours. This process causes the helical structure of collagen molecules to disintegrate into a random coil organisation, induced by the cleavage of hydrogen bonds and cross-linking between them (Chen et al. 2014). After gelatinisation, the solution consists of a mixture of gelatinised collagen and other non-collagenous proteins, and other insoluble residues. Through an Ezee-filter step, all inorganic material or other aggregates larger than ~60-80 μm are filtered down, and the process can continue with a purified collagen (gelatine) solution.

The gelatine was frozen overnight and subsequently lyophilised in a freeze-dryer for 48 hours. After this, the collagen had a white, cotton-like texture and was weighed into small tin cups which were combusted in an Isotope Ratio Mass Spectrometer. Combusted at over 1000°C the gelatine is converted into gas, which is then ionised and directed into an evacuated flight tube, were strong magnets deflect and separate the gas according to its mass. At the end of the flight, the molecules fly against a Faraday collector, creating a weak electrical signal which is measured and converted into the isotopic ratios (Ben-David & Flaherty 2012). An international standard is also measured at the same time to enable direct comparisons with results from other labs.

Stable isotope measurement
$\delta^{13}C$ and $\delta^{15}N$ measurements were conducted in two different laboratories. The Max-Plank-Institute of Geoanthropology in Jena and the SILVER Lab facility at the University of Vienna. The Max Plank laboratory uses a Thermo Scientific Flash 2000 Elemental Analyser coupled to a Thermo Delta V advantage mass spectrometer. The SILVER Lab

is equipped with three continuous-flow isotope ratio mass spectrometers which are interfaced with an elemental analyser.

The wet lab preparation was done in the Laboratory of the University of Vienna (Douka Lab). Minor differences observed in the results between the two facilities are consistent and probably caused by a different calibration of the systems. For the comparison between these measurements, the results have been averaged.

Results

Zooarchaeology by Mass Spectrometry

Layer 14

247 bones from Layer 14 were analysed, of which 227 samples were assigned to a taxonomic group (91% success rate). Only 20 samples could not be identified, 8 were classified as unknown (3%) and 12 (5%) as failed (Figure 8).
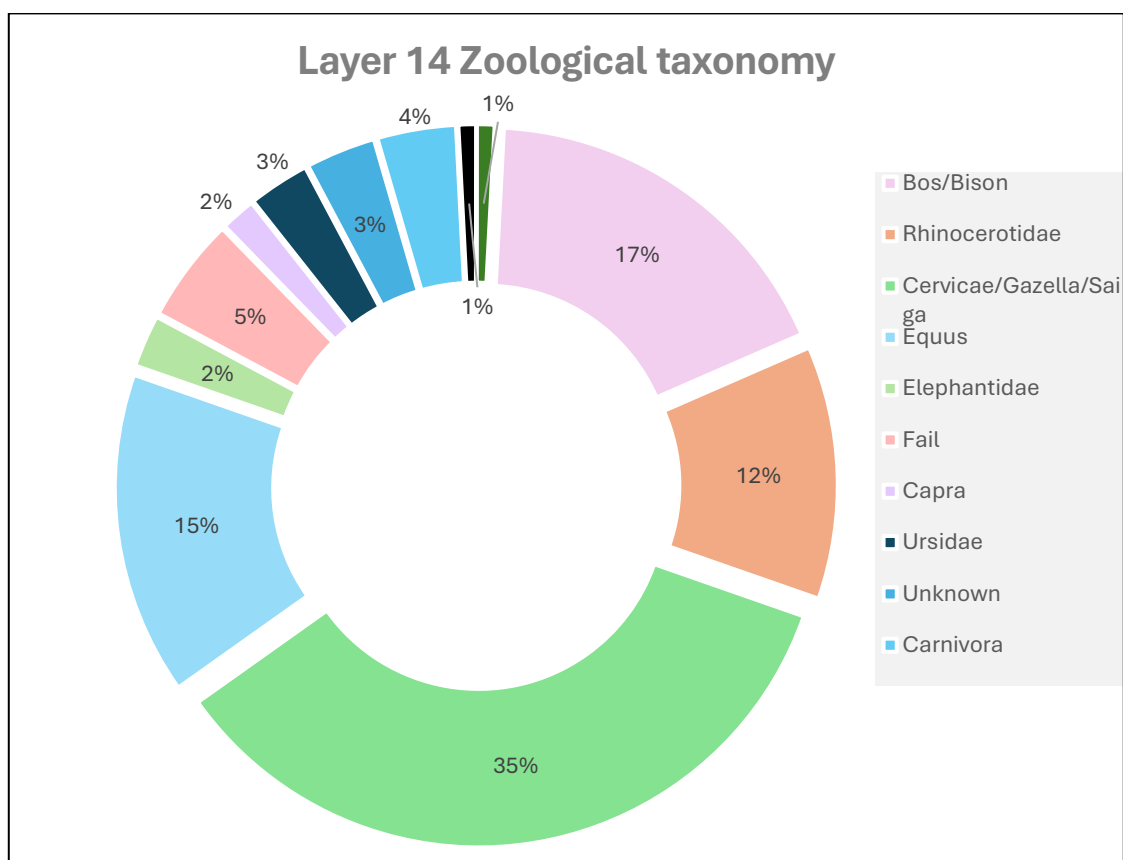
Figure 8: Taxonomic distribution (in percentage) of ZooMS-analysed bone fragments from Layer 14, East Chamber of Denisova Cave.

Of all these identified samples, 17% were identified as Bos/Bison, 12% as Rhinocerotidae, 35% as Cervicae/Gazella/Saiga, while 15% were *Equus* sp. Other taxa were rarer, and these included: Elephantidae (2%), Capra (3%), Ursidae (3%), Carnivora (4%), Ovis (1%). In addition, 2 Hominidae (1%) were also identified in this layer. (Figure 8; Table 4)

The hominin samples (DC 15833; hereafter, DC 33 and DC 15891; hereafter DC 35) (Figure 10) preserved the specific peptide marker used in the identification of Hominidae, marker B (COL1α2 484 – 498) at m/z 1477.7, alongside other peptide markers.

Undergoing aDNA analyses, performed at the Max-Plank-Institute for Evolutionary Anthropology in Leipzig, revealed Denisovan mtDNA for both samples (preliminary data; Janet Kelso, *pers. comm*).

Figure 9: DC 15833, or DC 33, a hominin bone fragment from Layer 14 of the East Chamber, Denisova Cave

Figure 10: DC 15891, or DC 35, a hominin bone fragment from Layer 14 of the East Chamber, Denisova Cave.

Layer 13

400 samples were analysed from Layer 13. Of these, 374 were identified successfully (94% success rate). Only 26 samples could not be identified; of these, 22 were unknown (5%), and 4 samples failed to yield collagen (1%). The largest group was Bos/Bison (31%), followed by Cervidae/Gazella/Saiga (23%), Rhinocerotidae (13%), Equus (9%), Carnivora (5%), Capra (3%) and about 1% are identified as Ursus (Figure 11; Table 4).

Table 4: NISP and Percentage of ZooMS-Taxonomies found in the different Layers.

ZooMS Taxon	Layer 13 (NISP)	Layer 13 (%)	Layer 14 (NISP)	Layer 14 (%)	Both Layers (NISP)	Both Layers %
Carnivora	21	6%	9	4%	30	5%
Cervidae/Gazella/Saiga	91	24%	85	38%	176	29%
Bos/Bison	124	33%	43	19%	167	28%
Rhinocerotidae	53	14%	29	13%	82	14%
Equus	37	10%	37	17%	74	12%
Elephantidae	35	9%	6	3%	41	7%
Capra/Ovis	12	3%	6	3%	18	3%
Ursidae	2	1%	7	3%	9	2%
Hominidae	0	0%	2	1%	2	0.3%
Total	**375**		**224**		**599**	
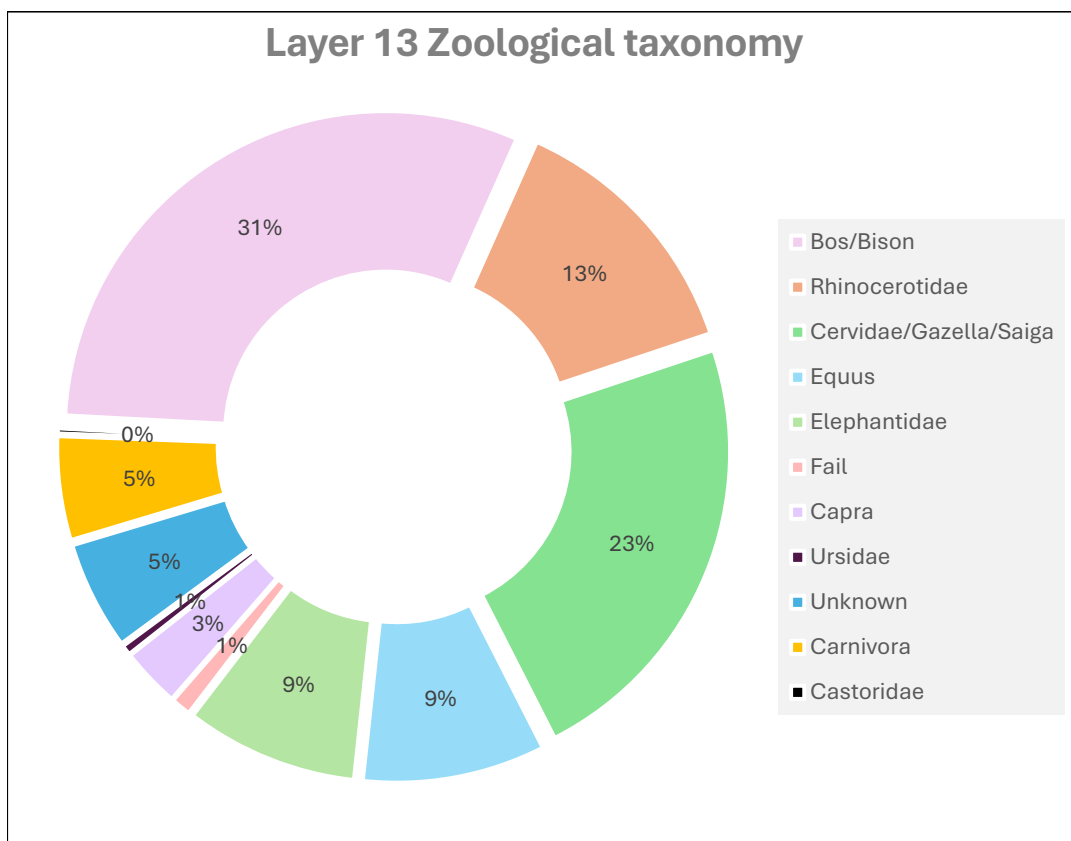
Figure 11: Taxonomic distribution (in percentage) of ZooMS-analysed bone fragments from Layer 13, East Chamber of Denisova Cave.

Stable Isotopes

In total, 116 bone fragments from four different layers of the East Chamber of Denisova Cave were selected and pretreated for stable isotope analyses (C and N). Of these, only 76 samples produced enough collagen (see Appendix Tablle 2a). These came from Layer 13 (n=23), Layer 14 (n=24), Layer 15 (n=20), and Layer 17 (n=9). For Layers 13, 14 and 15 a variety of bones from different animal species have been selected to create a range of fragments mirroring a broad spectrum of trophic levels. Layer 17 represents the smallest sample number and a selection of animals inconsistent with the other layers.

Table 5: Number of bone fragments of different species analysed for stable isotopes, per Layer.

Taxon	Layer 13	Layer 14	Layer 15	Layer 17
Bos/Bison	5	4	5	0
Canidae	5	5	6	0
Elephantidae	3	4	4	0
Equidae	5	3	5	1
Panthera/Crocuta	2	4	0	0
Panthera/Crocuta/ Mustelidae	3	0	0	0
Capra	0	0	0	1
Cervidae/Gazella/Saiga	0	0	0	1
Felidae/Ursidae	0	0	0	1
Ursidae	0	0	0	4
Vulpes vulpes	0	0	0	1
Hominidae	0	4	0	0
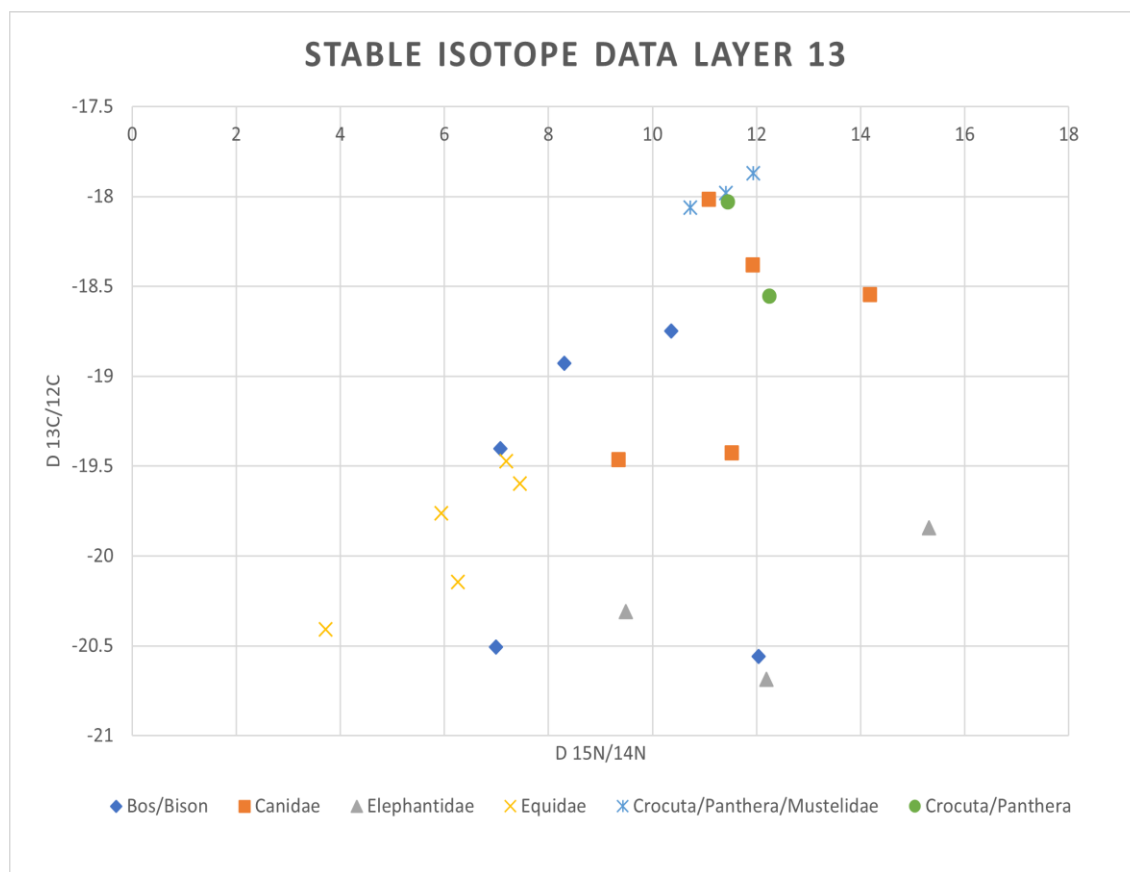
Figure 12: Stable isotope data for analysed bones of Layer 13.

Four hominin bones, all from Layer 14 of the East Chamber were also analysed. DC28 (*ZooMS ID: DC 13142*) and DC35 (*ZooMS ID: DC 15891*), are previously discovered but unpublished hominins from the same layer and year of excavation (2012-13), as DC33 and DC34 were discovered during this dissertation.
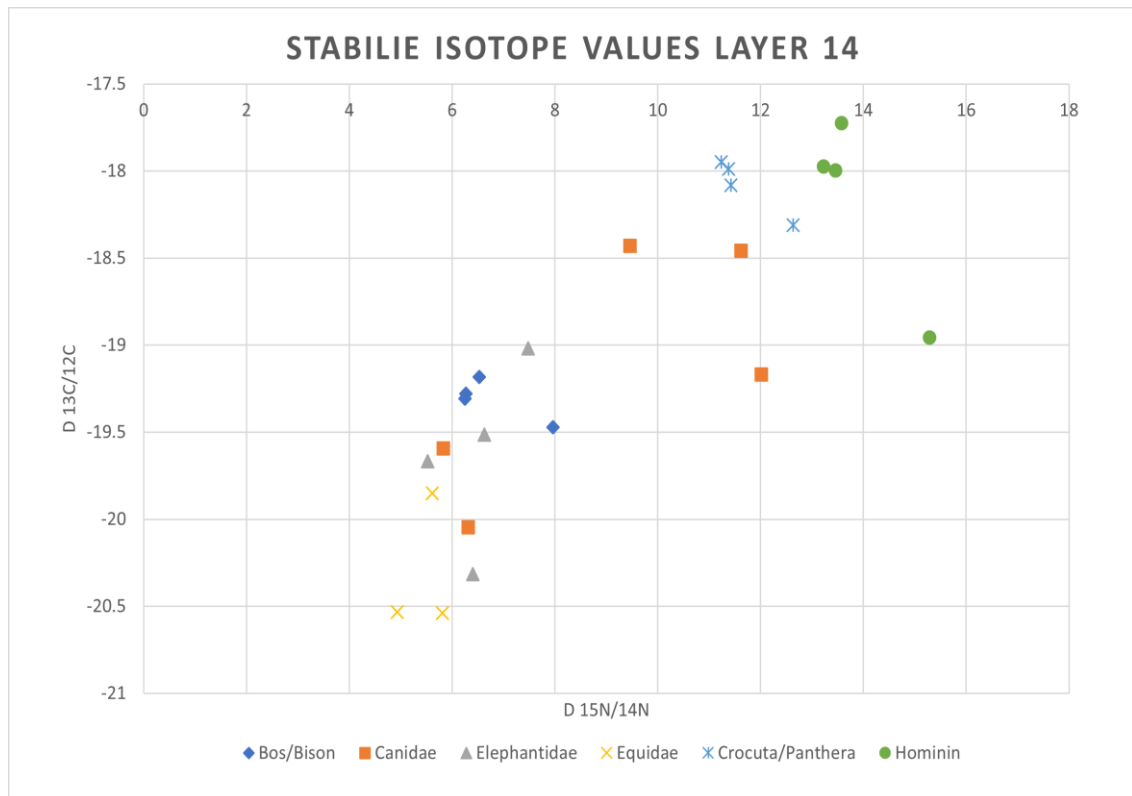
Figure 13: Stable isotope data for analysed bones of Layer 14.

The stable isotope results show interesting patterns. Starting with the hominins (DC28, DC33, DC34, DC35) their values range between $\delta^{13}C$ – 17.73 to – 18.96 ‰ and their $\delta^{15}N$ range between 13.23 – 15,.0 ‰. Their variation is overall low, no greater than 2 ‰ for ^{15}N and 1 ‰ for ^{13}C. Interestingly, DC34, DC33, DC35 group together while DC28 shows higher $\delta^{15}N$ and lower $\delta^{13}C$ values (Figure 13).
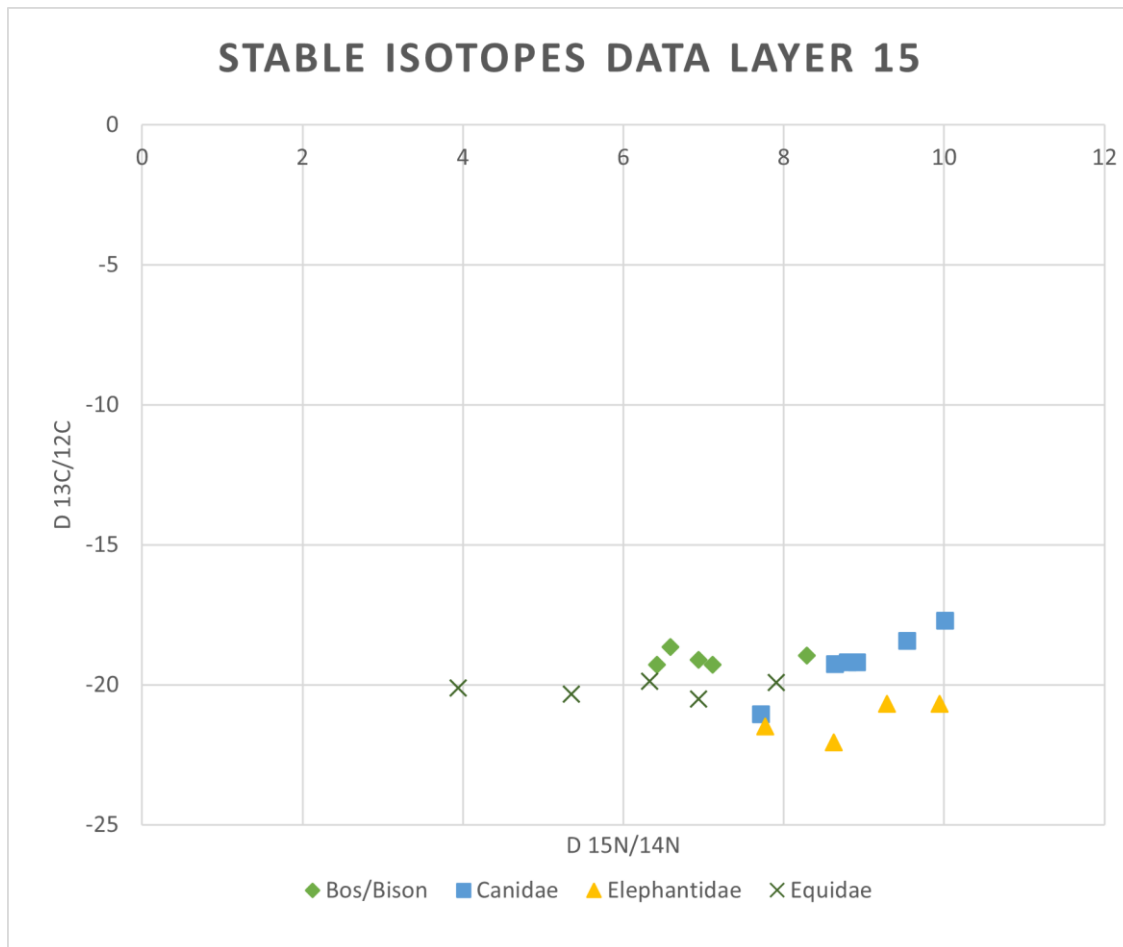
Figure 14: Stable isotope data for analysed bones of Layer 15.

Carnivores fall into two ZooMS taxa: Panthera/Crocuta or Panthera/Crocuta/Mustelidae ($\delta^{15}N_{aver}$=11.61 ‰) and Canidae ($\delta^{15}N_{aver}$=9.82 ‰). As expected, they show higher $\delta^{15}N$ values than herbivore and omnivore taxa, with hominins ($\delta^{15}N_{aver}$=13.89 ‰) showing higher values. Their $\delta^{13}C$ values are variable and do not significantly differ from other taxa analysed, although Felidae $\delta^{13}C$ values range between -18.55 and – 17.87 ‰. The Canidae do not stand out from other taxa in their $\delta^{13}C$ values. with an average $\delta^{13}C$ values of -19.03 ‰, and ranges between -21.07 to -17.72 ‰.

The herbivores analysed here (Bos/Bison, Equidae, Capra, Elephantidae, Cervidae/Gazella/Saiga), show a great range in δ^{15}N values, and overlap with each other. Clustering between different taxa was visible for Equidae (*Equus hydruntinus, Equus ovodovi, Equus ferus*). Equid δ^{15}N values range between 3.72 to 7.91 ‰ (δ^{15}N$_{aver}$=5.86 ‰), and δ^{13}C values between -20.54 and -19.47 ‰ (δ^{13}C$_{aver}$=-20.11 ‰).
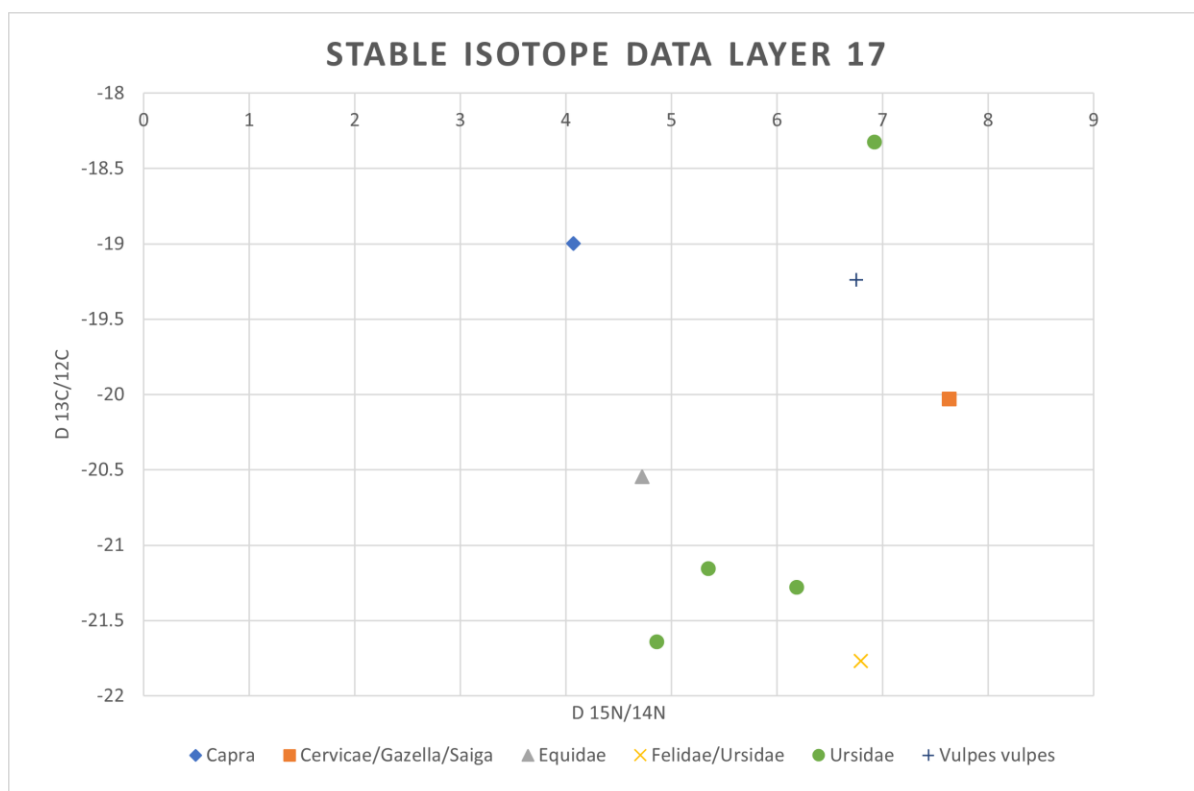
Figure 15: Stable isotope data for analysed bones of Layer 17.

The remaining herbivore species show more widespread δ^{15}N values. Bos/Bison for example have an average δ^{15}N value of 7.62 ‰, ranging from 6.25 to 12.04 ‰, and therefore overlap with almost all other taxa analysed. The δ^{13}C values too are comparable to the ones generated for other taxa.

Similar variation can be observed for the Elephantidae (woolly mammoth), showing an average δ^{15}N value of 8.97 ‰ but distributed in an extremely high range of 5.52 to 15.31 ‰.

For Layer 17, only single bone fragments contain enough collagen to be analysed, representing only one taxonomy. Leading to a single stable isotope value for a Capra bone fragment (δ^{15}N = 4.07 ‰; δ^{13}C = -18.99 ‰), a fragment identified as Cervidae/Gazella/Saiga with a δ^{15}N value of 7.63 ‰ and a δ^{13}C value of -20.04 ‰, a δ^{15}N value of 6.79 ‰ and a δ^{13}C value of -21.77 ‰ for a bone fragment identified as Felidae/Ursidae.

When the data is compared based on layers (which naturally correspond to specific paleoenvironmental conditions), some taxa demonstrate clearer clustering (for example the hominins in Layer 14; Fig. 15). Nevertheless, a clear separation of taxa based on their stable isotope levels is not possible.

Discussion

ZooMS analyses

As described above, environmental changes have a huge impact on the living conditions and food resources of the inhabitants of a certain habitat. Ecological niches must fit the individual needs of a species. Rapid changes in the environment can lead to extinction if the species has no opportunity to adapt properly. Likewise, populations tend to migrate to areas that suit their needs more.

This study focused on the analyses of bone fragments from Layer 13 and Layer 14 of the East Chamber of Denisova Cave. Layer 13 in particular has not been analysed before using ZooMS (only 25 such identifications existed) and is classified as archaeologically semi-sterile based on the absence of an archaeological assemblage. The climatic conditions change strongly between the two analysed layers, showing a rather warm and humid pattern in the beginning of the timeframe in which Layer 14 accumulated (around 187 – 193 ka) (Bolikhovskaya et al. 2015; 2014; Jacobs et al. 2019), whereas colder and more arid conditions prevailed during the accumulation of Layer 13.

These changes are reflected in the distribution of different fauna taxa discovered macroscopically (Vasiliev et al. 2017) and in our new ZooMS data. For example, in Layer 13 a higher amount of steppe animals (like Bos/Bison) could be seen, while in Layer 14 forest species were higher in number (like Cervidae, Gazella, Saiga). This is also seen in the data of Vasiliev et al. (2017) where a four-fold increase of deer species was observed between Layer 14 and Layer 13. This is consistent with a change from interglacial (warmer) to glacial (cooler) conditions.

An increase of large sized animals is observed in Layer 13, as seen in the higher number of Rhinocerotidae (woolly rhino) and Elephantidae (woolly mammoth), species that prefer open landscapes such as those forming during glacial periods (Vasiliev S.K. et al. 2017). Surprisingly, other than in the analysed data for this thesis, no major changes for Equus between those two layers were observed, neither in the external analysed ZooMS data (see Figure 17) (Brown et al. 2021) nor in the morphology-based fauna data (Bolikhovskaya & Shunkov 2014; Vasiliev et al. 2017).

To place the new ZooMS results in context, I compare the newly generated data with a large dataset of ZooMS published by Brown et al. (2021). Both studies show a similar change in the distribution of the taxas as mentioned earlier, between Layers 13 and 14, with a decrease in animals adapted to forest habitats like deer (included in the ZooMS categories of Cervidae/Gazella/Saiga) and an increase in steppe-adapted animals like Bos/Bison from Layer 13 to Layer 14.
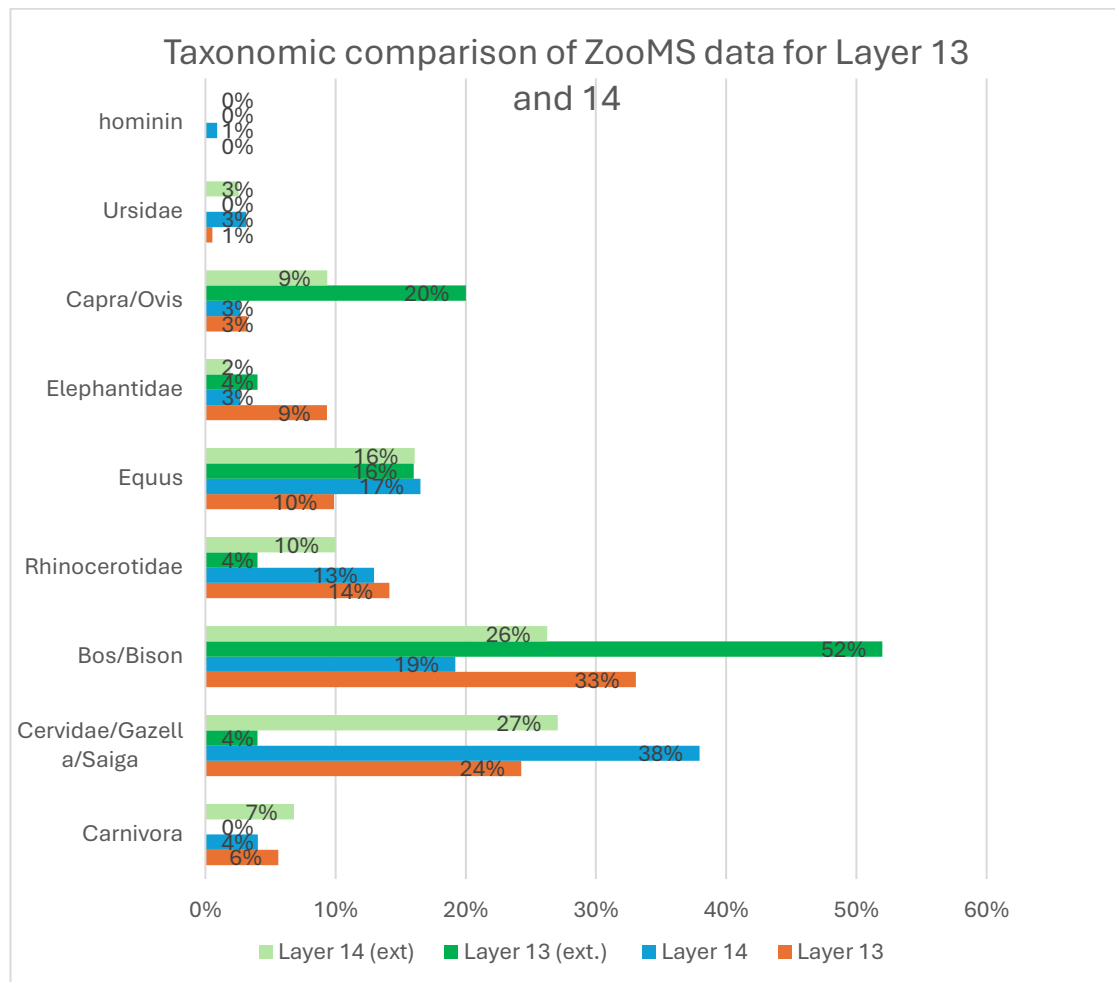
Figure 16: Comparison of external and internal generated ZooMS Data of Layer 13 and 14

Brown et al. (2021) show a decrease in carnivores from Layer 14 to Layer 13 but overall, no significant change of predator remains throughout the layers.

This contrasts the findings from this thesis, as well as the data from Vasiliev et al. (2017), since both studies show an increase of carnivores from Layer 14 to 13, linked to a continuous use of Denisova Cave as a resort for predator species. Especially cave hyena is believed to be an almost steady occupant of the cave, while the occupation and usage of the spaces by hominin groups is believed to be rather irregular as also shown by the distribution of human DNA in the sediment (Zavala et al. 2021). Co-habitation is nearly impossible (Morley et al. 2019). However, it is possible that the short hominin occupation episodes were beneficial for scavenging animals like the cave hyena. Morley et al. (2019) suggest that parts of the cave could have been used as a waste deposition for food scraps, attracting animals when the hominis were not around (Morley et al. 2019). Additionally, previous studies have shown that predator species were targeted for their fur in this region (Borgia 2017; Vasil'ev 2003).

Another difference between our data and the findings of Brown et al. (2021) concerns the decline of *Equus* specimens from Layer 14 (17%) to Layer 13 (10%) identified in the current data, which was not present in Brown et al. (2021).

I ought to note here, however, that Brown et al. (2021) identified only 25 bones from Layer 13 using ZooMS (whilst 1054 samples were analysed for Layer 14). The identified specimens in this study are 375 bones for Layer 13 and 224 bones for Layer 14. It is certain that the small size of bones analysed from Layer 13 in the study by Brown et al. (2021) renders direct comparisons of the data very challenging.

Table 6: Fauna data based on ZooMS analyses by Brown et al. (2021) for Layer 13 and 14 of the East Chamber of Denisova Cave.

ZooMS Taxon	Layer 13 (NISP)	Layer 13 (%)	Layer 14 (NISP)	Layer 14 (%)
Carnivora	0	0%	75	7%
Cervidae/Gazella/Saiga	1	4%	298	27%
Bos/Bison	13	52%	289	26%
Rhinocerotidae	1	4%	110	10%
Equus	4	16%	177	16%
Elephantidae	1	4%	21	2%
Capra/Ovis	5	20%	103	9%
Ursidae	0	0%	28	3%
Hominidae	0	0%	0	0%

Stable Isotope analyses

In order to convert isotopic values to trophic level positioning of an organism, an average increase of 3 ‰ in the δ^{15}N value between trophic levels is used to reconstruct food webs (Minagawa & Wada 1984). Further studies have shown that this factor cannot be used universally (Kelly & Del Rio 2010; Martínez Del Rio et al. 2009; Vanderklift & Ponsard 2003). This suggests that the δ^{15}N enrichment from one trophic level to another is highly dependent on the species-specific predator-prey relationship. Given the variation that Middle and Upper Palaeolithic European terrestrial ecosystems show, several studies suggested the use of a higher enrichment factor, ranging between 0 – 2 ‰ for δ^{13}C and 3 – 5 ‰ for δ^{15}N (Ambrose 1991; Bocherens & Drucker 2003).

In this study, almost all species show δ^{15}N values elevated above the expected range. Elephantidae for example, show extremely high δ^{15}N values. Such elevation in N has been observed before for mammoths, for example, by Jacobi et al. (2009) where δ^{15}N values ranging from 7.6 to 9.7 ‰ were observed for mammoth bones found in the Camp de Fouilles, an Early Upper Palaeolithic site in Belgium (Jacobi et al. 2009).

Interestingly, certain taxa demonstrate a wide distribution in δ^{15}N values too. This can be as much as 10 ‰, as in the case of Elephantidae (most likely woolly mammoth). Felidae had an average δ^{15}N value of 11.61 ‰, therefore their prey would need to show an

average δ^{15}N value from between 6.61 to 8.61 ‰. In this study, only the Bos/Bison ZooMS taxa shows an average δ^{15}N value of 7.62 ‰, matching the range for the prey species of Felidae.

The hominin bones show an average δ^{15}N value of 13.89 ‰, hence, the δ^{15}N value of their prey species should have ranged between 8.89 to 10.89 ‰, which overlaps with the δ^{15}N values of Elephantidae (δ^{15}N=8.97 ‰)(Ambrose 1991; Bocherens & Drucker 2003). These assumptions agree with Dobrovskaya and Tiunov (2011) who suggested that the hominin from Okladnikov Cave show δ^{15}N values that match large herbivore mammals like mammoths and woolly rhinos as prey species. This led to the assumption that the hominins in this area evolved a carnivore diet strategy based on large herbivore mammals (Derevianko et al. 2011).

Nonetheless, European Neanderthals have been assigned to highly carnivorous diets on the basis of their stable isotope values, with ranges of δ^{15}N between 7.9 – 11.8 ‰ (Richards et al. 2000; Richards & Trinkaus 2009). Yet their δ^{15}N values differ significantly from the Denisova and Okladnikov Cave hominins (Figure 17). Both sites show highly elevated δ^{15}N values for hominins compared to other Eastern European sites (Bocherens et al. 1991; Richards et al. 2000; Richards & Trinkaus 2009). Another Palaeolithic human, this time an early upper Palaeolithic modern human from Kostenki 1, shows elevated δ^{15}N values, with a δ^{15}N value of 15.3 ‰ (δ^{13}C -18.2 ‰ and δ^{15}N 15.3 ‰) (Richards et al. 2001) but comparable to the values measured from the Okladnikov Neanderthals and the Denisova hominins.
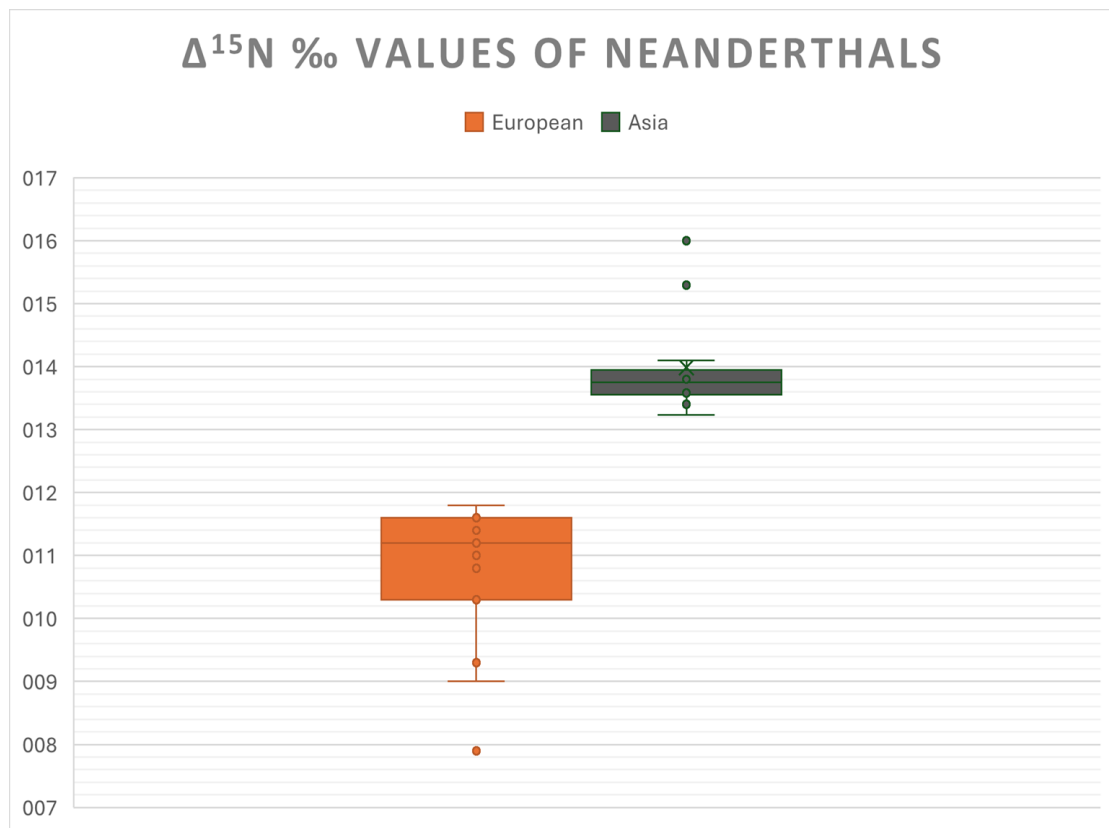
Figure 17: Boxplot showing the difference in δ15N between hominins found in Europe and hominins found in Asia (Richards et al. 2000; Richards & Trinkaus 2009).

The hominins analysed in this study most likely belonged to Denisovans, based on their stratigraphic provenance and preliminary aDNA data. This leads to the assumption that the $\delta^{15}N$ value of Neanderthals and Denisovans is highly elevated in the Altai, which was also found in a previous study (Dobrovolskaya & Tiunov 2011). The average European Pleistocene Neanderthal has $\delta^{15}N$ value around 11 ‰ (Richards et al. 2000), whereas the average hominin $\delta^{15}N$ value for the hominins in this study is 13.89 ‰. Interestingly, not only the hominin but also some Bos/Bison specimens exhibit slightly elevated $\delta^{15}N$ values.

This higher $\delta^{15}N$ value can be caused by many factors. Climatic conditions have a strong influence on the $\delta^{15}N$ value incorporated into an animal's body tissue. Arid climatic conditions and high temperatures influence the nitrogen-stable-isotope values, due to evapotranspiration (Ben-David & Flaherty 2012; Szpak 2014). This can not only be seen in primary producers but also in water-conserving mammals in arid regions (Ambrose 1991).

The incorporation of N into plants is highly dependent on the available nitrogen, and differences may be observed depending on which form and whether the plant itself can

incorporate N, or hast to interact with specific Mycorrhiza that are able to supplement N for the plants (Szpak 2014). The soil itself, and the plants growing on it, are another factor, leading to varied δ^{15}N values (Szpak 2014), as well as the availability of light for the plant (Ben-David & Flaherty 2012) and the discrimination the plant itself has between different N in the nitrification process (Szpak 2014).

Not only does the environment influence the stable isotope values, but the age of the specimen itself is a dependent factor for the ^{15}N incorporation. Adult herbivores for example will incorporate the δ^{15}N signature of the plants they are eating slowly if their intake is poor in nitrogen since they will first recycle their body nitrogen as much as possible (Ben-David & Flaherty 2012; Martínez Del Rio et al. 2005, 2009; Martínez Del Rio & Carleton 2012). The opposite is shown in growing animals, when on a high-protein diet, the juveniles show a fast incorporation of the isotopic signature of the food (Martínez Del Rio et al. 2009; Martínez Del Rio & Carleton 2012).

Hence, it becomes clear that the isotopic signature of an organism is influenced by the nutritional status, size, and the age of the animal as well as the macronutrient composition of the diet (Martínez Del Rio et al. 2009; Martínez Del Rio & Carleton 2012). Weaning individuals also differ in their stable isotope values, compared to their adult species members, and they show a high amount of δ^{15}N values. This could be the case for some of our Elephantidae samples, showing high δ^{15}N values (15.31 ‰), nevertheless, this cannot be verified, since there is no possibility of aging the bone fragments used for this analysis.

For the hominins, these elevated δ^{15}N values could be caused by another diet not displayed in our analysis of the mammal taxa found in the cave. A diet based on aquatic ecosystems leads to higher δ^{15}N values, even though the δ^{13}C value is very variable (Koch 2007). Even though there are several freshwater lakes in the area around Denisova Cave, the hypothesis that the main nitrogen intake of hominins at the time was based on fishing seems quite unlikely. This is consistent with the zooarchaeological collections found in Denisova Cave which show only a small number of freshwater fish remains, considered to have been introduced into this cave through other animals, like otters or owls. These fish show no modification by hominins.

Furthermore, it is quite rare that animals only depend on one food source, instead they have multiple food sources (Bond et al. 2016; Carleton et al. 2008). This can also be seen in the behaviour of *H. sapiens* from the Upper Palaeolithic, showing a spectrum of various food sources (Richards et al. 2001). Not only is the food source of a species quite broad but it also changes several times during its life, faster than the turnover rates

of some of their tissues (Bond et al. 2016; Carleton et al. 2008) making it impossible to be fully reflected in the isotopic signature of the body. Even with animals highly specialised to one food source, this source is usually temporally very variable in macronutrients and isotopic composition among others, based on the different habitats the food source was found in (Flaherty & Ben-David 2010; Martínez Del Rio et al. 2005; Martínez Del Rio & Carleton 2012).

Starvation as well as N-poor nutrition may influence the $\delta^{15}N$ and $\delta^{13}C$ values in an increasing manner. This can be explained by a change in protein and carbohydrate metabolism or intensified dependence on internal N resources, leading to a higher absorption and excretion of ^{14}N. Studies have shown that even when there is no new N and C intake, the excretion and respiration loss of an individual stays the same, leading to an even greater reduction of ^{14}N in the body and therefore an enrichment of the $\delta^{15}N$ values. The length of the starvation or poor nitrogen diet is thereby a decisive factor (Doi et al. 2017).

Large environmental changes could influence the $\delta^{15}N$ values of the specimens. Glaciers and permafrost influence the stable isotope values due to their introduction of nutrients like nitrogen into the soil when melting down, leading to enriched nitrogen values in the plants growing on this soil (Beermann et al. 2017; Göransson et al. 2016). These high values are introduced through atmospheric nitrogen captured in the ice as well as microbial weathering processes (Burpee et al. 2018; Williams et al. 2007). These elevations are mirrored in plants and are introduced into the body of herbivores through them and consequently found in carnivores too. Denisova Cave is located on the Altai mountains, an area that had been and is partially covered in ice and which was influenced from glaciation and deglaciation cycles. The high nitrogen values found in the bones I analysed may be an indication for nutrient rich soil conditions of this area during this time. The hominin bones in Layer 14 (dated to a time of 193 ± 12 to 187 ± 14 ka) (Jacobs et al. 2019) correspond to milder climatic conditions, that would have exposed permafrost soils to thawing.

As outlined, the estimation of how and why stable isotope signatures are shown is complex and creates the necessity to reconstruct several possible scenarios of the lifestyle of previous generations. These scenarios must be compared to each and induced with data from further studies.

Conclusion

Environmental changes are a constant process, leading to a constant change in living conditions. Influencing fitness through diet opportunities and habitat chances leads to the necessity to adapt or to move. This creates a constant change of taxonomic constellation in a region. For the Altai region this is especially important, looking at the significance of this region as the melting pot of hominin occupation. Especially Denisova Cave with its remarkable preservation is a key point when it comes to research on hominins and their lifestyle.

This crucial site combined with biochemical methods like the ZooMS method to identify further bone fragments, even if these are morphologically not to analyse, or the stable isotope analyses, creates the opportunity to generate more information that cannot be captured in any other way and is needed for a further understanding of human development.

The biomolecular taxonomical determination of 647 bone fragments from Layers 13 and 14 of the East Chamber gives us information about the taxonomic changes. Changes in the taxonomic distribution of some species offer us insights into the environmental changes between those two layers and create therefore a higher understanding of the living conditions Neanderthals and Denisovans faced. The identification of two hominin bones in Layer 14, DC33 and DC35, make them one of the first hominin species from this layer. Further genetic analyses of these bone fragments will allow us to place them into a wider context.

In addition to the palaeoproteomic data, this study generated and analysed stable isotope values for 77 bones from four different layers (Layers 13, 14, 15 and 17) in the East Chamber of Denisova Cave. This data provides the necessary background upon which we can place the hominin isotope results.

Overall, this thesis succeeded to provide further information about the species living next to our ancestors and their close relatives, leading into a better understanding of the subsistence behaviour, and the interaction between hominins and their environment. The combination of ZooMS and stable isotope analyses offers great possibilities for further understanding late human evolution.

References

Agadjanian, A. K., Shunkov, M. V., & Kozlikin, M. B. (2019). Remains of Small Vertebrates from the Eastern Chamber of Denisova Cave. *Problems of Archaeology, Ethnography, Anthropology of Siberia and Neighboring Territories*, 25, 7–13. https://doi.org/10.17746/2658-6193.2019.25.007-013

Agatova, A. R., Nepop, R. K., Bronnikova, M. A., Slyusarenko, I. Y., & Orlova, L. A. (2016). Human occupation of South Eastern Altai highlands (Russia) in the context of environmental changes. *Archaeological and Anthropological Sciences*, 8(3), 419–440. https://doi.org/10.1007/s12520-014-0202-7

Ambrose, S. H. (1991). Effects of Diet, Climate and Physiology on Nitrogen Isotope Abundances in Terrestrial Foodwebs. *Journal of Archaeological Science*, 18, 293-317.

Arnold, L. J., Demuro, M., Parés, J. M., Arsuaga, J. L., Aranburu, A., Bermúdez de Castro, J. M., & Carbonell, E. (2014). Luminescence dating and palaeomagnetic age constraint on hominins from Sima de los Huesos, Atapuerca, Spain. *Journal of Human Evolution*, 67(1), 85–107. https://doi.org/10.1016/j.jhevol.2013.12.001

Bae, C. J., Douka, K., & Petraglia, M. D. (2017). Human colonization of Asia in the late Pleistocene an introduction to supplement 17. *Current Anthropology*, 58, S373–S382. https://doi.org/10.1086/694420

Bar-Yosef, O. (1994). The Lower Paleolithic of the Near East. *Journal of World Prehistory*, 8(3), 211-265. https://doi.org/10.1007/BF02221050

Beermann, F., Langer, M., Wetterich, S., Strauss, J., Boike, J., Fiencke, C., Schirrmeister, L., Pfeiffer, E.-M., & Kutzbach, L. (2017). Permafrost Thaw and Liberation of Inorganic Nitrogen in Eastern Siberia. *Permafrost and Periglacial Processes*. https://doi.org/10.1002/ppp.1958

Behar, D. M., Villems, R., Soodyall, H., Blue-Smith, J., Pereira, L., Metspalu, E., Scozzari, R., Makkan, H., Tzur, S., Comas, D., Bertranpetit, J., Quintana-Murci, L., Tyler-Smith, C., Wells, R. S., & Rosset, S. (2008). The Dawn of Human Matrilineal Diversity. *American Journal of Human Genetics*, 82(5), 1130–1140. https://doi.org/10.1016/j.ajhg.2008.04.002

Benazzi, S., Douka, K., Fornai, C., Bauer, C. C., Kullmer, O., Svoboda, J., Pap, I., Mallegni, F., Bayle, P., Coquerelle, M., Condemi, S., Ronchitelli, A., Harvati, K., & Weber, G. W. (2011). Early dispersal of modern humans in Europe and implications for Neanderthal behaviour. *Nature*, 479(7374), 525–528. https://doi.org/10.1038/nature10617

Ben-David, M., & Flaherty, E. A. (2012). Stable isotopes in mammalian research: A beginner's guide. *Journal of Mammalogy*, 93(2), 312–328. https://doi.org/10.1644/11-MAMM-S-166.1

Bergström, A., Stringer, C., Hajdinjak, M., Scerri, E. M. L., & Skoglund, P. (2021). Origins of modern human ancestry. *Nature*, 590(7845), 229–237. https://doi.org/10.1038/s41586-021-03244-5

Bergström, A., McCarthy, S. A., Hui, R., Almarri, M. A., Ayub, Q., Danecek, P., Chen, Y., Felkel, S., Hallast, P., Kamm, J., Blanché, H., Deleuze, J. F., Cann, H., Mallick, S., Reich, D., Sandhu, M. S., Skoglund, P., Scally, A., Xue, Y., & Tyler-Smith, C. (2020). Insights into human genetic variation and population history from 929 diverse genomes. *Science*, 367(6484). https://doi.org/10.1126/science.aay5012

Bocherens Hervt, Fizet, M., Mariottil, A., Lange-Badre, B., Vanderrneersch, B., Borel, J. P., & Bellon, G. (1991). Isotopic biogeochemistry (13C, 15N) of fossil vertebrate collagen: implications for the study of fossil food web including Neanderthal Man. *Journal of Human Evolution , 20, 481-492.* https://doi.org/10.1016/0047-2484(91)90021-M

Bocherens, H., Drucker, D. G., Billiou, D., Patou-Mathis, M., & Vandermeersch, B. (2005). Isotopic evidence for diet and subsistence pattern of the Saint-Césaire I Neanderthal. *Journal of Human Evolution*, 49(1), 71–87. https://doi.org/10.1016/j.jhevol.2005.03.003

Bocherens, H., & Drucker, D. (2003). Trophic level isotopic enrichment of carbon and nitrogen in bone collagen. *International Journal of Osteoarchaeology*, 13(1–2), 46–53. https://doi.org/10.1002/oa.662

Bond, A. L., Jardine, T. D., & Hobson, K. A. (2016). *Multi-tissue stable-isotope analyses can identify dietary specialization*. 7. 1428-1437. https://doi.org/10.1111/2041-210X.12620

Buckley, M., Collins, M., Thomas-Oaies, J., & Wilson, J. C. (2009). Species identification by analysis of bone collagen using matrix-assisted laser desorption/ionisation time-of-flight mass spectrometry. *Rapid Communications in Mass Spectrometry*, 23(23), 3843–3854. https://doi.org/10.1002/rcm.4316

Buckley, M., Fraser, S., Herman, J., Melton, N. D., Mulville, J., & Pálsdóttir, A. H. (2014). Species identification of archaeological marine mammals using collagen fingerprinting. *Journal of Archaeological Science*, *41*, 631–641. https://doi.org/10.1016/j.jas.2013.08.021

Buckley, M. (2017). Zooarchaeology by mass spectrometry (ZooMS) collagen fingerprinting for the species identification of archaeological bone fragments. In *Zooarchaeology in Practice: Case Studies in Methodology and Interpretation in Archaeofaunal Analysis* (pp. 227–247). Springer International Publishing. https://doi.org/10.1007/978-3-319-64763-0_12

Bolikhovskaya, N. S., & Shunkov, M. V. (2014). Pleistocene environments of northwestern Altai: Vegetation and climate. *Archaeology, Ethnology and Anthropology of Eurasia*, *42*(2), 2–17. https://doi.org/10.1016/j.aeae.2015.01.001

Bolikhovskaya, N. S., Kozlikin, M. B., Shunkov, M. V. (2015). Plalynostratigraphy and Preliminary Reconstruction of Environmental conditions in formin the Upper part of Pleistocene section in eastern galley of Denisova Cave. Problems of Archaeology, Ethnography, Anthropology of Siberia and Neighboring Territories. 21. 28-30.

Borgia, V. (2017). Hunting high and low: Gravettian hunting weapons from Southern Italy to the Russian Plain. *Open Archaeology*, 3(1), 376–391. https://doi.org/10.1515/opar-2017-0024

Brown, S., Higham, T., Slon, V., Paabo, S., Meyer, M., Douka, K., Brock, F., Comeskey, D., Procopio, N., Shunkov, M., Derevianko, A., & Buckley, M. (2016). Identification of a new hominin bone from Denisova Cave, Siberia using collagen fingerprinting and mitochondrial DNA analysis. *Scientific Reports*, *6*. https://doi.org/10.1038/srep23559

Brown, S., Massilani, D., Kozlikin, M. B., Shunkov, M. v., Derevianko, A. P., Stoessel, A., Jope-Street, B., Meyer, M., Kelso, J., Pääbo, S., Higham, T., & Douka, K. (2022). The earliest Denisovans and their cultural adaptation. *Nature Ecology and Evolution*, *6*(1), 28–35. https://doi.org/10.1038/s41559-021-01581-2

Brown, S., Wang, N., Oertle, A., Kozlikin, M. B., Shunkov, M. V., Derevianko, A. P., Comeskey, D., Jope-Street, B., Harvey, V. L., Chowdhury, M. P., Buckley, M., Higham, T., & Douka, K. (2021). Zooarchaeology through the lens of collagen fingerprinting at Denisova Cave. *Scientific Reports*, 11(1). https://doi.org/10.1038/s41598-021-94731-2

Browning, S. R., Browning, B. L., Zhou, Y., Tucci, S., & Akey, J. M. (2018). Analysis of Human Sequence Data Reveals Two Pulses of Archaic Denisovan Admixture. *Cell*, 173(1), 53-61.e9. https://doi.org/10.1016/j.cell.2018.02.031

Burpee, B. T., Anderson, D., & Saros, J. E. (2018). Assessing ecological effects of glacial meltwater on lakes fed by the Greenland Ice Sheet: The role of nutrient subsidies and turbidity. *Arctic, Antarctic, and Alpine Research*, 50(1). https://doi.org/10.1080/15230430.2017.1420953

Carleton, S. A., Kelly, L., Anderson-Sprecher, R., & del Rio, C. M. (2008). Should we use one-, or multi-compartment models to describe 13C incorporation into animal tissues? *Rapid Communications in Mass Spectrometry*, *22*(19), 3008–3014. https://doi.org/10.1002/rcm.3691

Carotenuto, F., Tsikaridze, N., Rook, L., Lordkipanidze, D., Longo, L., Condemi, S., & Raia, P. (2016). Venturing out safely: The biogeography of Homo erectus dispersal out of Africa. *Journal of Biogeography*. https://doi.org/10.1016/j.jbioge.2016.02.013

Chen, L., Ma, L., Zhou, M., Liu, Y., & Zhang, Y. (2014). Effects of pressure on gelatinization of collagen and properties of extracted gelatins. *Food Hydrocolloids*, *36*, 316–322. https://doi.org/10.1016/j.foodhyd.2013.10.012Bo

Chen, F., Welker, F., Shen, C. C., Bailey, S. E., Bergmann, I., Davis, S., Xia, H., Wang, H., Fischer, R., Freidline, S. E., Yu, T. L., Skinner, M. M., Stelzer, S., Dong, G., Fu, Q., Dong, G., Wang, J., Zhang, D., & Hublin, J. J. (2019). A late Middle Pleistocene Denisovan mandible from the Tibetan Plateau. *Nature*, 569(7756), 409–412. https://doi.org/10.1038/s41586-019-1139-x

Chisholm, B. S., Nelson, D. E., Hobson, K. A., Schwarcz, H. P., & Knyf, M. (1983). Carbon Isotope Measurement Techniques for Bone Collagen: Notes for the Archaeologist. In *Journal of Archaeological Science* (Vol. 10). http://dx.doi.org/10.1016/0305-4403(83)90073-0

Chlachula, J. (2001). Pleistocene climate change, natural environments and palaeolithic o ccupation of the Altai area, west-central Siberia. *Quaternary International*. 80-81. 131-167. https://doi.org/10.1016/S1040-6182(01)00023-4

Chlachula, J. (2019). Environmental context and adaptations of prehistoric and early historical occupation in the Southern Altai (SW Siberia–East Kazakhstan). *Archaeological and Anthropological Sciences*, *11*(5), 2215–2236. https://doi.org/10.1007/s12520-018-0664-0

Choudhury, D., Timmermann, A., Schloesser, F., Heinemann, M., & Pollard, D. (2020). Simulating Marine Isotope Stage 7 with a coupled climate-ice sheet model. *Climate of the Past*, 16(6), 2183–2201. https://doi.org/10.5194/cp-16-2183-2020

Chu, A. C. (2023). Natural selection and Neanderthal extinction in a Malthusian economy. *Springer Nature* , *36*, 1641–1656. https://doi.org/10.1007/s00148-023-00939-z

Dawson, T. E., Mambelli, S., Plamboeck, A. H., Templer, P. H., & Tu, K. P. (2002). Stable isotopes in plant ecology. In *Annual Review of Ecology and Systematics* (Vol. 33, pp. 507–559). https://doi.org/10.1146/annurev.ecolsys.33.020602.095451

Demeter, F., Zanolli, C., Westaway, K. E., Joannes-Boyau, R., Duringer, P., Morley, M. W., Welker, F., Rüther, P. L., Skinner, M. M., McColl, H., Gaunitz, C., Vinner, L., Dunn, T. E., Olsen, J. V., Sikora, M., Ponche, J. L., Suzzoni, E., Frangeul, S., Boesch, Q., ... Shackelford, L. (2022). A Middle Pleistocene Denisovan molar from the Annamite Chain of northern Laos. *Nature Communications*, 13(1). https://doi.org/10.1038/s41467-022-29923-z

Derevianko, A. P. (2011). The origin of anatomically modern humans and their behavior in africa and eurasia. *Archaeology, Ethnology and Anthropology of Eurasia*, *39*(3), 2–31. https://doi.org/10.1016/j.aeae.2011.09.001

Derevianko, A. P., & Shunkov, M. V. (2009). Development of early human culture in northern Asia. *Paleontological Journal*, 43(8), 881–889. https://doi.org/10.1134/S0031030109080061

Derevianko, A. P., Shunkov, M. v., & Volkov, P. v. (2008). A PALEOLITHIC BRACELET FROM DENISOVA CAVE*. *Archaeology, Ethnology and Anthropology of Eurasia*, *34*(2), 13–25. https://doi.org/10.1016/j.aeae.2008.07.002

Di Vincenzo, F., & Manzi, G. (2023). Homo heidelbergensis as the Middle Pleistocene common ancestorof Denisovans, Neanderthals and modern humans. *Journal of Mediterranean Earth Sciences*, *15*, 161–173. https://doi.org/10.13133/2280-6148/18074

Dobrovolskaya M.V., & Tiunov A.V. (2011). STABLE ISOTOPE (13C/12C AND 15N/14 N) EVIDENCE FOR LATE PLEISTOCENE HOMININES' PALAEODIETS IN GORNY ALTAI. *Publishing Department of the Institute of Archaeology and Ethnography SB RAS*, 81–90.

Doi, H., Akamatsu, F., & González, A. L. (2017). Starvation effects on nitrogen and carbon stable isotopes of animals: An insight from meta-analysis of fasting experiments. *Royal Society Open Science*, *4*(8). https://doi.org/10.1098/rsos.170633

Douka, K., Slon, V., Jacobs, Z., Bronk Ramsey, C., Shunkov, M. V., Derevianko, A. P., Mafessoni, F., Li, B., Grün, R., Comeskey, D., Devièse, T., Viola, B., Kinsley, L., Buckley, M., Meyer, M., Roberts, R. G., Pääbo, S., Kelso, J., & Higham, T. (2019). Age estimates for hominin fossils and the onset of the Upper Palaeolithic. *Nature*, 565(7741), 640-644. https://doi.org/10.1038/s41586-018-0870-z

Ferring, R., Oms, O., Agustí, J., Berna, F., Nioradze, M., Shelia, T., Tappen, M., Vekua, A., Zhvania, D., & Lordkipanidze, D. (2011). Earliest human occupations at Dmanisi (Georgian Caucasus) dated to 1.85-1.78 Ma. *Proceedings of the National Academy of Sciences of the United States of America*, 108(26), 10432–10436. https://doi.org/10.1073/pnas.1106638108

Fu, Q., Hajdinjak, M., Moldovan, O. T., Constantin, S., Mallick, S., Skoglund, P., Patterson, N., Rohland, N., Lazaridis, I., Nickel, B., Viola, B., Prüfer, K., Meyer, M., Kelso, J., Reich, D., & Pääbo, S. (2015). An early modern human from Romania with a recent Neanderthal ancestor. *Nature*, 524, 216–219. https://doi.org/10.1038/nature14558

Fu, Q., Li, H., Moorjani, P., Jay, F., Slepchenko, S. M., Bondarev, A. A., Johnson, P. L. F., Aximu-Petri, A., Prüfer, K., de Filippo, C., Meyer, M., Zwyns, N., Salazar-García, D. C., Kuzmin, Y. v., Keates, S. G., Kosintsev, P. A., Razhev, D. I., Richards, M. P., Peristov, N. v., … Pääbo, S. (2014). Genome sequence of a 45,000-year-old modern human from western Siberia. *Nature*, *514*(7253), 445–449. https://doi.org/10.1038/nature13810

Gavan, Z. (2018). Neanderthals (Homo neanderthalensis): An Adaptive Paradox. *The Human Voyage 2 (July)*. *https://studentjournals.anu.edu.au/index.php/hv/article/view/77*

Gómez-Robles, A. (2019). Dental evolutionary rates and its implications for the Neanderthal-modern human divergence. 5 (5). https://doi.org/10.1126/sciadv.

Göransson, H., Welc, M., Bünemann, E. K., Christl, I., & Venterink, H. O. (2016). Nitrogen and phosphorus availability at early stages of soil development in the Damma glacier forefield, Switzerland; implications for establishment of N2-fixing plants. *Plant and Soil*, *404*(1–2), 251–261. https://doi.org/10.1007/s11104-016-2821-5

Green, R. E., Krause, J., Briggs, A. W., Maricic, T., Stenzel, U., Kircher, M., Patterson, N., Li, H., Zhai, W., Fritz, M. H.-Y., Hansen, N. F., Durand, E. Y., Malaspinas, A., Jensen, J. D., Marques-Bonet, T., Alkan, C., Prüfer, K., Meyer, M., Burbano, H. A., … Pääbo, S. (2010). A Draft Sequence of the Neandertal Genome. *Science*, 328(5979), 710–722. https://doi.org/10.1126/science.1188021

Grün, R., Brink, J. S. , Spooner, N. A. . , Taylor, L. , Stringer, C. B. , Franciscus, R. G. , & Murray, A. S. (1996). Direct dating of Florisbad hominid. *Nature , 382(6591)*, 500–501. https://doi.org/10.1038/382500a

Hajdinjak, M., Mafessoni, F., Skov, L., Vernot, B., Hübner, A., Fu, Q., Essel, E., Nagel, S., Nickel, B., Richter, J., Moldovan, O. T., Constantin, S., Endarova, E., Zahariev, N., Spasov, R., Peter, B. M., Meyer, M., Skoglund, P., Kelso, J., & Pääbo, S. (2021). Initial Upper Palaeolithic humans in Europe had recent Neanderthal ancestry. *Nature*, 592(11), 17. https://doi.org/10.1038/s41586-021-03335-3

Hajdinjak, M., Fu, Q., Hübner, A., Petr, M., Mafessoni, F., Grote, S., Skoglund, P., Narasimham, V., Rougier, H., Crevecoeur, I., Semal, P., Soressi, M., Talamo, S., Hublin, J. J., Gušić, I., Kućan, Z., Rudan, P., Golovanova, L. v., Doronichev, V. B., ... Kelso, J. (2018). Reconstructing the genetic history of late Neanderthals. *Nature*, *555*(7698), 652–656. https://doi.org/10.1038/nature26151

Hardy, B. L., & Moncel, M. H. (2011). Neanderthal use of fish, mammals, birds, starchy plants and wood 125-250,000 years ago. *PLoS ONE*, *6*(8). https://doi.org/10.1371/JOURNAL.PONE.0023768

Hardy, K., Buckley, S., Collins, M. J., Estalrrich, A., Brothwell, D., Copeland, L., García-Tabernero, A., García-Vargas, S., de La Rasilla, M., Lalueza-Fox, C., Huguet, R., Bastir, M., Santamaría, D., Madella, M., Wilson, J., Cortés, Á. F., & Rosas, A. (2012). Neanderthal medics? Evidence for food, cooking, and medicinal plants entrapped in dental calculus. *Naturwissenschaften*, *99*(8), 617–626. https://doi.org/10.1007/s00114-012-0942-0

Hardy, B. L., Moncel, M., Lebon, M., & Bellot-Gurlet, L. (2020). Direct evidence of neanderthal fibre technology and its cognitive and behavioral implications. *Nature Ecology and Evolution* , *5*, 1263–1282. https://doi.org/10.1038/s41598-020-61839-w

Harvati, K., Röding, C., Bosman, A. M., Karakostis, F. A., Grün, R., Stringer, C., Karkanas, P., Thompson, N. C., Koutoulidis, V., Moulopoulos, L. A., Gorgoulis, V. G., & Kouloukoussa, M. (2019). Apidima Cave fossils provide earliest evidence of Homo sapiens in Eurasia. *Nature*, 571, 500–502. https://doi.org/10.1038/s41586-019-1376-z

Harvati, K., Stringer, C., Grü, R., Aubert, M., Allsworth-Jones, P., & Folorunso, C. A. (2011). The Later Stone Age Calvaria from Iwo Eleru, Nigeria: Morphology and Chronology. *PLOS ONE*, 6(9), 1–8. https://doi.org/10.1371/journal.pone.0024024

Hedges, R. E. M., Stevens, R. E., & Richards, M. P. (2004). Bone as a stable isotope archive for local climatic information. *Quaternary Science Reviews*, *23*(7–8), 959–965. https://doi.org/10.1016/j.quascirev.2003.06.022

Hendy, J., Welker, F., Demarchi, B., Speller, C., Warinner, C. and Collins, M.J. (2018). A guide to ancient protein studies. *Nature ecology & evolution*, *2*(5), pp.791-799. https://doi.org/10.1038/s41559-018-0510-x

Hendy, J. (2021). Ancient protein analysis in archaeology. In *Hendy, Sci. Adv* (Vol. 7) Issue 3. https://doi.org/10.1126/sciadv.abb9314

Henry, A. G., Brooks, A. S., & Piperno, D. R. (2011). Microfossils in calculus demonstrate consumption of plants and cooked foods in Neanderthal diets (Shanidar III, Iraq; Spy I and II, Belgium). *Proceedings of the National Academy of Sciences of the United States of America*, *108*(2), 486–491. https://doi.org/10.1073/pnas.1016868108

Hershkovitz, I., Marder, O., Ayalon, A., Bar-Matthews, M., Yasur, G., Boaretto, E., Caracuta, V., Alex, B., Frumkin, A., Goder-Goldberger, M., Gunz, P., Holloway, R. L., Latimer, B., Lavi, R., Matthews, A., Slon, V., Mayer, D. B. Y., Berna, F., Bar-Oz, G., ... Barzilai, O. (2015). Levantine cranium from Manot Cave (Israel) foreshadows the first European modern humans. *Nature, 520*(7546), 216–219. https://doi.org/10.1038/nature14134

Hershkovitz, I., Weber, G. W., Quam, R., Duval, M., Grün, R., Kinsley, L., Ayalon, A., Bar-Matthews, M., Valladas, H., Mercier, N., Arsuaga, J. L., Martinón-Torres, M., Bermúdez de Castro, J. M., Fornai, C., Martín-Francés, L., Sarig, R., May, H., Krenn, V. A., Slon, V., ... Weinstein-Evron, M. (2018). The earliest modern humans outside Africa. In *Jose Miguel Carretero* (Vol. 5). http://science.sciencemag.org/

Higham, T., Douka, K., Wood, R., Ramsey, C. B., Brock, F., Basell, L., Camps, M., Arrizabalaga, A., Baena, J., Barroso-Ruíz, C., Bergman, C., Boitard, C., Boscato, P., Caparrós, M., Conard, N. J., Draily, C., Froment, A., Galván, B., Gambassini, P., ... Jacobi, R. (2014). The timing and spatiotemporal

patterning of Neanderthal disappearance. *Nature*, 512(7514), 306–309. https://doi.org/10.1038/nature13621

Hublin, J. J. (2009). The origin of Neandertals. *Proceedings of the National Academy of Sciences*. www.pnas.orgcgidoi10.1073pnas.0904119106

Hublin, J. J. (2015). The modern human colonization of western Eurasia: When and where? In *Quaternary Science Reviews* (Vol. 118, pp. 194–210). Elsevier Ltd. https://doi.org/10.1016/j.quascirev.2014.08.011

Hublin, J. J., Sirakov, N., Aldeias, V., Bailey, S., Bard, E., Delvigne, V., Endarova, E., Fagault, Y., Sinet-Mathiot, V., Meyer, M., Pääbo, S., Popov, V., ... Tsanova, T. (2020). Initial Upper Palaeolithic Homo sapiens from Bacho Kiro Cave, Bulgaria. *Nature*, 581(7808), 299–302. https://doi.org/10.1038/s41586-020-2259-z

Hublin, J.-J., Ben-Ncer, A., Bailey, S. E., Freidline, S. E., Neubauer, S., Skinner, M. M., Bergmann, I., le Cabec, A., Benazzi, S., Harvati, K., & Gunz, P. (2017). New fossils from Jebel Irhoud, Morocco and the pan-African origin of Homo sapiens. *Nature Publishing Group*. https://doi.org/10.1038/nature22336

Jacobi, R. M., Higham, T. F. G., Haesaerts, P., Jadin, I., & Basell, L. S. (2009). Radiocarbon chronology for the Early Gravettian of northern Europe: new AMS determinations for Maisì eres-Canal, Belgium. *Cambridge University Press* , *84*, 26–40. https://doi.org/10.1017/S0003598X00099749

Jacobs, Z., Li, B., Shunkov, M. V., Kozlikin, M. B., Bolikhovskaya, N. S., Agadjanian, A. K., Uliyanov, V. A., Vasiliev, S. K., O'gorman, K., Derevianko, A. P., & Roberts, G. (2019). Timing of archaic hominin occupation of Denisova Cave in southern Siberia. *Nature*, 565(7741), 594–599. https://doi.org/10.1038/s41586-018-0843-2

Kelly, L. J., & del Rio, C. M. (2010). The fate of carbon in growing fish: An experimental study of isotopic routing. *Physiological and Biochemical Zoology*, *83*(3), 473–480. https://doi.org/10.1086/649628

Kowalczyk, M., Staniszewski, A., Kamiñska, K., Domaradzki, P., & Horecka, B. (2021). Advantages, Possibilities, and Limitations of Mitochondrial DNA Analysis in Molecular Identification. *Folia Biologica (Poland)*, *69*(3), 101–111. https://doi.org/10.3409/fb_69-3.12

Krause, J., Fu, Q., Good, J. M., Viola, B., Shunkov, M. v., Derevianko, A. P., & Pääbo, S. (2010). The complete mitochondrial DNA genome of an unknown hominin from southern Siberia. *Nature*, *464*(7290), 894–897. https://doi.org/10.1038/nature08976

Kuhlwilm, M., Gronau, I., Hubisz, M. J., de Filippo, C., Prado-Martinez, J., Kircher, M., Fu, Q., Burbano, H. A., Lalueza-Fox, C., de La Rasilla, M., Rosas, A., Rudan, P., Brajkovic, D., Kucan, Ž., Gušic, I., Marques-Bonet, T., Andrés, A. M., Viola, B., Pääbo, S., ... Castellano, S. (2016). Ancient gene flow from early modern humans into Eastern Neanderthals. *Nature*, 530(7591), 429–433. https://doi.org/10.1038/nature16544

Kuzmin, Y. v., Bondarev, A. A., Kosintsev, P. A., & Zazovskaya, E. P. (2021). The Paleolithic diet of Siberia and Eastern Europe: evidence based on stable isotopes (δ13C and δ15N) in hominin and animal bone collagen. *Archaeological and Anthropological Sciences*, *13*(10). https://doi.org/10.1007/s12520-021-01439-5

Lambacher, N., Gerdau-Radonic, K., Bonthorne, E., & Valle de Tarazaga Montero, F. J. (2016). Evaluating three methods to estimate the number of individuals from a commingled context. *Journal of Archaeological Science: Reports*, 10, 674–683. https://doi.org/10.1016/j.jasrep.2016.07.008

Leder, D., Hermann, R., Hüls, M., Russo, G., Hoelzmann, P., Nielbock, R., Böhner, U., Lehmann, J., Meier, M., Schwalb, A., Tröller-Reimer, A., Koddenberg, T., & Terberger, T. (2021). A 51,000-year-old engraved bone reveals Neanderthals' capacity for symbolic behaviour. *Nature Ecology and Evolution*, *5*(9), 1273–1282. https://doi.org/10.1038/s41559-021-01487-z

Liden, K., Takahashi, C., & Nelson, D. E. (1995). The Effects of Lipids in Stable Carbon Isotope Analysis and the Effects of NaOH Treatment on the Composition of Extracted Bone Collagen. In *Journal of Archaeological Science* (Vol. 22). https://doi.org/10.1006/jasc.1995.0034

Longin E. J., Marien R., G., & Pachiaudi, C. (1971). Lyon, natural radiocarbon measurements II. American Journan of Science, Radiocarbon, 13(1), 52-73. https://doi.org/10.1017/S0033822200000850

Lordkipanidze, D., Vekua, A., Ferring, R., Rightmire, G.P., Agusti, J., Kiladze, G., Mouskhelishvili, A., Nioradze, M., De León, M.S.P., Tappen, M. and Zollikofer, C.P. (2005). The earliest toothless hominin skull. *Nature*, *434*(7034), pp.717-718. https://doi.org/10.1038/434717b

Lyman, R. L. (2002). Taxonomic identification of zooarchaeological remains. *The Review of Archaeology*, 23,13–20.

Marshall, J. D., Renée Brooks, J., & Lajtha, K. (2007). *Sources of variation in the stable isotopic composition of plants**. http://dx.doi.org/10.1002/9780470691854.ch2

Martínez Del Rio, C., Wolf, N., Carleton, S. A., & Gannes, L. Z. (2009). Isotopic ecology ten years after a call for more laboratory experiments. In *Biological Reviews* (Vol. 84, Issue 1, pp. 91–111). https://doi.org/10.1111/j.1469-185X.2008.00064.x

Martínez del Rio, C. and Wolf, B.O. (2005) Mass-Balance Models for Animal Isotopic Ecology. In: Starck, J.M., Wang, T. and Wang, T., Eds., Physiological and Ecological Adaptations to Feeding in Vertebrates, Science Publishers, Enfield, Chapter 6, 141-174.

Martínez del Rio, C., & Carleton, S. A. (2012). How fast and how faithful: The dynamics of isotopic incorporation into animal tissues. In *Journal of Mammalogy* (Vol. 93, Issue 2, pp. 353–359). https://doi.org/10.1644/11-MAMM-S-165.1

Massilani, D., Skov, L., Hajdinjak, M., Gunchinsuren, B., Tseveendorj, D., Yi, S., Lee, J., Nagel, S., Nickel, B., Devièse, T., Higham, T., Meyer, M., Kelso, J., Peter, B. M., & Pääbo, S. (2020). *Denisovan ancestry and population history of early East Asians*. Science, 370(6516), 579-583 https://doi.org/https://doi.org/10.1126/science.abc1166

Mellars, P., (2004). Neanderthals and the modern human colonization of Europe. *Nature*, *432*(7016), pp.461-465. https://doi.org/10.1038/nature03103

Mellars, P., (2006). Going East: New Genetic and Archaeological Perspectives on the Modern Human Colonization of Eurasia. In *Science* (Vol. 313, Issue 5788, pp. 796–800). https://doi.org/10.1126/science.1127272

Mellars, P. (2005). The impossible coincidence. A single-species model for the origins of modern human behavior in Europe. In *Evolutionary Anthropology* (Vol. 14, Issue 1, pp. 12–27). https://doi.org/10.1002/evan.20037

Meyer, M., Kircher, M., Gansauge, M.-T., Li, H., Racimo, F., Mallick, S., Schraiber, J. G., Jay, F., Prüfer, K., de Filippo, C., Sudmant, P. H., Alkan, C., Fu, Q., Do, R., Rohland, N., Tandon, A., Siebauer, M., Green, R. E., Bryc, K., … Pääbo, S. (2012). A High Coverage Genome Sequence from an Archaic Denisovan Individual. *Science*, 338(6104), 222–226. https://doi.org/10.1126/science.1224344

Koch, P. L. (2007). Stable Isotopes in Ecology and Environmental Science *SECOND EDITION*. *Pp. 99 -154*. *https://doi.org/10.1002/9780470691854.ch5*

Minagawa, M., & Wada, E. (1984). Stepwise enrichment of "N along food chains: Further evidence and the relation between 615N and animal age. *Geochimicaet Cosmochimica Acta*, 48, 1135-1140. https://doi.org/10.1016/0016-7037(84)90204-7

Morin, E., Ready, E., Boileau, A., Beauval, C., & Coumont, M. P. (2017). Problems of Identification and Quantification in Archaeozoological Analysis, Part I: Insights from a Blind Test. *Journal of Archaeological Method and Theory*, 24(3), 886–937. https://doi.org/10.1007/s10816-016-9300-4

Morley, M. W., Goldberg, P., Uliyanov, V. A., Kozlikin, M. B., Shunkov, M. v., Derevianko, A. P., Jacobs, Z., & Roberts, R. G. (2019). Hominin and animal activities in the microstratigraphic record from Denisova Cave (Altai Mountains, Russia). *Scientific Reports*, 9(1). https://doi.org/10.1038/s41598-019-49930-3

Ocobock, C., Lacy, S., & Niclou, A. (2021). Between a rock and a cold place: Neanderthal biocultural cold adaptations. *Evolutionary Anthropology*, 30(4), 262–279. https://doi.org/10.1002/evan.21894

Orlando, L., Allaby, R., Skoglund, P., Der Sarkissian, C., Stockhammer, P.W., Ávila-Arcos, M.C., Fu, Q., Krause, J., Willerslev, E., Stone, A.C. and Warinner, C., 2021. Ancient DNA analysis. *Nature reviews methods primers*, 1(1), p.14. https://doi.org/10.1038/s43586-020-00011-0

Pappu, S., Gunnell, Y., Akhilesh, K., Braucher, R., Taieb, M., Demory, F., & Thouveny, N. (2011). Early Pleistocene presence of Acheulian hominins in South India. *Science*, 331(6024), 1596–1599. https://doi.org/10.1126/science.1200183

Pedro, N., Brucato, N., Fernandes, V. *et al*. (2020). Papuan mitochondrial genomes and the settlement of Sahul. *J Hum Genet* 65, 875–887. https://doi.org/10.1038/s10038-020-0781-3

Peyrégne, S., Slon, V., & Kelso, J. (2024). More than a decade of genetic research on the Denisovans. *Nature Reviews Genetics |*, *25*, 83–103. https://doi.org/10.1038/s41576-023-00643-4

Power, R. C., Salazar-García, D. C., Rubini, M., Darlas, A., Havarti, K., Walker, M., Hublin, J. J., & Henry, A. G. (2018). Dental calculus indicates widespread plant use within the stable Neanderthal dietary niche. *Journal of Human Evolution*, 119, 27–41. https://doi.org/10.1016/j.jhevol.2018.02.009

Prüfer, K., de Filippo, C., Grote, S., Mafessoni, † Fabrizio, Korlević, P., Hajdinjak, M., Vernot, B., Skov, L., Hsieh, P., Peyrégne, S., Reher, D., Hopfe, C., Nagel, S., Maricic, T., Fu, Q., Theunert, C., Rogers, R., Skoglund, P., Chintalapati, M., ... Pääbo, S. (2017). *A high-coverage Neandertal genome from Vindija Cave in Croatia*. https://doi.org/10.1126/science.aao1887

Prüfer, K., Racimo, F., Patterson, N., Jay, F., Sankararaman, S., Sawyer, S., Heinze, A., Renaud, G., Sudmant, P. H., de Filippo, C., Li, H., Mallick, S., Dannemann, M., Fu, Q., Kircher, M., Kuhlwilm, M., Lachmann, M., Meyer, M., Ongyerth, M., ... Pääbo, S. (2014). The complete genome sequence of a Neanderthal from the Altai Mountains. *Nature*, 505(7481), 43–49. https://doi.org/10.1038/nature12886

Radovčić, D., Sršen, A. O., Radovčić, J., & Frayer, D. W. (2015). Evidence for neandertal jewelry: Modified white-tailed eagle claws at krapina. *PLoS ONE*, *10*(3). https://doi.org/10.1371/journal.pone.0119802

Reich, D., Green, R. E., Kircher, M., Krause, J., Patterson, N., Durand, E. Y., Viola, B., Briggs, A. W., Stenzel, U., Johnson, P. L. F., Maricic, T., Good, J. M., Marques-Bonet, T., Alkan, C., Fu, Q., Mallick, S., Li, H., Meyer, M., Eichler, E. E., ... Pääbo, S. (2010). Genetic history of an archaic hominin group from Denisova cave in Siberia. *Nature*, 468(7327), 1053–1060. https://doi.org/10.1038/nature09710

Reich, D., Patterson, N., Kircher, M., Delfin, F., Nandineni, M. R., Pugach, I., Ko, A. M. S., Ko, Y. C., Jinam, T. A., Phipps, M. E., Saitou, N., Wollstein, A., Kayser, M., Pääbo, S., & Stoneking, M. (2011). Denisova admixture and the first modern human dispersals into Southeast Asia and Oceania. *American Journal of Human Genetics*, *89*(4), 516–528. https://doi.org/10.1016/j.ajhg.2011.09.005

Richards, M. P., Pettitt, P. B., Stiner, M. C., & Trinkaus, E. (2001). *Stable isotope evidence for increasing dietary breadth in the European mid-Upper Paleolithic*. www.pnas.orgcgidoi10.1073pnas.111155298

Richards, M. P., Pettitt, P. B., Trinkaus, E., Smith, F. H., & Paunović, M. (2000). Neanderthal diet at Vindija and Neanderthal predation: The evidence from stable isotopes. *Proceedings of the National Academy of Sciences*. www.pnas.orgcgidoi10.1073pnas.120178997

Richards, M. P., & Trinkaus, E. (2009). *Isotopic evidence for the diets of European Neanderthals and early modern humans*. Proc. Natl. Acad. Sci. U.S.A. 106 (38) 16034-16039, https://doi.org/10.1073/pnas.0903821106

Richter, D., Grün, R., Joannes-Boyau, R., Steele, T. E., Amani, F., Rué, M., Fernandes, P., Raynal, J.-P., Geraads, D., Ben-Ncer, A., Hublin, J.-J., & Mcpherron, S. P. (2017). The age of the hominin fossils from Jebel Irhoud, Morocco, and the origins of the Middle Stone Age. *Nature Publishing Group*. https://doi.org/10.1038/nature22335

Richter, K. K., Codlin, M. C., Seabrook, M., & Warinner, C. (2022). *A primer for ZooMS applications in archaeology*. 119 (20). https://doi.org/10.1073/pnas.2109323119/-/DCSupplemental

Rightmire, G. P. (1998). Human evolution in the Middle Pleistocene: The role of Homo heidelbergensis. *Evolutionary Anthropology*, 6, 218–227.

Sankararaman, S., Mallick, S., Patterson, N., & Reich, D. (2016). The Combined Landscape of Denisovan and Neanderthal Ancestry in Present-Day Humans. *Current Biology*, 26(9), 1241–1247. https://doi.org/10.1016/j.cub.2016.03.037

Shipman, P., & Rose, J. (1983). Early Hominid Hunting, Butchering, and Carcass-Processing Behaviors: Approaches to the Fossil Record. *Journal of Anthropological Archaeology*, 2.

Shunkov, M. v., Kulik, N. A., Kozlikin, M. B., Sokol, E. v., Miroshnichenko, L. v., & Ulianov, V. A. (2018). The Phosphates of Pleistocene–Holocene Sediments of the Eastern Gallery of Denisova Cave. *Doklady Earth Sciences*, *478*(1), 46–50. https://doi.org/10.1134/S1028334X18010270

Skov, L., Peyrégne, S., Popli, D., Iasi, L. N. M., Devièse, T., Slon, V., Zavala, E. I., Hajdinjak, M., Sümer, A. P., Grote, S., Bossoms Mesa, A., López Herráez, D., Nickel, B., Nagel, S., Richter, J., Essel, E., Gansauge, M., Schmidt, A., Korlević, P., … Peter, B. M. (2022). Genetic insights into the social organization of Neanderthals. *Nature*, *610*(7932), 519–525. https://doi.org/10.1038/s41586-022-05283-y

Slimak, L., Zanolli, C., Higham, T., Frouin, M., Schwenninger, J.-L., Arnold, L. J., Demuro, M., Douka, K., Mercier, N., Guérin, G., Valladas, H., Yvorra, P., Giraud, Y., Seguin-Orlando, A., Orlando, L., & Lewis, J. E. (2022). Modern human incursion into Neanderthal territories 54,000 years ago at Mandrin, France. *Science Advances*, 8(6), eabj9496. https://doi.org/10.1126/sciadv.abj9496

Slon, V., Mafessoni, F., Vernot, B., de Filippo, C., Grote, S., Viola, B., Hajdinjak, M., Peyrégne, S., Nagel, S., Brown, S., Douka, K., Higham, T., Kozlikin, M. B., Shunkov, M. v., Derevianko, A. P., Kelso, J., Meyer, M., Prüfer, K., & Pääbo, S. (2018). The genome of the offspring of a Neanderthal mother and a Denisovan father. *Nature*, *561*(7721), 113–116. https://doi.org/10.1038/s41586-018-0455-x

Smith, B. N., & Epsten, S. (1971). Two Categories of 1CC/12C Ratios for Higher Plants. In *Plant PhysioL* (Vol. 47). https://doi.org/10.1104/pp.47.3.380

Stewart, J. R., García-Rodríguez, O., Knul, M. V., Sewell, L., Montgomery, H., Thomas, M. G., & Diekmann, Y. (2019). Palaeoecological and genetic evidence for Neanderthal power locomotion as an adaptation to a woodland environment. *Quaternary Science Reviews*, 217, 310-315. https://doi.org/10.1016/j.quascirev.2018.12.023

Stringer, C. B., & Andrews, P. (1988). Genetic and Fossil Evidence for the Origin of Modern Humans. *Science*, 239(4845) https://doi.org/10.1126/science.3125610

Stringer, C. (2012). The status of Homo heidelbergensis (Schoetensack 1908). *Evolutionary Anthropology*, 21, 101–107.

Shunkov, M. V., Kozlikin, M. B. & Derevianko, A. P. (2020). Dynamics of the Altai Paleolithic industries in the archaeological record of Denisova Cave. *Quat. Int.* https://doi.org/10.1016/j.quaint.2020.02.017

Szpak, P. (2014). Complexities of nitrogen isotope biogeochemistry in plant-soil systems: Implications for the study of ancient agricultural and animal management practices. In *Frontiers in Plant Science* (Vol. 5, Issue JUN). Frontiers Research Foundation. https://doi.org/10.3389/fpls.2014.00288

Szpak, P., Krippner, K., & Richards, M. P. (2017). Effects of Sodium Hydroxide Treatment and Ultrafiltration on the Removal of Humic Contaminants from Archaeological Bone. *International Journal of Osteoarchaeology*, *27*(6), 1070–1077. https://doi.org/10.1002/oa.2630

Timmermann, A. (2020). Quantifying the potential causes of Neanderthal extinction: Abrupt climate change versus competition and interbreeding. *Quaternary Science Reviews*, 238. https://doi.org/10.1016/j.quascirev.2020.106331

van Holstein, L. A., & Foley, R. A. (2024). Diversity-dependent speciation and extinction in hominins. *Nature Ecology and Evolution*, 8(6), 1180–1190. https://doi.org/10.1038/s41559-024-02390-z

Vallini, L., Zampieri, C., Shoaee, M. J., Bortolini, E., Marciani, G., Aneli, S., Pievani, T., Benazzi, S., Barausse, A., Mezzavilla, M., Petraglia, M. D., & Pagani, L. (2024). The Persian plateau served as hub for Homo sapiens after the main out of Africa dispersal. *Nature Communications*, 15(1). https://doi.org/10.1038/s41467-024-46161-7

Vanderklift, M. A., & Ponsard, S. (2003). Sources of variation in consumer-diet δ15N enrichment: A meta-analysis. *Oecologia*, *136*(2), 169–182. https://doi.org/10.1007/s00442-003-1270-z

Vasiliev S.K., Shunkov M.V., Kozlikin M.B. (2017). Megafaunal remains from the eastern chamber of Denisova Cave and problems of reconstructing the Pleistocene environments in the Northwestern Altai. in *Problems of Archaeology, Ethnography, Anthropology of Siberia and Neighboring Territories* Vol. XXIII (2017). https://doi.org/10.1038/s41586-018-0843-2

Vasiliev, S.K., Shunkov, M. V., Kozlikin, M.B., (2013). Preliminary results of the study of Meagafauna Remains from Pleistocene Deposits in the eastern Gallery of Denisova Cave. *Problems of Archaeology, Ethnography, Anthropology of Siberia and Neighboring Territories. Vol XIX.*

Vasil´ev, S. A. (2003). *Faunal exploitation, subsistence practices and Pleistocene extinctions in Paleolithic Siberia*. Vol. 9. 513-556.

Warinner, C., Korzow Richter, K. and Collins, M.J., 2022. Paleoproteomics. *Chemical reviews*, *122*(16), pp.13401-13446. https://doi.org/10.1021/acs.chemrev.1c00703

Welker, F. (2018). Palaeoproteomics for human evolution studies. *Quaternary Science Reviews*, *190*, 137–147. https://doi.org/10.1016/j.quascirev.2018.04.033

White, T. E. (1953). A Method of Calculating the Dietary Percentage of Various Food Animals Utilized by Aboriginal Peoples. *American Antiquity*, *18*(4), 396–398. https://doi.org/10.2307/277116

Williams, M. W., Knauf, M., Cory, R., Caine, N., & Liu, F. (2007). Earth Surface Processes and Landforms Earth Surf. *Earth Surf. Process. Landforms*, *32*, 1032–1047. https://doi.org/10.1002/esp

Xia, H., Zhang, D., Wang, J., Fagernäs, Z., Li, T., Li, Y., Yao, J., Lin, D., Troché, G., Smith, G. M., Chen, X., Cheng, T., Shen, X., Han, Y., Olsen, J. v., Shen, Z., Pei, Z., Hublin, J.-J., Chen, F., & Welker, F. (2024). Middle and Late Pleistocene Denisovan subsistence at Baishiya Karst Cave. *Nature*. https://doi.org/10.1038/s41586-024-07612-9

Yaworsky, P. M., Nielsen, E. S., & Nielsen, T. K. (2024). The Neanderthal niche space of Western Eurasia 145 ka to 30 ka ago. *Nature*, 15(2). https://doi.org/10.1038/s41598-024-57490-4

Zavala, E. I., Jacobs, Z., Vernot, B., Shunkov, M. V., Kozlikin, M. B., Derevianko, A. P., Essel, E., de Fillipo, C., Nagel, S., Richter, J., Romagné, F., Schmidt, A., Li, B., O'Gorman, K., Slon, V., Kelso, J., Pääbo, S., Roberts, R. G., & Meyer, M. (2021). Pleistocene sediment DNA reveals hominin and faunal turnovers at Denisova Cave. *Nature*, 595(7867), 399–403. https://doi.org/10.1038/s41586-021-03675-0

Zilhão, J., Angelucci, D. E., Badal-García, E., D'Errico, F., Daniel, F., Dayet, L., Douka, K., Higham, T. F. G., Martínez-Sánchez, M. J., Montes-Bernárdez, R., Murcia-Mascarós, S., Pérez-Sirvent, C., Roldán-García, C., Vanhaeren, M., Villaverde, V., Wood, R., & Zapata, J. (2010). Symbolic use of marine shells and mineral pigments by Iberian Neandertals. *Proceedings of the National Academy of Sciences of the United States of America*, 107(3), 1023–1028. https://doi.org/10.1073/pnas.0914088107

Zhang, P., Zhang, X., Zhang, X., Gao, X., Huerta-Sanchez, E., & Zwyns, N. (2022). Denisovans and Homo sapiens on the Tibetan Plateau: dispersals and adaptations. *Trends in Ecology & Evolution*, 37(3), 257–267. https://doi.org/10.1016/j.tree.2021.11.004

Figure References

Figure 1.: A graphic of the Denisovan, Neanderthal and modern human relationship; Peyrégne, S., Slon, V., & Kelso, J. (2024). More than a decade of genetic research on the Denisovans. *Nature Reviews Genetics |*, *25*, 83–103. https://doi.org/10.1038/s41576-023-00643-4

Figure 2: Entrance of the Denisova cave; Siberia; https://www.flickr.com/photos/loronet/14645660133; CC BY -NC-ND 2.0

Figure 3: Plan of Denisova Cave, drawn based on graphics in Jacobs, Z., Li, B., Shunkov, M. V., Kozlikin, M. B., Bolikhovskaya, N. S., Agadjanian, A. K., Uliyanov, V. A., Vasiliev, S. K., O'gorman, K., Derevianko, A. P., & Roberts, G. (2019). Timing of archaic hominin occupation of Denisova Cave in southern Siberia. *Nature*, 565(7741), 594–599. https://doi.org/10.1038/s41586-018-0843-2

Figure 4: Stratigraphy of the East Chamber, drawn based on graphic in Jacobs, Z., Li, B., Shunkov, M. V., Kozlikin, M. B., Bolikhovskaya, N. S., Agadjanian, A. K., Uliyanov, V. A., Vasiliev, S. K., O'gorman, K., Derevianko, A. P., & Roberts, G. (2019). Timing of archaic hominin occupation of Denisova Cave in southern Siberia. *Nature*, 565(7741), 594–599. https://doi.org/10.1038/s41586-018-0843-2

Figure 5: Timeline of layer information and Marine-Isotope Stages after Jacobs, Z., Li, B., Shunkov, M. V., Kozlikin, M. B., Bolikhovskaya, N. S., Agadjanian, A. K., Uliyanov, V. A., Vasiliev, S. K., O'gorman, K., Derevianko, A. P., & Roberts, G. (2019). Timing of archaic hominin occupation of Denisova Cave in southern Siberia. *Nature*, 565(7741), 594–599. https://doi.org/10.1038/s41586-018-0843-2

Figure 5: Screenshot of a DC sample analysed in the open-source program mMass version 6.0.2 (created by Martin Strohalm 2005-13).

Figure 6: Figure 5: Screenshot of a DC sample analysed in the open-source program mMass version 6.0.2 (created by Martin Strohalm 2005-13).

Appendix

Appendix 1a: ZooMS analysed Data

Zooms_ID	Context Information	Order	Family	ZooMS taxon
DC15294	Layer 14	Artiodactyla	Bovidae	Bos/Bison
DC15295	Layer 14	Perissodactyla	Rhinocerotidae	Rhinocerotidae
DC15296	Layer 14	Artiodactyla	Bovidae/Cervidae	Cervidae/Gazella/Saiga
DC15297	Layer 14	Artiodactyla	Bovidae/Cervidae	Cervidae/Gazella/Saiga
DC15298	Layer 14	Artiodactyla	Bovidae/Cervidae	Cervidae/Gazella/Saiga
DC15299	Layer 14	Perissodactyla	Rhinocerotidae	Rhinocerotidae
DC15300	Layer 14	Perissodactyla	Equidae	Equus
DC15301	Layer 14	Artiodactyla	Bovidae	Bos/Bison
DC15302	Layer 14	Artiodactyla	Bovidae	Bos/Bison
DC15303	Layer 14	Perissodactyla	Equidae	Equus
DC15304	Layer 14	Artiodactyla	Bovidae/Cervidae	Cervidae/Gazella/Saiga
DC15305	Layer 14	Artiodactyla	Bovidae/Cervidae	Cervidae/Gazella/Saiga
DC15306	Layer 14	Proboscidea	Elephantidae	Elephantidae
DC15307	Layer 14	Artiodactyla	Bovidae/Cervidae	Cervidae/Gazella/Saiga
DC15308	Layer 14	Artiodactyla	Bovidae/Cervidae	Cervidae/Gazella/Saiga
DC15309	Layer 14	Carnivora	Felidae	Felidae
DC15310	Layer 14	Perissodactyla	Equidae	Equus
DC15311	Layer 14	Artiodactyla	Bovidae/Cervidae	Cervidae/Gazella/Saiga
DC15312	Layer 14	Perissodactyla	Equidae	Equus
DC15313	Layer 14	Perissodactyla	Rhinocerotidae	Rhinocerotidae
DC15314	Layer 14	Artiodactyla	Bovidae/Cervidae	Cervidae/Gazella/Saiga
DC15315	Layer 14	Artiodactyla	Bovidae/Cervidae	Cervidae/Gazella/Saiga
DC15317	Layer 14	Artiodactyla	Bovidae/Cervidae	Cervidae/Gazella/Saiga
DC15318	Layer 14	Perissodactyla	Rhinocerotidae	Rhinocerotidae
DC15319	Layer 14	Artiodactyla	Bovidae/Cervidae	Cervidae/Gazella/Saiga
DC15320	Layer 14	Perissodactyla	Equidae	Equus
DC15321	Layer 14	Perissodactyla	Rhinocerotidae	Rhinocerotidae
DC15322	Layer 14	Perissodactyla	Equidae	Equus

DC15323	Layer 14	Artiodactyla	Bovidae	Bos/Bison
DC15324	Layer 14	Artiodactyla	Bovidae/Cervidae	Cervidae/Gazella/Saiga
DC15325	Layer 14	Artiodactyla	Bovidae/Cervidae	Cervidae/Gazella/Saiga
DC15326	Layer 14	Artiodactyla	Bovidae/Cervidae	Cervidae/Gazella/Saiga
DC15327	Layer 14			fail
DC15328	Layer 14	Artiodactyla	Bovidae	Bos/Bison
DC15329	Layer 14	Artiodactyla	Bovidae/Cervidae	Cervidae/Gazella/Saiga
DC15330	Layer 14			Unknown
DC15331	Layer 14	Artiodactyla	Bovidae	Bos/Bison
DC15332	Layer 14			Unknown
DC15333	Layer 14	Artiodactyla	Bovidae/Cervidae	Cervidae/Gazella/Saiga
DC15334	Layer 14	Proboscidea	Elephantidae	Elephantidae
DC15335	Layer 14	Artiodactyla	Bovidae	Bos/Bison
DC15336	Layer 14			fail
DC15337	Layer 14	Artiodactyla	Bovidae	Bos/Bison
DC15338	Layer 14	Artiodactyla	Bovidae/Cervidae	Cervidae/Gazella/Saiga
DC15339	Layer 14	Perissodactyla	Equidae	Equus
DC15340	Layer 14			Fail
DC15341	Layer 14			Fail
DC15342	Layer 14	Artiodactyla	Bovidae	Bos/Bison
DC15343	Layer 14	Artiodactyla	Bovidae/Cervidae	Cervidae/Gazella/Saiga
DC15344	Layer 14	Artiodactyla	Bovidae	Bos/Bison
DC15345	Layer 14	Artiodactyla	Bovidae/Cervidae	Cervidae/Gazella/Saiga
DC15346	Layer 14			Fail
DC15347	Layer 14	Artiodactyla	Bovidae/Cervidae	Cervidae/Gazella/Saiga
DC15348	Layer 14	Artiodactyla	Bovidae	Bos/Bison
DC15349	Layer 14			Fail
DC15350	Layer 14			fail
DC15351	Layer 14	Perissodactyla	Equidae	Equus
DC15352	Layer 14	Perissodactyla	Rhinocerotidae	Rhinocerotidae
DC15353	Layer 14			Fail
DC15354	Layer 14	Artiodactyla	Bovidae/Cervidae	Cervidae/Gazella/Saiga
DC15355	Layer 14	Artiodactyla	Bovidae/Cervidae	Cervidae/Gazella/Saiga
DC15356	Layer 14			fail
DC15357	Layer 14	Perissodactyla	Rhinocerotidae	Rhinocerotidae
DC15358	Layer 14	Artiodactyla	Bovidae/Cervidae	Cervidae/Gazella/Saiga

DC15359	Layer 14			Fail
DC15360	Layer 14	Artiodactyla	Bovidae	Bos/Bison
DC15361	Layer 14	Perissodactyla	Rhinocerotidae	Rhinocerotidae
DC15362	Layer 14	Carnivora	Felidae	Felidae
DC15363	Layer 14	Artiodactyla	Bovidae/Cervidae	Cervidae/Gazella/Saiga
DC15364	Layer 14	Perissodactyla	Equidae	Equus
DC15365	Layer 14	Artiodactyla	Bovidae/Cervidae	Cervidae/Gazella/Saiga
DC15366	Layer 14	Artiodactyla	Bovidae/Cervidae	Cervidae/Gazella/Saiga
DC15367	Layer 14	Artiodactyla	Bovidae/Cervidae	Cervidae/Gazella/Saiga
DC15368	Layer 14	Artiodactyla	Bovidae/Cervidae	Cervidae/Gazella/Saiga
DC15369	Layer 14	Carnivora	Canidae	Canidae
DC15370	Layer 14	Artiodactyla	Bovidae	Bos/Bison
DC15371	Layer 14	Artiodactyla	Bovidae/Cervidae	Cervidae/Gazella/Saiga
DC15372	Layer 14	Artiodactyla	Bovidae	Bos/Bison
DC15373	Layer 14	Perissodactyla	Equidae	Equus
DC15374	Layer 14	Artiodactyla	Bovidae/Cervidae	Cervidae/Gazella/Saiga
DC15375	Layer 14	Artiodactyla	Bovidae/Cervidae	Cervidae/Gazella/Saiga
DC15376	Layer 14			Fail
DC15377	Layer 14	Artiodactyla	Bovidae	Bos/Bison
DC15378	Layer 14	Artiodactyla	Bovidae/Cervidae	Cervidae/Gazella/Saiga
DC15379	Layer 14	Perissodactyla	Equidae	Equus
DC15380	Layer 14	Artiodactyla	Bovidae	Bos/Bison
DC15381	Layer 14	Artiodactyla	Bovidae	Bos/Bison
DC15382	Layer 14	Artiodactyla	Bovidae	Bos/Bison
DC15383	Layer 14	Artiodactyla	Bovidae	Bos/Bison
DC15384	Layer 14	Artiodactyla	Bovidae	Bos/Bison
DC15385	Layer 14	Proboscidea	Elephantidae	Elephantidae
DC15386	Layer 14	Perissodactyla	Equidae	Equus
DC15387	Layer 14	Perissodactyla	Rhinocerotidae	Rhinocerotidae
DC15388	Layer 14	Perissodactyla	Equidae	Equus
DC15389	Layer 14	Perissodactyla	Rhinocerotidae	Rhinocerotidae
DC15390	Layer 14	Artiodactyla	Bovidae/Cervidae	Cervidae/Gazella/Saiga
DC15391	Layer 14	Artiodactyla	Bovidae	Bos/Bison
DC15392	Layer 14	Perissodactyla	Equidae	Equus
DC15393	Layer 14	Artiodactyla	Bovidae	Bos/Bison
DC15394	Layer 14	Perissodactyla	Equidae	Equus
DC15395	Layer 14	Artiodactyla	Bovidae	Bos/Bison
DC15396	Layer 14	Perissodactyla	Rhinocerotidae	Rhinocerotidae

DC15397	Layer 14	Artiodactyla	Bovidae/Cervidae	Cervidae/Gazella/ Saiga
DC15398	Layer 14			Fail
DC15399	Layer 14	Artiodactyla	Bovidae/Cervidae	Cervidae/Gazella/ Saiga
DC15400	Layer 14	Perissodactyla	Rhinocerotidae	Rhinocerotidae
DC15401	Layer 14	Artiodactyla	Bovidae	Capra
DC15402	Layer 14	Carnivora	Felidae	Felidae
DC15403	Layer 14	Artiodactyla	Bovidae/Cervidae	Cervidae/Gazella/ Saiga
DC15404	Layer 14	Artiodactyla	Bovidae/Cervidae	Cervidae/Gazella/ Saiga
DC15405	Layer 14	Proboscidea	Elephantidae	Elephantidae
DC15406	Layer 14	Artiodactyla	Bovidae/Cervidae	Cervidae/Gazella/ Saiga
DC15407	Layer 14	Artiodactyla	Bovidae	Bos/Bison
DC15408	Layer 14	Perissodactyla	Rhinocerotidae	Rhinocerotidae
DC15409	Layer 14	Artiodactyla	Bovidae/Cervidae	Cervidae/Gazella/ Saiga
DC15410	Layer 14	Artiodactyla	Bovidae/Cervidae	Cervidae/Gazella/ Saiga
DC15411	Layer 14	Artiodactyla	Bovidae	Bos/Bison
DC15412	Layer 14	Artiodactyla	Bovidae/Cervidae	Cervidae/Gazella/ Saiga
DC15413	Layer 14	Perissodactyla	Equidae	Equus
DC15414	Layer 14	Artiodactyla	Bovidae	Bos/Bison
DC15415	Layer 14			Unknown
DC15416	Layer 14	Artiodactyla	Bovidae/Cervidae	Cervidae/Gazella/ Saiga
DC15417	Layer 14	Artiodactyla	Bovidae	Capra
DC15418	Layer 14	Carnivora	Canidae	Canidae
DC15419	Layer 14			Unknown
DC15420	Layer 14	Perissodactyla	Rhinocerotidae	Rhinocerotidae
DC15421	Layer 14	Artiodactyla	Bovidae/Cervidae	Cervidae/Gazella/ Saiga
DC15422	Layer 14	Proboscidea	Elephantidae	Elephantidae
DC15423	Layer 14	Artiodactyla	Bovidae	Bos/Bison
DC15424	Layer 14	Artiodactyla	Bovidae/Cervidae	Cervidae/Gazella/ Saiga
DC15425	Layer 14	Artiodactyla	Bovidae/Cervidae	Cervidae/Gazella/ Saiga
DC15426	Layer 14	Artiodactyla	Bovidae	Bos/Bison
DC15427	Layer 13	Artiodactyla	Bovidae	Bos/Bison
DC15428	Layer 13	Artiodactyla	Bovidae	Bos/Bison
DC15429	Layer 13	Artiodactyla	Bovidae	Bos/Bison
DC15430	Layer 13	Artiodactyla	Bovidae/Cervidae	Cervidae/Gazella/ Saiga
DC15431	Layer 13	Perissodactyla	Rhinocerotidae	Rhinocerotidae

DC15432	Layer 13	Artiodactyla	Bovidae/Cervidae	Cervidae/Gazella/Saiga
DC15433	Layer 13	Artiodactyla	Bovidae	Bos/Bison
DC15434	Layer 13	Artiodactyla	Bovidae	Bos/Bison
DC15435	Layer 13	Artiodactyla	Bovidae	Bos/Bison
DC15436	Layer 13	Artiodactyla	Bovidae	Bos/Bison
DC15437	Layer 13	Perissodactyla	Equidae	Equus
DC15438	Layer 13	Artiodactyla	Bovidae	Bos/Bison
DC15439	Layer 13			Unknown
DC15440	Layer 13	Artiodactyla	Bovidae	Bos/Bison
DC15441	Layer 13	Perissodactyla	Equidae	Equus
DC15442	Layer 13	Artiodactyla	Bovidae	Bos/Bison
DC15443	Layer 13	Perissodactyla	Equidae	Equus
DC15444	Layer 13	Artiodactyla	Bovidae	Bos/Bison
DC15445	Layer 13	Proboscidea	Elephantidae	Elephantidae
DC15446	Layer 13	Carnivora	Felidae/Hyaenidae/Mustelidae	Panthera/Crocuta/Mustelidae
DC15447	Layer 13	Artiodactyla	Bovidae	Bos/Bison
DC15448	Layer 13			Unknown
DC15449	Layer 13	Perissodactyla	Equidae	Equus
DC15450	Layer 13	Carnivora	Canidae	Canidae
DC15451	Layer 13	Perissodactyla	Rhinocerotidae	Rhinocerotidae
DC15452	Layer 13			Unknown
DC15453	Layer 13	Perissodactyla	Rhinocerotidae	Rhinocerotidae
DC15454	Layer 13	Perissodactyla	Rhinocerotidae	Rhinocerotidae
DC15455	Layer 13	Perissodactyla	Rhinocerotidae	Rhinocerotidae
DC15456	Layer 13	Artiodactyla	Bovidae/Cervidae	Cervidae/Gazella/Saiga
DC15457	Layer 13	Artiodactyla	Bovidae/Cervidae	Cervidae/Gazella/Saiga
DC15458	Layer 13	Artiodactyla	Bovidae/Cervidae	Cervidae/Gazella/Saiga
DC15459	Layer 13	Artiodactyla	Bovidae/Cervidae	Cervidae/Gazella/Saiga
DC15460	Layer 13	Perissodactyla	Rhinocerotidae	Rhinocerotidae
DC15461	Layer 13	Artiodactyla	Bovidae	Bos/Bison
DC15462	Layer 13	Perissodactyla	Rhinocerotidae	Rhinocerotidae
DC15463	Layer 13	Artiodactyla	Bovidae/Cervidae	Cervidae/Gazella/Saiga
DC15464	Layer 13	Artiodactyla	Bovidae	Bos/Bison
DC15465	Layer 13	Perissodactyla	Equidae	Equus
DC15466	Layer 13	Perissodactyla	Equidae	Equus
DC15467	Layer 13	Perissodactyla	Rhinocerotidae	Rhinocerotidae
DC15468	Layer 13	Artiodactyla	Bovidae/Cervidae	Cervidae/Gazella/Saiga
DC15469	Layer 13	Proboscidea	Elephantidae	Elephantidae

DC15470	Layer 13	Proboscidea	Elephantidae	Elephantidae
DC15471	Layer 13	Perissodactyla	Rhinocerotidae	Rhinocerotidae
DC15472	Layer 13	Artiodactyla	Bovidae	Bos/Bison
DC15473	Layer 13	Proboscidea	Elephantidae	Elephantidae
DC15474	Layer 13	Perissodactyla	Rhinocerotidae	Rhinocerotidae
DC15475	Layer 13	Artiodactyla	Bovidae	Bos/Bison
DC15476	Layer 13	Artiodactyla	Bovidae/Cervidae	Cervidae/Gazella/Saiga
DC15477	Layer 13	Artiodactyla	Bovidae/Cervidae	Cervidae/Gazella/Saiga
DC15478	Layer 13	Perissodactyla	Rhinocerotidae	Rhinocerotidae
DC15479	Layer 13	Artiodactyla	Bovidae/Cervidae	Cervidae/Gazella/Saiga
DC15480	Layer 13	Proboscidea	Elephantidae	Elephantidae
DC15481	Layer 13	Artiodactyla	Bovidae/Cervidae	Cervidae/Gazella/Saiga
DC15482	Layer 13	Artiodactyla	Bovidae/Cervidae	Cervidae/Gazella/Saiga
DC15483	Layer 13	Artiodactyla	Bovidae	Bos/Bison
DC15484	Layer 13	Perissodactyla	Rhinocerotidae	Rhinocerotidae
DC15485	Layer 13	Perissodactyla	Rhinocerotidae	Rhinocerotidae
DC15486	Layer 13	Perissodactyla	Rhinocerotidae	Rhinocerotidae
DC15487	Layer 13	Artiodactyla	Bovidae/Cervidae	Cervidae/Gazella/Saiga
DC15488	Layer 13	Artiodactyla	Bovidae/Cervidae	Cervidae/Gazella/Saiga
DC15489	Layer 13	Artiodactyla	Bovidae/Cervidae	Cervidae/Gazella/Saiga
DC15490	Layer 13	Artiodactyla	Bovidae	Bos/Bison
DC15491	Layer 13	Artiodactyla	Bovidae	Bos/Bison
DC15492	Layer 13	Artiodactyla	Bovidae	Bos/Bison
DC15493	Layer 13			Unknown
DC15494	Layer 13	Artiodactyla	Bovidae/Cervidae	Cervidae/Gazella/Saiga
DC15495	Layer 13	Artiodactyla	Bovidae	Bos/Bison
DC15496	Layer 13	Artiodactyla	Bovidae/Cervidae	Cervidae/Gazella/Saiga
DC15497	Layer 13	Proboscidea	Elephantidae	Elephantidae
DC15498	Layer 13	Proboscidea	Elephantidae	Elephantidae
DC15499	Layer 13	Artiodactyla	Bovidae	Bos/Bison
DC15500	Layer 13	Artiodactyla	Bovidae	Bos/Bison
DC15501	Layer 13	Perissodactyla	Equidae	Equus
DC15502	Layer 13	Proboscidea	Elephantidae	Elephantidae
DC15503	Layer 13	Artiodactyla	Bovidae	Bos/Bison
DC15504	Layer 13	Artiodactyla	Bovidae/Cervidae	Cervidae/Gazella/Saiga
DC15505	Layer 13	Artiodactyla	Bovidae	Bos/Bison
DC15506	Layer 13	Perissodactyla	Equidae	Equus

DC15507	Layer 13	Perissodactyla	Equidae	Equus
DC15508	Layer 13	Artiodactyla	Bovidae/Cervidae	Cervidae/Gazella/Saiga
DC15509	Layer 13	Artiodactyla	Bovidae/Cervidae	Cervidae/Gazella/Saiga
DC15510	Layer 13	Artiodactyla	Bovidae/Cervidae	Cervidae/Gazella/Saiga
DC15511	Layer 13	Carnivora	Felidae/Hyaenidae/Mustelidae	Panthera/Crocuta/Mustelidae
DC15512	Layer 13	Perissodactyla	Equidae	Equus
DC15513	Layer 13	Artiodactyla	Bovidae	Bos/Bison
DC15514	Layer 13	Perissodactyla	Equidae	Equus
DC15515	Layer 13	Perissodactyla	Rhinocerotidae	Rhinocerotidae
DC15516	Layer 13	Proboscidea	Elephantidae	Elephantidae
DC15517	Layer 13	Artiodactyla	Bovidae	Bos/Bison
DC15518	Layer 13	Artiodactyla	Bovidae	Bos/Bison
DC15519	Layer 13	Artiodactyla	Bovidae	Capra
DC15520	Layer 13	Perissodactyla	Equidae	Equus
DC15521	Layer 13	Artiodactyla	Bovidae/Cervidae	Cervidae/Gazella/Saiga
DC15522	Layer 13	Perissodactyla	Rhinocerotidae	Rhinocerotidae
DC15523	Layer 13	Carnivora	Felidae/Hyaenidae/Mustelidae	Panthera/Crocuta/Mustelidae
DC15524	Layer 13	Artiodactyla	Bovidae/Cervidae	Cervidae/Gazella/Saiga
DC15525	Layer 13	Carnivora	Canidae	Canidae
DC15526	Layer 13			Unknown
DC15527	Layer 13	Proboscidea	Elephantidae	Elephantidae
DC15528	Layer 13	Artiodactyla	Bovidae/Cervidae	Cervidae/Gazella/Saiga
DC15529	Layer 13			Unknown
DC15530	Layer 13	Perissodactyla	Equidae	Equus
DC15531	Layer 13			Unknown
DC15532	Layer 13			Unknown
DC15533	Layer 13	Artiodactyla	Bovidae	Bos/Bison
DC15534	Layer 13	Artiodactyla	Bovidae/Cervidae	Cervidae/Gazella/Saiga
DC15535	Layer 13	Artiodactyla	Bovidae/Cervidae	Cervidae/Gazella/Saiga
DC15536	Layer 13	Proboscidea	Elephantidae	Elephantidae
DC15537	Layer 13	Proboscidea	Elephantidae	Elephantidae
DC15538	Layer 13	Artiodactyla	Bovidae/Cervidae	Cervidae/Gazella/Saiga
DC15539	Layer 13	Artiodactyla	Bovidae/Cervidae	Cervidae/Gazella/Saiga
DC15540	Layer 13	Artiodactyla	Bovidae	Bos/Bison
DC15541	Layer 13	Artiodactyla	Bovidae/Cervidae	Cervidae/Gazella/Saiga

DC15542	Layer 13	Proboscidea	Elephantidae	Elephantidae
DC15543	Layer 13	Artiodactyla	Bovidae	Bos/Bison
DC15544	Layer 13	Artiodactyla	Bovidae	Bos/Bison
DC15545	Layer 13	Artiodactyla	Bovidae	Bos/Bison
DC15546	Layer 13	Artiodactyla	Bovidae	Bos/Bison
DC15547	Layer 13	Proboscidea	Elephantidae	Elephantidae
DC15548	Layer 13	Artiodactyla	Bovidae	Bos/Bison
DC15549	Layer 13	Artiodactyla	Bovidae/Cervidae	Cervidae/Gazella/Saiga
DC15550	Layer 13	Artiodactyla	Bovidae	Bos/Bison
DC15551	Layer 13	Artiodactyla	Bovidae	Capra
DC15552	Layer 13	Perissodactyla	Rhinocerotidae	Rhinocerotidae
DC15553	Layer 13	Proboscidea	Elephantidae	Elephantidae
DC15554	Layer 13	Perissodactyla	Rhinocerotidae	Rhinocerotidae
DC15555	Layer 13	Perissodactyla	Equidae	Equus
DC15556	Layer 13	Artiodactyla	Bovidae	Bos/Bison
DC15557	Layer 13	Proboscidea	Elephantidae	Elephantidae
DC15558	Layer 13	Artiodactyla	Bovidae/Cervidae	Cervidae/Gazella/Saiga
DC15559	Layer 13	Carnivora	Canidae	Canidae
DC15560	Layer 13	Perissodactyla	Equidae	Equus
DC15561	Layer 13	Artiodactyla	Bovidae	Bos/Bison
DC15562	Layer 13	Artiodactyla	Bovidae	Bos/Bison
DC15563	Layer 13	Perissodactyla	Rhinocerotidae	Rhinocerotidae
DC15564	Layer 13	Perissodactyla	Rhinocerotidae	Rhinocerotidae
DC15565	Layer 13	Artiodactyla	Bovidae	Bos/Bison
DC15566	Layer 13	Perissodactyla	Rhinocerotidae	Rhinocerotidae
DC15567	Layer 13	Perissodactyla	Rhinocerotidae	Rhinocerotidae
DC15568	Layer 13	Perissodactyla	Equidae	Equus
DC15569	Layer 13	Proboscidea	Elephantidae	Elephantidae
DC15570	Layer 13			Unknown
DC15571	Layer 13	Artiodactyla	Bovidae	Bos/Bison
DC15572	Layer 13	Perissodactyla	Equidae	Equus
DC15573	Layer 13	Artiodactyla	Bovidae/Cervidae	Cervidae/Gazella/Saiga
DC15574	Layer 13	Perissodactyla	Rhinocerotidae	Rhinocerotidae
DC15575	Layer 13	Artiodactyla	Bovidae/Cervidae	Cervidae/Gazella/Saiga
DC15576	Layer 13	Proboscidea	Elephantidae	Elephantidae
DC15577	Layer 13	Artiodactyla	Bovidae	Bos/Bison
DC15578	Layer 13	Artiodactyla	Bovidae	Bos/Bison
DC15579	Layer 13	Artiodactyla	Bovidae	Bos/Bison
DC15580	Layer 13	Artiodactyla	Bovidae	Bos/Bison
DC15581	Layer 13			Unknown
DC15582	Layer 13	Perissodactyla	Rhinocerotidae	Rhinocerotidae

DC15583	Layer 13	Proboscidea	Elephantidae	Elephantidae
DC15584	Layer 13	Proboscidea	Elephantidae	Elephantidae
DC15585	Layer 13	Artiodactyla	Bovidae	Bos/Bison
DC15586	Layer 13	Artiodactyla	Bovidae	Bos/Bison
DC15587	Layer 13	Artiodactyla	Bovidae	Bos/Bison
DC15588	Layer 13	Perissodactyla	Equidae	Equus
DC15589	Layer 13	Artiodactyla	Bovidae	Bos/Bison
DC15590	Layer 13	Artiodactyla	Bovidae	Bos/Bison
DC15591	Layer 13			Unknown
DC15592	Layer 13	Artiodactyla	Bovidae	Bos/Bison
DC15593	Layer 13	Perissodactyla	Rhinocerotidae	Rhinocerotidae
DC15594	Layer 13	Artiodactyla	Bovidae	Bos/Bison
DC15595	Layer 13	Perissodactyla	Rhinocerotidae	Rhinocerotidae
DC15596	Layer 13	Artiodactyla	Bovidae	Bos/Bison
DC15597	Layer 13	Artiodactyla	Bovidae	Bos/Bison
DC15598	Layer 13	Artiodactyla	Bovidae	Capra
DC15599	Layer 13	Artiodactyla	Bovidae	Bos/Bison
DC15600	Layer 13	Artiodactyla	Bovidae/Cervidae	Cervidae/Gazella/Saiga
DC15601	Layer 13	Artiodactyla	Bovidae	Bos/Bison
DC15602	Layer 13	Artiodactyla	Bovidae	Bos/Bison
DC15603	Layer 13	Artiodactyla	Bovidae	Bos/Bison
DC15604	Layer 13	Artiodactyla	Bovidae	Bos/Bison
DC15605	Layer 13	Artiodactyla	Bovidae	Capra
DC15606	Layer 13	Artiodactyla	Bovidae	Bos/Bison
DC15607	Layer 13	Perissodactyla	Equidae	Equus
DC15608	Layer 13	Artiodactyla	Bovidae/Cervidae	Cervidae/Gazella/Saiga
DC15609	Layer 13	Artiodactyla	Bovidae/Cervidae	Cervidae/Gazella/Saiga
DC15610	Layer 13	Proboscidea	Elephantidae	Elephantidae
DC15611	Layer 13	Artiodactyla	Bovidae	Bos/Bison
DC15612	Layer 13			fail
DC15613	Layer 13	Carnivora	Canidae	Canidae
DC15614	Layer 13	Artiodactyla	Bovidae/Cervidae	Cervidae/Gazella/Saiga
DC15615	Layer 13	Perissodactyla	Rhinocerotidae	Rhinocerotidae
DC15616	Layer 13	Carnivora	Canidae	Canidae
DC15617	Layer 13	Artiodactyla	Bovidae	Bos/Bison
DC15618	Layer 13	Artiodactyla	Bovidae/Cervidae	Cervidae/Gazella/Saiga
DC15619	Layer 13	Artiodactyla	Bovidae/Cervidae	Cervidae/Gazella/Saiga
DC15620	Layer 13	Artiodactyla	Bovidae/Cervidae	Cervidae/Gazella/Saiga
DC15621	Layer 13	Artiodactyla	Bovidae	Bos/Bison

DC15622	Layer 13	Perissodactyla	Rhinocerotidae	Rhinocerotidae
DC15623	Layer 13			Unknown
DC15624	Layer 13	Carnivora	Felidae	Felidae
DC15625	Layer 13	Carnivora	Felidae	Felidae
DC15626	Layer 13	Artiodactyla	Bovidae	Bos/Bison
DC15627	Layer 13	Artiodactyla	Bovidae	Bos/Bison
DC15628	Layer 13	Artiodactyla	Bovidae/Cervidae	Cervidae/Gazella/Saiga
DC15629	Layer 13	Artiodactyla	Bovidae/Cervidae	Cervidae/Gazella/Saiga
DC15630	Layer 13	Artiodactyla	Bovidae	Bos/Bison
DC15631	Layer 13	Artiodactyla	Bovidae/Cervidae	Cervidae/Gazella/Saiga
DC15632	Layer 13	Artiodactyla	Bovidae	Bos/Bison
DC15633	Layer 13	Artiodactyla	Bovidae/Cervidae	Cervidae/Gazella/Saiga
DC15634	Layer 13	Perissodactyla	Equidae	Equus
DC15635	Layer 13	Artiodactyla	Bovidae	Bos/Bison
DC15636	Layer 13	Perissodactyla	Equidae	Equus
DC15637	Layer 13	Rodentia	Castoridae	Castoridae
DC15638	Layer 13	Artiodactyla	Bovidae	Bos/Bison
DC15639	Layer 13	Artiodactyla	Bovidae	Bos/Bison
DC15640	Layer 13	Artiodactyla	Bovidae	Bos/Bison
DC15641	Layer 13	Perissodactyla	Rhinocerotidae	Rhinocerotidae
DC15642	Layer 13	Artiodactyla	Bovidae/Cervidae	Cervidae/Gazella/Saiga
DC15643	Layer 13	Artiodactyla	Bovidae	Bos/Bison
DC15644	Layer 13	Perissodactyla	Rhinocerotidae	Rhinocerotidae
DC15645	Layer 13	Proboscidea	Elephantidae	Elephantidae
DC15646	Layer 13	Artiodactyla	Bovidae	Bos/Bison
DC15647	Layer 13	Artiodactyla	Bovidae/Cervidae	Cervidae/Gazella/Saiga
DC15648	Layer 13	Proboscidea	Elephantidae	Elephantidae
DC15649	Layer 13	Artiodactyla	Bovidae	Bos/Bison
DC15650	Layer 13	Artiodactyla	Bovidae/Cervidae	Cervidae/Gazella/Saiga
DC15651	Layer 13	Artiodactyla	Bovidae	Bos/Bison
DC15652	Layer 13	Perissodactyla	Rhinocerotidae	Rhinocerotidae
DC15653	Layer 13	Artiodactyla	Bovidae	Bos/Bison
DC15654	Layer 13	Perissodactyla	Rhinocerotidae	Rhinocerotidae
DC15655	Layer 13	Artiodactyla	Bovidae	Bos/Bison
DC15656	Layer 13	Artiodactyla	Bovidae	Bos/Bison
DC15657	Layer 13	Carnivora	Canidae	Canidae
DC15658	Layer 13	Perissodactyla	Rhinocerotidae	Rhinocerotidae
DC15659	Layer 13			fail
DC15660	Layer 13	Carnivora	Canidae	Canidae

DC15661	Layer 13	Artiodactyla	Bovidae/Cervidae	Cervidae/Gazella/Saiga
DC15662	Layer 13	Perissodactyla	Rhinocerotidae	Rhinocerotidae
DC15663	Layer 13	Artiodactyla	Bovidae/Cervidae	Cervidae/Gazella/Saiga
DC15664	Layer 13			Unknown
DC15665	Layer 13	Artiodactyla	Bovidae	Bos/Bison
DC15666	Layer 13	Artiodactyla	Bovidae/Cervidae	Cervidae/Gazella/Saiga
DC15667	Layer 13			Unknown
DC15668	Layer 13	Proboscidea	Elephantidae	Elephantidae
DC15669	Layer 13			Unknown
DC15670	Layer 13	Artiodactyla	Bovidae/Cervidae	Cervidae/Gazella/Saiga
DC15671	Layer 13	Perissodactyla	Rhinocerotidae	Rhinocerotidae
DC15672	Layer 13	Perissodactyla	Rhinocerotidae	Rhinocerotidae
DC15673	Layer 13	Artiodactyla	Bovidae	Bos/Bison
DC15674	Layer 13	Artiodactyla	Bovidae/Cervidae	Cervidae/Gazella/Saiga
DC15675	Layer 13	Perissodactyla	Rhinocerotidae	Rhinocerotidae
DC15676	Layer 13	Artiodactyla	Bovidae	Bos/Bison
DC15677	Layer 13			Unknown
DC15678	Layer 13	Artiodactyla	Bovidae/Cervidae	Cervidae/Gazella/Saiga
DC15679	Layer 13	Artiodactyla	Bovidae	Bos/Bison
DC15680	Layer 13			Unknown
DC15681	Layer 13	Artiodactyla	Bovidae/Cervidae	Cervidae/Gazella/Saiga
DC15682	Layer 13	Artiodactyla	Bovidae	Bos/Bison
DC15683	Layer 13	Artiodactyla	Bovidae	Bos/Bison
DC15684	Layer 13			fail
DC15685	Layer 13	Artiodactyla	Bovidae/Cervidae	Cervidae/Gazella/Saiga
DC15686	Layer 13	Artiodactyla	Bovidae/Cervidae	Cervidae/Gazella/Saiga
DC15687	Layer 13	Artiodactyla	Bovidae/Cervidae	Cervidae/Gazella/Saiga
DC15688	Layer 13	Perissodactyla	Rhinocerotidae	Rhinocerotidae
DC15689	Layer 13	Perissodactyla	Rhinocerotidae	Rhinocerotidae
DC15690	Layer 13			Unknown
DC15691	Layer 13	Proboscidea	Elephantidae	Elephantidae
DC15692	Layer 13	Perissodactyla	Rhinocerotidae	Rhinocerotidae
DC15693	Layer 13	Artiodactyla	Bovidae/Cervidae	Cervidae/Gazella/Saiga
DC15694	Layer 13	Artiodactyla	Bovidae	Bos/Bison
DC15695	Layer 13	Artiodactyla	Bovidae	Bos/Bison
DC15696	Layer 13	Artiodactyla	Bovidae/Cervidae	Cervidae/Gazella/Saiga

DC15697	Layer 13	Perissodactyla	Rhinocerotidae	Rhinocerotidae
DC15698	Layer 13	Artiodactyla	Bovidae	Bos/Bison
DC15699	Layer 13			Unknown
DC15700	Layer 13	Artiodactyla	Bovidae	Bos/Bison
DC15701	Layer 13	Artiodactyla	Bovidae	Bos/Bison
DC15702	Layer 13	Artiodactyla	Bovidae/Cervidae	Cervidae/Gazella/Saiga
DC15703	Layer 13	Proboscidea	Elephantidae	Elephantidae
DC15704	Layer 13	Artiodactyla	Bovidae	Bos/Bison
DC15705	Layer 13	Artiodactyla	Bovidae	Bos/Bison
DC15706	Layer 13	Carnivora	Canidae	Canidae
DC15707	Layer 13	Carnivora	Ursidae	Ursus
DC15708	Layer 13	Artiodactyla	Bovidae	Capra
DC15709	Layer 13	Perissodactyla	Rhinocerotidae	Rhinocerotidae
DC15710	Layer 13	Artiodactyla	Bovidae	Capra
DC15711	Layer 13	Artiodactyla	Bovidae	Capra
DC15712	Layer 13	Carnivora	Felidae/Hyaenidae	Panthera/Crocuta
DC15713	Layer 13	Artiodactyla	Bovidae	Capra
DC15714	Layer 13	Artiodactyla	Bovidae	Bos/Bison
DC15715	Layer 13	Artiodactyla	Bovidae	Bos/Bison
DC15716	Layer 13	Perissodactyla	Rhinocerotidae	Rhinocerotidae
DC15717	Layer 13	Perissodactyla	Equidae	Equus
DC15718	Layer 13	Perissodactyla	Equidae	Equus
DC15719	Layer 13	Perissodactyla	Equidae	Equus
DC15720	Layer 13	Carnivora	Felidae/Hyaenidae	Panthera/Crocuta
DC15721	Layer 13	Artiodactyla	Bovidae	Bos/Bison
DC15722	Layer 13	Artiodactyla	Bovidae	Bos/Bison
DC15723	Layer 13	Artiodactyla	Bovidae	Bos/Bison
DC15724	Layer 13	Artiodactyla	Bovidae	Bos/Bison
DC15725	Layer 13	Artiodactyla	Bovidae/Cervidae	Cervidae/Gazella/Saiga
DC15726	Layer 13	Artiodactyla	Bovidae	Capra
DC15727	Layer 13	Artiodactyla	Bovidae/Cervidae	Cervidae/Gazella/Saiga
DC15728	Layer 13	Carnivora	Canidae	Canidae
DC15729	Layer 13	Perissodactyla	Equidae	Equus
DC15730	Layer 13	Artiodactyla	Bovidae	Bos/Bison
DC15731	Layer 13	Proboscidea	Elephantidae	Elephantidae
DC15732	Layer 13	Carnivora	Canidae	Canidae
DC15733	Layer 13	Perissodactyla	Equidae	Equus
DC15734	Layer 13	Artiodactyla	Bovidae	Bos/Bison
DC15735	Layer 13	Artiodactyla	Bovidae	Bos/Bison
DC15736	Layer 13	Carnivora	Ursidae	Ursus
DC15737	Layer 13	Proboscidea	Elephantidae	Elephantidae

DC15738	Layer 13	Perissodactyla	Equidae	Equus
DC15739	Layer 13	Artiodactyla	Bovidae	Capra
DC15740	Layer 13	Artiodactyla	Bovidae	Bos/Bison
DC15741	Layer 13	Artiodactyla	Bovidae	Bos/Bison
DC15742	Layer 13	Artiodactyla	Bovidae/Cervidae	Cervidae/Gazella/Saiga
DC15743	Layer 13	Artiodactyla	Bovidae/Cervidae	Cervidae/Gazella/Saiga
DC15744	Layer 13	Perissodactyla	Equidae	Equus
DC15745	Layer 13	Artiodactyla	Bovidae	Bos/Bison
DC15746	Layer 13	Artiodactyla	Bovidae	Bos/Bison
DC15747	Layer 13	Perissodactyla	Rhinocerotidae	Rhinocerotidae
DC15748	Layer 13	Artiodactyla	Bovidae/Cervidae	Cervidae/Gazella/Saiga
DC15749	Layer 13	Artiodactyla	Bovidae	Bos/Bison
DC15750	Layer 13	Perissodactyla	Equidae	Equus
DC15751	Layer 13	Artiodactyla	Bovidae	Bos/Bison
DC15752	Layer 13	Artiodactyla	Bovidae	Bos/Bison
DC15753	Layer 13	Carnivora	Canidae	Canidae
DC15754	Layer 13	Artiodactyla	Bovidae/Cervidae	Cervidae/Gazella/Saiga
DC15755	Layer 13	Perissodactyla	Equidae	Equus
DC15756	Layer 13	Artiodactyla	Bovidae	Bos/Bison
DC15757	Layer 13	Artiodactyla	Bovidae	Bos/Bison
DC15758	Layer 13	Proboscidea	Elephantidae	Elephantidae
DC15759	Layer 13	Artiodactyla	Bovidae	Bos/Bison
DC15760	Layer 13	Artiodactyla	Bovidae	Bos/Bison
DC15761	Layer 13	Perissodactyla	Equidae	Equus
DC15762	Layer 13	Artiodactyla	Bovidae/Cervidae	Cervidae/Gazella/Saiga
DC15763	Layer 13	Artiodactyla	Bovidae	Bos/Bison
DC15764	Layer 13	Artiodactyla	Bovidae	Bos/Bison
DC15765	Layer 13	Proboscidea	Elephantidae	Elephantidae
DC15766	Layer 13	Perissodactyla	Equidae	Equus
DC15767	Layer 13	Artiodactyla	Bovidae	Bos/Bison
DC15768	Layer 13	Perissodactyla	Equidae	Equus
DC15769	Layer 13	Proboscidea	Elephantidae	Elephantidae
DC15770	Layer 13	Artiodactyla	Bovidae/Cervidae	Cervidae/Gazella/Saiga
DC15771	Layer 13	Artiodactyla	Bovidae	Bos/Bison
DC15772	Layer 13	Artiodactyla	Bovidae	Bos/Bison
DC15773	Layer 13	Perissodactyla	Rhinocerotidae	Rhinocerotidae
DC15774	Layer 13	Perissodactyla	Equidae	Equus
DC15775	Layer 13	Perissodactyla	Rhinocerotidae	Rhinocerotidae
DC15776	Layer 13	Artiodactyla	Bovidae/Cervidae	Cervidae/Gazella/Saiga

DC15777	Layer 13	Perissodactyla	Equidae	Equus
DC15778	Layer 13	Perissodactyla	Equidae	Equus
DC15779	Layer 13	Artiodactyla	Bovidae	Bos/Bison
DC15780	Layer 13	Perissodactyla	Rhinocerotidae	Rhinocerotidae
DC15781	Layer 13	Artiodactyla	Bovidae	Bos/Bison
DC15782	Layer 13	Artiodactyla	Bovidae	Capra
DC15783	Layer 13	Artiodactyla	Bovidae	Capra
DC15784	Layer 13	Artiodactyla	Bovidae/Cervidae	Cervidae/Gazella/ Saiga
DC15785	Layer 13	Proboscidea	Elephantidae	Elephantidae
DC15786	Layer 13	Artiodactyla	Bovidae	Bos/Bison
DC15787	Layer 13	Artiodactyla	Bovidae/Cervidae	Cervidae/Gazella/ Saiga
DC15788	Layer 13	Perissodactyla	Rhinocerotidae	Rhinocerotidae
DC15789	Layer 13	Artiodactyla	Bovidae	Bos/Bison
DC15790	Layer 13	Artiodactyla	Bovidae	Bos/Bison
DC15791	Layer 13	Perissodactyla	Equidae	Equus
DC15792	Layer 13			Unknown
DC15793	Layer 13	Artiodactyla	Bovidae/Cervidae	Cervidae/Gazella/ Saiga
DC15794	Layer 13	Carnivora	Canidae	Canidae
DC15795	Layer 13	Artiodactyla	Bovidae/Cervidae	Cervidae/Gazella/ Saiga
DC15796	Layer 13	Artiodactyla	Bovidae	Bos/Bison
DC15797	Layer 13	Artiodactyla	Bovidae/Cervidae	Cervidae/Gazella/ Saiga
DC15798	Layer 13	Proboscidea	Elephantidae	Elephantidae
DC15799	Layer 13	Artiodactyla	Bovidae	Bos/Bison
DC15800	Layer 13			Unknown
DC15801	Layer 13	Artiodactyla	Bovidae/Cervidae	Cervidae/Gazella/ Saiga
DC15802	Layer 13	Artiodactyla	Bovidae/Cervidae	Cervidae/Gazella/ Saiga
DC15803	Layer 13	Artiodactyla	Bovidae/Cervidae	Cervidae/Gazella/ Saiga
DC15804	Layer 13	Artiodactyla	Bovidae/Cervidae	Cervidae/Gazella/ Saiga
DC15805	Layer 13	Proboscidea	Elephantidae	Elephantidae
DC15806	Layer 13	Artiodactyla	Bovidae/Cervidae	Cervidae/Gazella/ Saiga
DC15807	Layer 13	Artiodactyla	Bovidae/Cervidae	Cervidae/Gazella/ Saiga
DC15808	Layer 13	Artiodactyla	Bovidae/Cervidae	Cervidae/Gazella/ Saiga
DC15809	Layer 13	Artiodactyla	Bovidae/Cervidae	Cervidae/Gazella/ Saiga
DC15810	Layer 13	Artiodactyla	Bovidae/Cervidae	Cervidae/Gazella/ Saiga
DC15811	Layer 13	Artiodactyla	Bovidae/Cervidae	Cervidae/Gazella/ Saiga

DC15812	Layer 13	Perissodactyla	Rhinocerotidae	Rhinocerotidae
DC15813	Layer 13			Unknown
DC15814	Layer 13	Perissodactyla	Rhinocerotidae	Rhinocerotidae
DC15815	Layer 13	Perissodactyla	Rhinocerotidae	Rhinocerotidae
DC15816	Layer 13			fail
DC15817	Layer 13	Artiodactyla	Bovidae/Cervidae	Cervidae/Gazella/Saiga
DC15818	Layer 13	Artiodactyla	Bovidae/Cervidae	Cervidae/Gazella/Saiga
DC15819	Layer 13	Carnivora	Canidae	Canidae
DC15820	Layer 13	Artiodactyla	Bovidae/Cervidae	Cervidae/Gazella/Saiga
DC15821	Layer 13	Proboscidea	Elephantidae	Elephantidae
DC15822	Layer 13	Perissodactyla	Rhinocerotidae	Rhinocerotidae
DC15823	Layer 13	Artiodactyla	Bovidae/Cervidae	Cervidae/Gazella/Saiga
DC15824	Layer 13	Perissodactyla	Rhinocerotidae	Rhinocerotidae
DC15825	Layer 13	Artiodactyla	Bovidae/Cervidae	Cervidae/Gazella/Saiga
DC15826	Layer 13	Artiodactyla	Bovidae	Bos/Bison
DC15827	Layer 13			Unknown
DC15828	Layer 13	Perissodactyla	Rhinocerotidae	Rhinocerotidae
DC15829	Layer 14	Artiodactyla	Bovidae/Cervidae	Cervidae/Gazella/Saiga
DC15830	Layer 14	Artiodactyla	Bovidae/Cervidae	Cervidae/Gazella/Saiga
DC15831	Layer 14	Perissodactyla	Equidae	Equus
DC15832	Layer 14	Artiodactyla	Bovidae/Cervidae	Cervidae/Gazella/Saiga
DC15833	Layer 14	Primates	Hominidae	Hominin
DC15834	Layer 14	Carnivora	Canidae	Canidae
DC15835	Layer 14	Artiodactyla	Bovidae/Cervidae	Cervidae/Gazella/Saiga
DC15836	Layer 14	Proboscidea	Elephantidae	Elephantidae
DC15837	Layer 14	Perissodactyla	Rhinocerotidae	Rhinocerotidae
DC15838	Layer 14	Perissodactyla	Equidae	Equus
DC15839	Layer 14	Perissodactyla	Equidae	Equus
DC15840	Layer 14	Artiodactyla	Bovidae	Bos/Bison
DC15841	Layer 14			Unknown
DC15842	Layer 14	Perissodactyla	Rhinocerotidae	Rhinocerotidae
DC15843	Layer 14	Perissodactyla	Equidae	Equus
DC15844	Layer 14	Perissodactyla	Equidae	Equus
DC15845	Layer 14	Artiodactyla	Bovidae/Cervidae	Cervidae/Gazella/Saiga
DC15846	Layer 14	Artiodactyla	Bovidae/Cervidae	Cervidae/Gazella/Saiga
DC15847	Layer 14	Artiodactyla	Bovidae/Cervidae	Cervidae/Gazella/Saiga

DC15848	Layer 14	Artiodactyla	Bovidae/Cervidae	Cervidae/Gazella/Saiga
DC15849	Layer 14	Perissodactyla	Equidae	Equus
DC15850	Layer 14	Artiodactyla	Bovidae	Bos/Bison
DC15851	Layer 14	Artiodactyla	Bovidae/Cervidae	Cervidae/Gazella/Saiga
DC15852	Layer 14	Artiodactyla	Bovidae	Bos/Bison
DC15853	Layer 14	Artiodactyla	Bovidae/Cervidae	Cervidae/Gazella/Saiga
DC15854	Layer 14	Artiodactyla	Bovidae/Cervidae	Cervidae/Gazella/Saiga
DC15855	Layer 14	Artiodactyla	Bovidae/Cervidae	Cervidae/Gazella/Saiga
DC15856	Layer 14	Artiodactyla	Bovidae	Bos/Bison
DC15857	Layer 14	Artiodactyla	Bovidae/Cervidae	Cervidae/Gazella/Saiga
DC15858	Layer 14	Artiodactyla	Bovidae/Cervidae	Cervidae/Gazella/Saiga
DC15859	Layer 14	Artiodactyla	Bovidae/Cervidae	Cervidae/Gazella/Saiga
DC15860	Layer 14	Artiodactyla	Bovidae	Bos/Bison
DC15861	Layer 14	Artiodactyla	Bovidae	Bos/Bison
DC15862	Layer 14	Perissodactyla	Equidae	Equus
DC15863	Layer 14	Perissodactyla	Rhinocerotidae	Rhinocerotidae
DC15864	Layer 14	Perissodactyla	Equidae	Equus
DC15865	Layer 14	Artiodactyla	Bovidae/Cervidae	Cervidae/Gazella/Saiga
DC15866	Layer 14	Perissodactyla	Equidae	Equus
DC15867	Layer 14	Artiodactyla	Bovidae	Bos/Bison
DC15868	Layer 14	Perissodactyla	Rhinocerotidae	Rhinocerotidae
DC15869	Layer 14	Carnivora	Felidae/Hyaenidae/Mustelidae	Panthera/Crocuta/Mustelidae
DC15870	Layer 14	Carnivora	Canidae	Canidae
DC15871	Layer 14	Artiodactyla	Bovidae	Bos/Bison
DC15872	Layer 14	Carnivora	Canidae	Canidae
DC15873	Layer 14	Artiodactyla	Bovidae/Cervidae	Cervidae/Gazella/Saiga
DC15874	Layer 14	Perissodactyla	Rhinocerotidae	Rhinocerotidae
DC15875	Layer 14	Artiodactyla	Bovidae/Cervidae	Cervidae/Gazella/Saiga
DC15876	Layer 14	Artiodactyla	Bovidae/Cervidae	Cervidae/Gazella/Saiga
DC15877	Layer 14	Artiodactyla	Bovidae/Cervidae	Cervidae/Gazella/Saiga
DC15878	Layer 14			Unknown
DC15879	Layer 14	Artiodactyla	Bovidae/Cervidae	Cervidae/Gazella/Saiga
DC15880	Layer 14	Perissodactyla	Rhinocerotidae	Rhinocerotidae
DC15881	Layer 14	Carnivora	Ursidae	Ursus

DC15882	Layer 14	Artiodactyla	Bovidae/Cervidae	Cervidae/Gazella/Saiga
DC15883	Layer 14	Artiodactyla	Bovidae/Cervidae	Cervidae/Gazella/Saiga
DC15884	Layer 14	Artiodactyla	Bovidae/Cervidae	Cervidae/Gazella/Saiga
DC15885	Layer 14	Perissodactyla	Rhinocerotidae	Rhinocerotidae
DC15886	Layer 14	Carnivora	Ursidae	Ursus
DC15887	Layer 14	Artiodactyla	Bovidae	Bos/Bison
DC15888	Layer 14	Artiodactyla	Bovidae/Cervidae	Cervidae/Gazella/Saiga
DC15889	Layer 14	Perissodactyla	Rhinocerotidae	Rhinocerotidae
DC15890	Layer 14	Artiodactyla	Bovidae	Bos/Bison
DC15891	Layer 14	Primates	Hominidae	Hominin
DC15892	Layer 14	Perissodactyla	Equidae	Equus
DC15893	Layer 14	Perissodactyla	Rhinocerotidae	Rhinocerotidae
DC15894	Layer 14	Perissodactyla	Equidae	Equus
DC15895	Layer 14	Artiodactyla	Bovidae/Cervidae	Cervidae/Gazella/Saiga
DC15896	Layer 14	Artiodactyla	Bovidae/Cervidae	Cervidae/Gazella/Saiga
DC15897	Layer 14	Perissodactyla	Equidae	Equus
DC15898	Layer 14	Perissodactyla	Equidae	Equus
DC15899	Layer 14	Perissodactyla	Rhinocerotidae	Rhinocerotidae
DC15900	Layer 14	Artiodactyla	Bovidae/Cervidae	Cervidae/Gazella/Saiga
DC15901	Layer 14			Unknown
DC15902	Layer 14	Carnivora	Canidae	Canidae
DC15903	Layer 14	Carnivora	Ursidae	Ursus
DC15904	Layer 14	Artiodactyla	Bovidae/Cervidae	Cervidae/Gazella/Saiga
DC15905	Layer 14	Perissodactyla	Rhinocerotidae	Rhinocerotidae
DC15906	Layer 14	Artiodactyla	Bovidae	Capra
DC15907	Layer 14	Artiodactyla	Bovidae	Bos/Bison
DC15908	Layer 14	Carnivora	Ursidae	Ursus
DC15909	Layer 14	Artiodactyla	Bovidae/Cervidae	Cervidae/Gazella/Saiga
DC15910	Layer 14	Perissodactyla	Rhinocerotidae	Rhinocerotidae
DC15911	Layer 14	Artiodactyla	Bovidae	Bos/Bison
DC15912	Layer 14	Perissodactyla	Equidae	Equus
DC15913	Layer 14	Perissodactyla	Equidae	Equus
DC15914	Layer 14	Perissodactyla	Equidae	Equus
DC15915	Layer 14	Perissodactyla	Equidae	Equus
DC15916	Layer 14	Perissodactyla	Equidae	Equus
DC15917	Layer 14	Artiodactyla	Bovidae	Bos/Bison
DC15918	Layer 14			Unknown
DC15919	Layer 14	Perissodactyla	Equidae	Equus

DC15920	Layer 14	Artiodactyla	Bovidae/Cervidae	Cervidae/Gazella/ Saiga
DC15921	Layer 14	Carnivora	Ursidae	Ursus
DC15922	Layer 14	Artiodactyla	Bovidae/Cervidae	Cervidae/Gazella/ Saiga
DC15923	Layer 14	Carnivora	Ursidae	Ursus
DC15924	Layer 14	Artiodactyla	Bovidae/Cervidae	Cervidae/Gazella/ Saiga
DC15925	Layer 14	Artiodactyla	Bovidae/Cervidae	Cervidae/Gazella/ Saiga
DC15926	Layer 14	Artiodactyla	Bovidae/Cervidae	Cervidae/Gazella/ Saiga
DC15927	Layer 14	Perissodactyla	Rhinocerotidae	Rhinocerotidae
DC15928	Layer 14	Artiodactyla	Bovidae/Cervidae	Cervidae/Gazella/ Saiga
DC15929	Layer 14	Perissodactyla	Rhinocerotidae	Rhinocerotidae
DC15930	Layer 14	Artiodactyla	Bovidae/Cervidae	Cervidae/Gazella/ Saiga
DC15931	Layer 14	Artiodactyla	Bovidae/Cervidae	Cervidae/Gazella/ Saiga
DC15932	Layer 14	Artiodactyla	Bovidae	Ovis
DC15933	Layer 14	Artiodactyla	Bovidae/Cervidae	Cervidae/Gazella/ Saiga
DC15934	Layer 14	Perissodactyla	Equidae	Equus
DC15935	Layer 14	Perissodactyla	Equidae	Equus
DC15936	Layer 14	Perissodactyla	Rhinocerotidae	Rhinocerotidae
DC15937	Layer 14	Artiodactyla	Bovidae/Cervidae	Cervidae/Gazella/ Saiga
DC15938	Layer 14	Artiodactyla	Bovidae	Ovis
DC15939	Layer 14	Artiodactyla	Bovidae	Bos/Bison
DC15940	Layer 14	Artiodactyla	Bovidae/Cervidae	Cervidae/Gazella/ Saiga
DC15941	Layer 14	Artiodactyla	Bovidae	Capra

Appendix 2: Analysed Stable Isotope Values

Zooms_ID	Layer	ZooMS taxon	d13C	d15N	C/N	Lab.
DC 15464	Layer 13	Bos/Bison	-18.75	10.36	2.3	MPL
DC 15472	Layer 13	Bos/Bison	-18.93	8.31	2.31	MPL
DC 15499	Layer 13	Bos/Bison	-20.51	6.993		SLV
DC 15503*	Layer 13	Bos/Bison	-20.56	12.04	2.30	MPL
DC 15540	Layer 13	Bos/Bison	-19.40	7.08	2.30	MPL
DC 15559*	Layer 13	Canidae	-19.43	11.53	2.30	MPL
DC 15616*	Layer 13	Canidae	-18.02	11.09	2.30	MPL
DC 15657	Layer 13	Canidae	-19.47	9.36	2.30	MPL

DC 15660	Layer 13	Canidae	-18.38	11.94	2.30	MPL
DC 15753	Layer 13	Canidae	-18.55	14.19	2.30	MPL
DC 15469*	Layer 13	Elephantidae	-20.31	9.49	2.30	MPL
DC 15473	Layer 13	Elephantidae	-20.69	12.19	2.30	MPL
DC 15547	Layer 13	Elephantidae	-19.84	15.31	2.30	MPL
DC 15733*	Layer 13	Equidae	-19.76	5.94	2.40	MPL
DC 15750	Layer 13	Equidae	-20.15	6.26	2.40	MPL
DC 15761	Layer 13	Equidae	-19.60	7.45	2.30	MPL
DC 15768	Layer 13	Equidae	-20.41	3.72	2.40	MPL
DC 15779	Layer 13	Equidae	-19.47	7.19	2.40	MPL
DC 15446	Layer 13	Crocuta/Panthera/Mustelidae	-17.87	11.94	2.30	MPL
DC 15511	Layer 13	Crocuta/Panthera/Mustelidae	-17.98	11.41	2.30	MPL
DC 15523*	Layer 13	Crocuta/Panthera/Mustelidae	-18.06	10.73	3.10	MPL
DC 15712	Layer 13	Crocuta/Panthera	-18.56	12.26	2.31	MPL
DC 15294*	Layer 14	Bos/Bison	-19.18	6.53	2.40	MPL
DC 5805	Layer 14	Bos/Bison	-19.31	6.25	2.30	MPL
DC 15316	Layer 14	Bos/Bison	-19.47	7.96	2.40	MPL
DC 5769	Layer 14	Bos/Bison	-19.28	6.27	2.40	MPL
DC 15870	Layer 14	Canidae	-20.05	6.32	2.40	MPL
DC 11274	Layer 14	Canidae	-18.46	11.63	2.40	MPL
DC 9606	Layer 14	Canidae	-19.60	5.84	2.40	MPL
DC 9580	Layer 14	Canidae	-19.17	12.02	2.40	MPL
DC 15418	Layer 14	Canidae	-18.43	9.47	2.40	MPL
DC 11227	Layer 14	Elephantidae	-19.02	7.48	2.40	MPL
DC 11219	Layer 14	Elephantidae	-20.31	6.4	2.40	MPL
DC 15385	Layer 14	Elephantidae	-19.67	5.52	2.40	MPL
DC 11221	Layer 14	Elephantidae	-19.51	6.63	2.50	MPL
DC 5785	Layer 14	Equidae	-19.85	5.61	2.40	MPL
DC 5811	Layer 14	Equidae	-20.54	5.81	2.40	MPL
DC 8255	Layer 14	Equidae	-20.53	4.93	2.40	MPL

DC 9021	Layer 14	Crocuta/Panthera	-18.31	12.63	2.30	MPL
DC 8956	Layer 14	Crocuta/Panthera	-17.95	11.23	2.30	MPL
DC 9009	Layer 14	Crocuta/Panthera	-17.99	11.38	2.40	MPL
DC 9066	Layer 14	Crocuta/Panthera	-18.08	11.42	2.40	MPL
DC 12777	Layer 14	Hominin	-18.00	13.47	1.50	MPL
DC 15833	Layer 14	Hominin	-17.73	13.58	2.50	MPL
DC 15891	Layer 14	Hominin	-17.98	13.23	2.40	MPL
DC 13142	Layer 14	Hominin	-18.96	15.291	2.40	MPL
DC 15720	Layer 13	Crocuta/Panthera	-18.03	11.46	2.30	MPL
DC 7332*	Layer 15	Bos/Bison	-19.28	7.11		SLV
DC 7409 *	Layer 15	Bos/Bison	-18.64	6.59	3.10	MPL
DC 7412*	Layer 15	Bos/Bison	-18.96	8.29	3.10	MPL
DC 7481*	Layer 15	Bos/Bison	-19.10	6.94	3.10	MPL
DC 7305	Layer 15	Bos/Bison	-19.28	6.418		SLV
DC 7722 *	Layer 15	Canidae	-18.46	9.55	3.00	MPL
DC 8802	Layer 15	Canidae	-19.21	8.81	3.00	MPL
DC 7760	Layer 15	Canidae	-19.28	8.65	3.00	MPL
DC 7370	Layer 15	Canidae	-21.07	7.72	3.10	MPL
DC 8674	Layer 15	Canidae	-19.21	8.92	3.10	MPL
DC 8825	Layer 15	Canidae	-17.73	10.02	3.00	MPL
DC 7563	Layer 15	Elephantidae	-20.68	9.29	3.00	MPL
DC 7322*	Layer 15	Elephantidae	-20.68	9.947		SLV
DC 7333*	Layer 15	Elephantidae	-21.49	7.772		SLV
DC 8844	Layer 15	Elephantidae	-22.07	8.623		SLV
DC 7349	Layer 15	Equidae	-20.34	5.35	3.10	MPL
DC 7615*	Layer 15	Equidae	-20.51	6.94	3.20	MPL
DC 7328	Layer 15	Equidae	-19.91	7.91	3.10	MPL
DC 7499	Layer 15	Equidae	-20.12	3.94	3.10	MPL
DC 7551	Layer 15	Equidae	-19.88	6.33	3.10	MPL
DC 10788*	Layer 17	Capra	-19.00	4.07	2.90	MPL
DC 10792*	Layer 17	Cervicae/Gazella/Saiga	-20.03	7.637		SLV

DC 10805*	Layer 17	Equidae	-20.54	4.723		SLV
DC 5981*	Layer 17	Felidae/Ursidae	-21.77	6.796		SLV
DC 10811*	Layer 17	Ursidae	-18.33	6.93	3.00	MPL
DC 10782*	Layer 17	Ursidae	-21.28	6.192		SLV
DC 6021*	Layer 17	Ursidae	-21.16	5.354		SLV
DC 6024*	Layer 17	Ursidae	-21.64	4.865		SLV
DC 10784*	Layer 17	Vulpes vulpes	-19.24	6.753		SLV